JOURNAL OF APPLIED PHYSICS

JOURNAL
OF
APPLIED PHYSICS

Vol. 14, No. 10 OCTOBER, 1943

In This Issue

Page

A National Headquarters for Physicists HENRY A. BARTON 499

The American Institute of Physics Building
I. Early History of the Building ROSE V. HUTCHISSON 501

Frictional Phenomena. XVI ANDREW GEMANT 510

Bibliography of Electron Microscopy
CLAIRE MARTON AND SAMUEL SASS 522

Contributed Original Research

Harmonic Analysis by Photographic Method
ARCHIE W. STRAITON AND GEORGE K. TERHUNE 535

Radiation Field of Long Wires, with Application to Vee Antennas CHARLES W. HARRISON, JR. 537

Dosimetry and Local Distribution of Energy in the Electric High Frequency Field K. S. LION 545

Erratum: The Penetrometer Method for Determining the Flow Properties of High Viscosity Fluids
WESLEY W. PENDLETON 551

Thermionic Emission from an Oxide-Coated Cathode
H. Y. FAN 552

In Every Issue

Calendar of Meetings 531

Here and There 532

Innovations in Instruments 533

New Instrument Booklets 533

Recent Applications of Physics 534

Index to Advertisers xviii

BOARD OF EDITORS

ELMER HUTCHISSON, *Editor*

Associate Editors

FRANCIS BITTER
W. F. BUSSE
S. H. CALDWELL
ROBLEY D. EVANS
SELIG HECHT
W. J. LYONS
MORRIS MUSKAT
THOMAS H. OSGOOD
PAUL E. SABINE
FREDERICK SEITZ
J. R. TOWNSEND
B. E. WARREN
J. B. WHITEHEAD

Publication of the American Institute of Physics

ADMINISTRATIVE STAFF

HENRY A. BARTON, *Director*

MADELINE M. MITCHELL, *Publications Manager*

JOHN T. TATE, *Adviser on Publications*

GOVERNING BOARD

PAUL E. KLOPSTEG, *Chairman*

GEORGE B. PEGRAM, *Secretary*

T. D. COPE
R. B. DOW
L. A. DUBRIDGE
FLOYD A. FIRESTONE
HARVEY FLETCHER
R. C. GIBBS
K. S. GIBSON
ARTHUR C. HARDY
HERMANN MARK
A. G. WORTHING
JOHN T. TATE
N. W. TAYLOR
WALLACE WATERFALL

The JOURNAL OF APPLIED PHYSICS, published monthly at Prince and Lemon Sts., Lancaster, Pa., is devoted to physics in its role as the science basic to other natural sciences and to the arts and industries. Previous to 1937 this publication was known as PHYSICS. The JOURNAL OF APPLIED PHYSICS publishes editorials, news of physicists and reviews, as well as technical papers of applied physics.

Manuscripts should be submitted to Elmer Hutchisson, Editor, 50th floor, 350 Fifth Avenue, New York 1, New York.

Subscriptions and orders for back numbers should be addressed to Prince and Lemon Streets, Lancaster, Pa. or to the American Institute of Physics, 175 Fifth Avenue, New York 10, N. Y.

Subscription Price

	U. S. AND CANADA	ELSEWHERE
To members of scientific societies	$5.00	$5.70
To all others	7.00	7.70

Back Number Prices

Complete set: Vol. 1, July, 1931–Vol. 13, 1942—**$80.50**
Yearly back number rate: **$7.70**
Single copies: **$0.70** each.

Changes of address and proofs should be addressed to the Publications Manager.

Advertising rates supplied on request. Orders, advertising copy, and cuts should be sent to the American Institute of Physics.

Entered as second class matter January 22, 1937, at the Post Office at Lancaster, Pennsylvania, under the Act of March 3, 1879. Accepted for mailing at the special rate of postage provided for in the Act of February 28, 1925, authorized May 2, 1932.

Copyright 1943, by the American Institute of Physics.

Journal
of
Applied Physics

Volume 14, Number 10 October, 1943

A National Headquarters for Physicists

By Henry A. Barton

Director of the American Institute of Physics

On August 20, 1943, authorized representatives of the American Institute of Physics negotiated a contract to purchase the building at 57 East 55 Street, New York City, as a national home office for the physicists of America. The passing of this milestone in the history of physics in America does not mean that the campaign to raise funds for the purchase of the building has attained its goal. It has not yet done so. It means not only that the Institute is committed to the purchase and that the campaign is progressing favorably enough to justify the action taken, but also that the remaining physicists and their friends, who have not yet joined over a thousand of their colleagues in supporting the project, must now be relied upon to bring the fund at least to the $75,000 total sought. Approximately $25,000 has still to be raised. Without question it can be done, but only with everyone helping.

Even physicists are likely to underestimate the value of their field of activity. Physics in this country has come from modest beginnings. Less than 50 years ago there did not exist any organized society through which all the physicists in America could gain the strength of mutual encouragement. There was no adequate provision for the sharing of information nor for the establishing of a professional status for physicists. In 1899, the American Physical Society was founded but it was some twenty years before its meetings became "crowded." Only in 1918 did the physicist, as a professional, begin to come into some prominence.

In 1918, the idea of a $75,000 building would have seemed far out of proportion. Now the situation has completely changed but even physicists themselves are likely not to realize how much it has changed. Instead of 1000 physicists there are 6500. Instead of annual services to physi-

cists, including publication, costing less than $12,000, such activities now require an outlay of more than $125,000. An investment of $75,000 in a headquarters building is now certainly not too much for physics and many physicists are proving by their contributions that it is not too much for them.

Now, in marked contrast to 1918, there are *five* large and strong national societies of physics which as entities are the "Members" of the American Institute of Physics. They really *are* the Institute. They control it. The fruits of its work and achievements belong to them and to their members. The new building, the national home office, is theirs. To these five societies other, as yet small, groups devoted to particular fields of physics are being added as Associates of the Institute. They are staying in the physics family. The Institute offers a way of conserving the unity of physicists without any sacrifice of independence and small-group enthusiasm.

Until about fifteen years ago physics was thought of mainly as a course of study or as a branch of higher scholarship. It was an area of knowledge fascinating in its known outline and rich in the possibilities of new exploration. Now, however, the habits of mind developed by the study of physics on the one hand, and the rapidity with which new discoveries have been made on the other, have combined to make it necessary for industries to turn to physicists themselves to supervise the application of physics to their problems. These problems have grown beyond the methods, the scope, and the capacities of the recognized fields of engineering and chemistry.

It is now barely a majority of physicists who are still to be found in academic surroundings, even though they too have increased in number. Some fear this swing and say that it will react against pure research—that the programs and character of the meetings of our societies will be unduly dominated by physics "at work" and that this will destroy the proper atmosphere for physics as a field of exploration after knowledge. There should be no basis for such fears for surely the development of applied physics should accelerate rather than retard the fundamental advance of the science. The Institute, at all events, will continue to represent all physicists and to provide a way for the strength of all to be imparted to the welfare of each.

The increased number of physicists, the increased importance of their industrial contribution, and the growth of organizational activities these developments necessitate combine to make the present a most opportune time for the acquisition by the Institute of a building of its own—a national headquarters through which may be focused the efforts of physicists to advance their science and their service to the community at large. The building at 57 East 55 Street, New York, is a fine building, handsome, well arranged, and a bargain. The estimated annual cost of its maintenance seems to be safely within the Institute's current means. It provides improved and expanded office space already seriously needed. It will permit many useful and desirable activities to be carried on that now are neglected. The purchase of the building, examined over a ten-year period in prospect, appears to be good business economy just as office space, but that is not the most important thing at all. The advantages of the building as an implement of professional unity and strength are of the greatest significance.

The American Institute of Physics Building

A HOME office for the American Institute of Physics, as well as a national headquarters for its member societies and for the physicists of America is no longer a dream but a definite accomplished fact. At a fraction of its former value, the Institute has obtained a building eminently suited to its needs. Because of the durable construction and fire-proof nature of the building, upkeep costs will be reasonably low. This fact together with the tax-free status of the Institute makes "home-ownership" decidedly a matter of good business.

The suitability of the building for the purposes of the Institute has been emphasized in the appeal for funds. The dignified entrance hall will make physicists proud of "their building." The large member's room on the second floor will provide a place for physicists visiting New York to read, write, telephone, and meet people. In addition, this room will make an excellent board room and meeting place for small groups. The other rooms on the second, third, and fourth floors will provide adequate space for the Director, Publications Manager, and other officers of the Institute, and for the publications staff. Fortunately there is room for the expansion of the activities of the Institute which is sure to come in the near future.

Many of the interior photographs in this issue of the Journal show the furnishings of the building when used as a residence. Naturally when used as an office some of the elegance will be sacrificed for utility. The Institute will of necessity carry out gradually interior decorations adapted to its new use. Since the building has not been used for several years minor repairs and a thorough cleaning will be in order first of all. Although the present appearance of the building inside and out is not as bright as the pictures used here indicate the architectural details are in sound condition underneath the grime.

Dr. Barton has pointed out that the goal of $75,000 which must be raised if this building is to be owned by the Institute free-of-debt has not yet been reached. Physicists are asked to send in their contributions soon. Every physicist will want to own a small part of this building. It is to be hoped that everyone will make a contribution even if it must be small so that the Institute will know that physicists are unanimously back of its carefully formulated program for the future of organized physics in America. Great credit is due to the Governing Board and the War Policy Committee, but those close to the Institute know that were it not for the hard work and unbounded enthusiasm of the Director and the Publications Manager, a national headquarters for physicists would not have been possible for a long time to come.

So that physicists may become better acquainted with their new headquarters, a series of articles describing the building is planned. The first of these is concerned with its early history and follows below.—THE EDITOR

I. Early History of the Building[1]

BY ROSE V. HUTCHISSON

THE new home of the American Institute of Physics at 57 East 55 Street, New York City, was known from the time of its construction in 1909 to its sale in 1937 as the Martin Erdmann Residence. It is a five-storied English Renaissance house, which was considered by contemporary critics a capable, daring, and clever work of architecture.[2] Its dignified limestone façade may have

[1] The author wishes to thank Mr. Julian Clarence Levi, architect, for information, sketches, and photographs pertaining to the building of the Erdmann Residence.

[2] Architecture **20**, 147 (October 15, 1909).

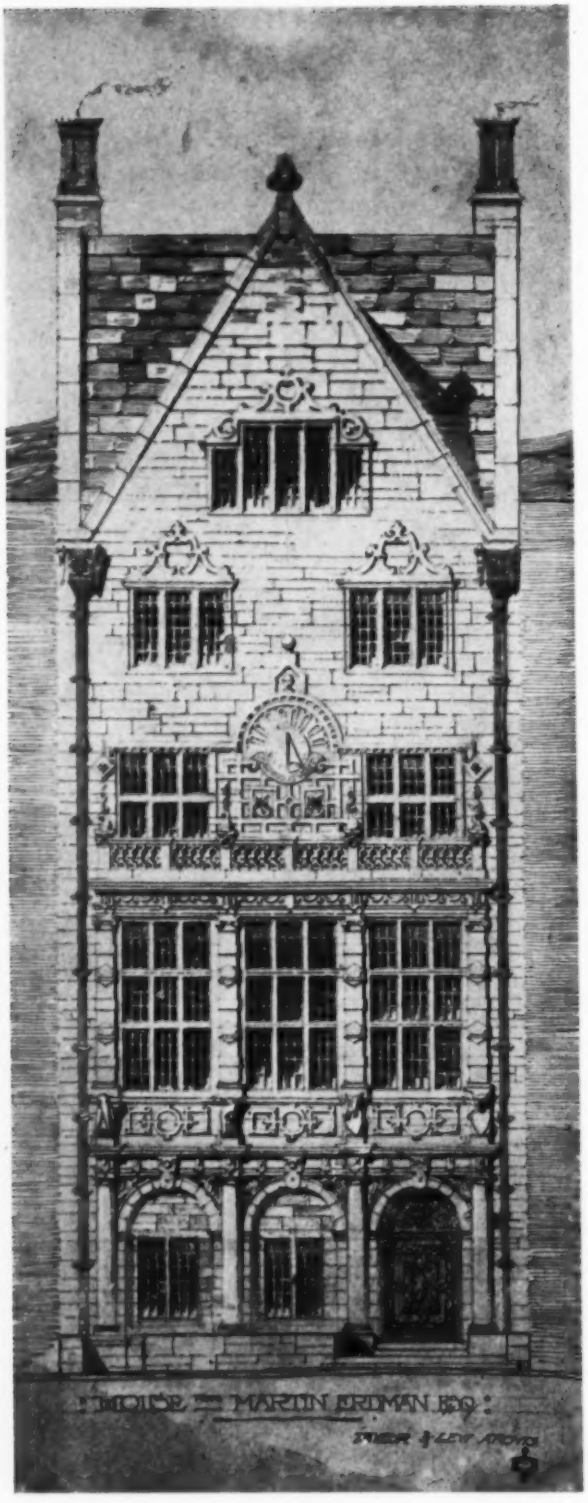

Architect's preliminary sketch of the facade.

seemed a bit incongruous among its nondescript brownstone neighbors, for it was built at a time when New York was a sea of almost identical brownstone fronts, a circumstance which gave rise to the then current comment that to have seen one New York house was to have seen them all. Now, however, mellowed by age, the house blends agreeably with its more recently built neighbors.

The decade in which it was erected was one of tremendous building activity on the part of wealthy merchants, manufacturers, and bankers, such as Andrew Carnegie, William Payne Whitney, the Astors, O. H. Havemeyer, Edward S. Harkness, F. W. Woolworth, and many others, all of whom built palatial residences. Occasionally the result was "a noble monument to the derivative genius of some American architect trained in Europe and given freedom to create."[3]

The late Mr. Martin Erdmann, a partner in the recently dissolved Speyer Corporation, international investment bankers, a bachelor, and a collector of English mezzotints, engaged the architectural firm of Taylor and Levi in 1908 to build a home for himself and his valuable art collection.[4] He had purchased two plots of ground on East 55 Street each having a frontage of sixteen and one-half feet and occupied by a four-storey brownstone house which was torn down to make room for the new structure. The location was in a fine residential section which had been guaranteed a dignified development by the inclusion of restrictive clauses in all the property deeds, forbidding the establishing of such nuisances as livery stables, breweries, tanneries, forge or blacksmith shops, glue factories, ink or vitriol manufactories, and others of equally noisome character. These restrictions still remain in the deed acquired by the American Institute of Physics, but ought not to hamper the work of the Institute.

The floor plan of the house was conditioned by the needs of a bachelor client rather than by the needs of a family and hence it differed somewhat from the conventional residence. After the plan

[3] Charles A. Beard and Mary R. Beard, *Rise of American Civilization* (Macmillan Co., New York, 1930), vol. II, p. 385.

[4] Nineteen of the mezzotints from the Erdmann Collection were acquired by the British Museum in 1937. See A. M. Hind, British Museum Quarterly **12**, 99 (1938).

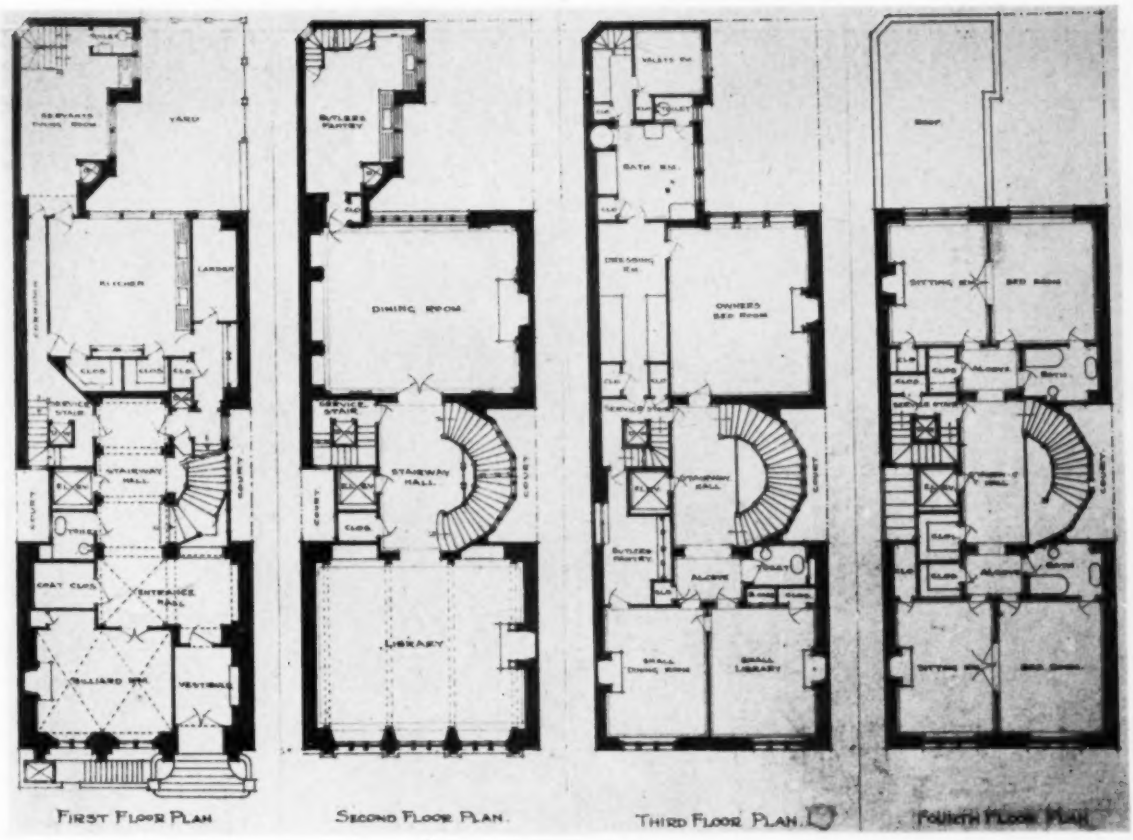

Floor plans which were followed in building the Martin Erdmann Residence.

had been approved, the architects made sketches for the façade in several styles including the Georgian, the Colonial, the Elizabethan, and the English Renaissance. The client chose the English Renaissance and the work of designing the interior in that style was begun. The architects were commissioned to design everything which was to go into the house including not only the panelling, the designs for the carving of the balustrades, moldings, cornices, doors and door-frames, the chandeliers, and iron work, but also the interior furnishings and draperies. As Mr. Levi, one of the architects, puts it, "We designed everything but the mezzotints and the oriental rugs." Three years passed from the time of the drawing of the first sketch to the completion of the furnishing.[5] All together, the sketches, designs, and working drawings filled eighty-five bulging portfolios. Everything in the house is real and genuine; neither Mr. Erdmann nor the architects would tolerate any shams or imitations.

The house is spacious, well built, and well preserved. It contains a wealth of beautiful architectural detail worthy of study, from the vaulted ceiling of its dignified marble entrance hall to the minutest detail of wood carving in the wall panels or in the magnificent railing leading from the second to the third floors. The decoration is never

[5] As a matter of record, a complete list of the builders is given here. The General Contractor was Mark Eidlitz and Son, well-known in New York as builder of fine houses. The following special contractors were employed: Heating, Johnson and Morris; Plumbing, James F. Gross & Company; Electric Installation, Western Electric Company; Elevator, Otis Elevator Company; Limestone for façade, from B. A. and G. M. Williams; Marble work, Traitel Marble Company; Leaded Glass, Harry Knox Smith; Lighting Fixtures (fixtures were executed from the architect's drawings), Sterling Bronze Company; Plaster (plaster forms made from molded designs created by the architects), Klee Thompson; Hardware, Russell and Irwin, Fritaine Cie., Paris, Krassner, Boston; Metal Sash, imported by Wragge from F. Draper in England; Cabinet work, A. J. Crawford; Floors, G. W. Koch and Son; Tile, William H. Jackson.

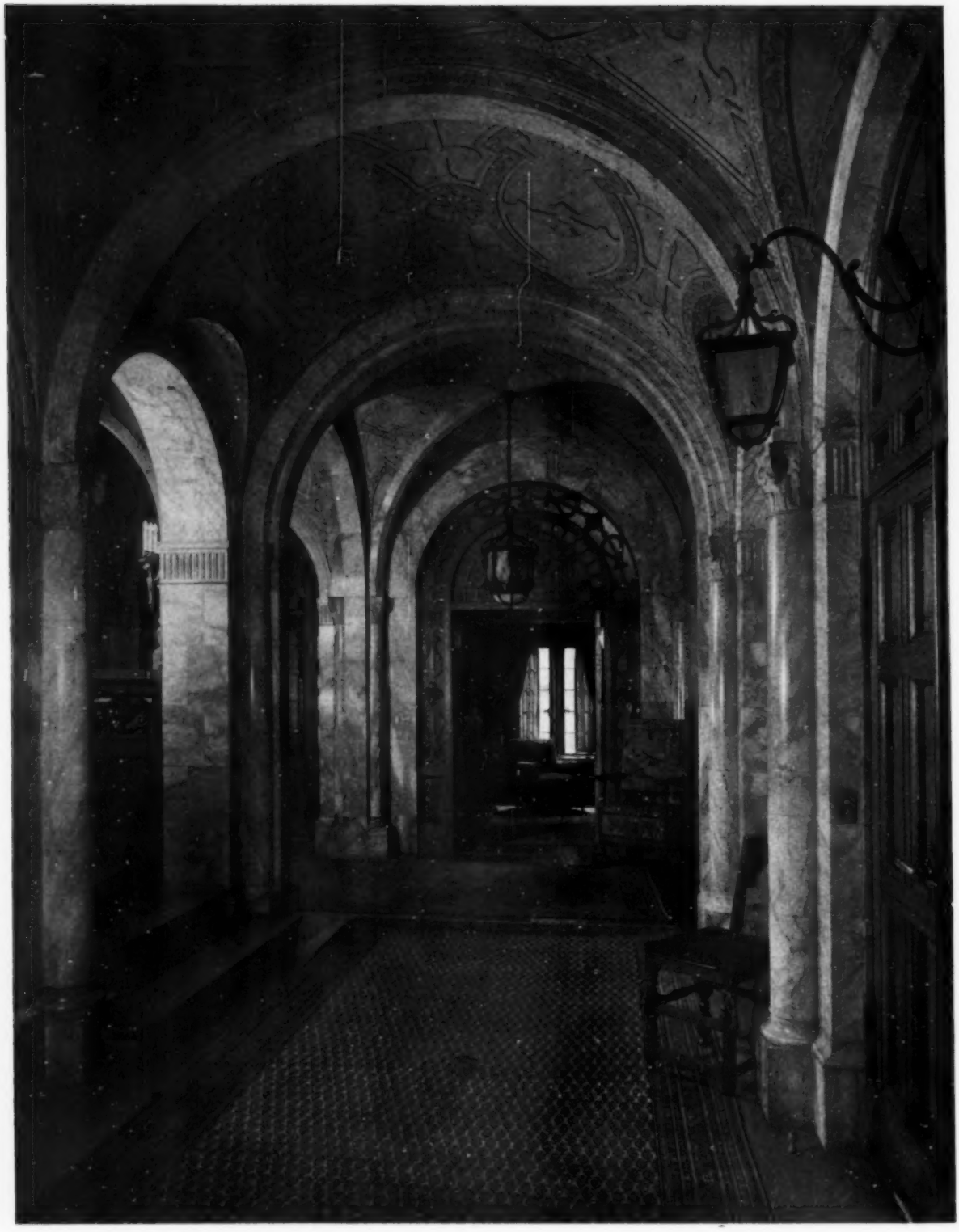

Entrance Hall as furnished when used as a residence. (Photo by M. E. Hewitt.)

Architect's water color rendering of preliminary design of Entrance Hall.

"fussy," overdone, nor effeminate. With a preponderance of oak panelling of simple design, and with restraint in the use of decorative pattern, the house is truly masculine in character. It gives promise of enduring a long time with a minimum of attention.

Two farsighted provisions of the original owner will benefit the American Institute of Physics. One is the care which was taken to make the building completely fireproof. According to the architects, it is "the most fireproof residence in Manhattan" and incidently gave the banker-client the lowest possible fire insurance rate. The other was the provision not only of a complete furnace system but also all the necessary arrangements for the utilization of steam heat supplied by the New York Steam Company. The latter provision, which was not at all usual at the time the house was built, will eliminate the handling of fuel and ashes on the premises.

A small modification in the external appearance of the house has taken place since its original construction. When the streets and lots were laid out in midtown Manhattan, each plot was marked with a building line, an area line (providing for light and an approach to the basement), and a stoop line. One was permitted to build to the area line and stoop line but had no legal title to this strip of land beyond the building line. The widening of East 55 Street in 1922 necessitated the removal of a stone railing originally enclosing the area way at the front of the Erdmann residence and the rebuilding of the projecting front stoop to make room for a sidewalk extending to the walls of the house. Grilles were put in the sidewalk to allow light to shine into the basement windows.

After Mr. Erdmann's death, his estate, in 1937, sold the house to Mr. Frederick Brown,[6] a prominent New York real estate broker, who bought it as an investment and who held it until the American Institute of Physics purchased it in August, 1943. Mr. Paul S. Dixon, broker of the Equity Conservation Corporation, located the house along with three or four others, none of which proved to be as suitable to the Institute's needs.

[6] Mr. Brown has very kindly loaned to the Institute several fine photographs of the house as it was when occupied by Mr. Erdmann. Five of these are included in this article.

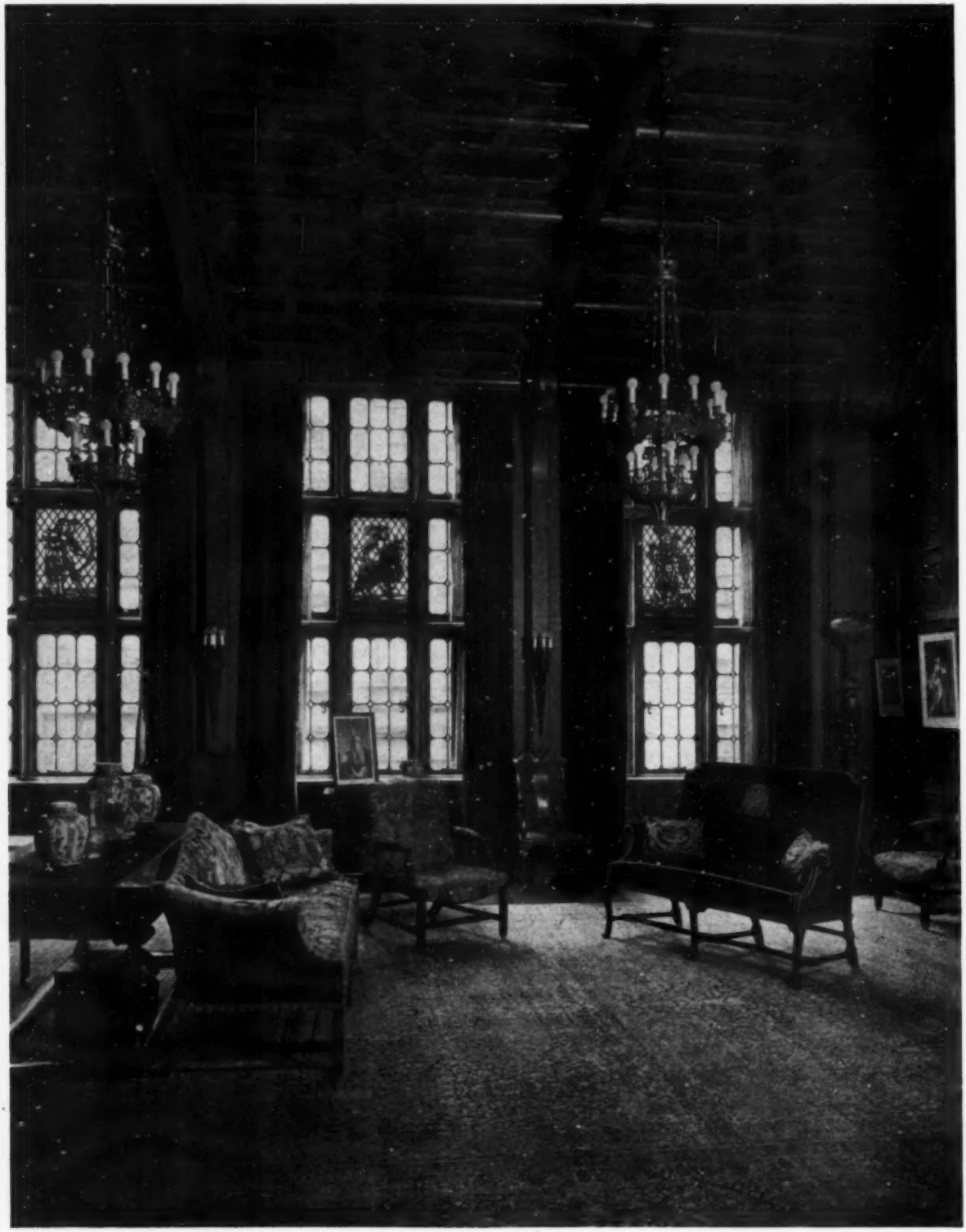

The library of Martin Erdmann. Furnishings and art objects were sold by the Estate at Mr. Erdmann's death. (Photo by M. E. Hewitt.)

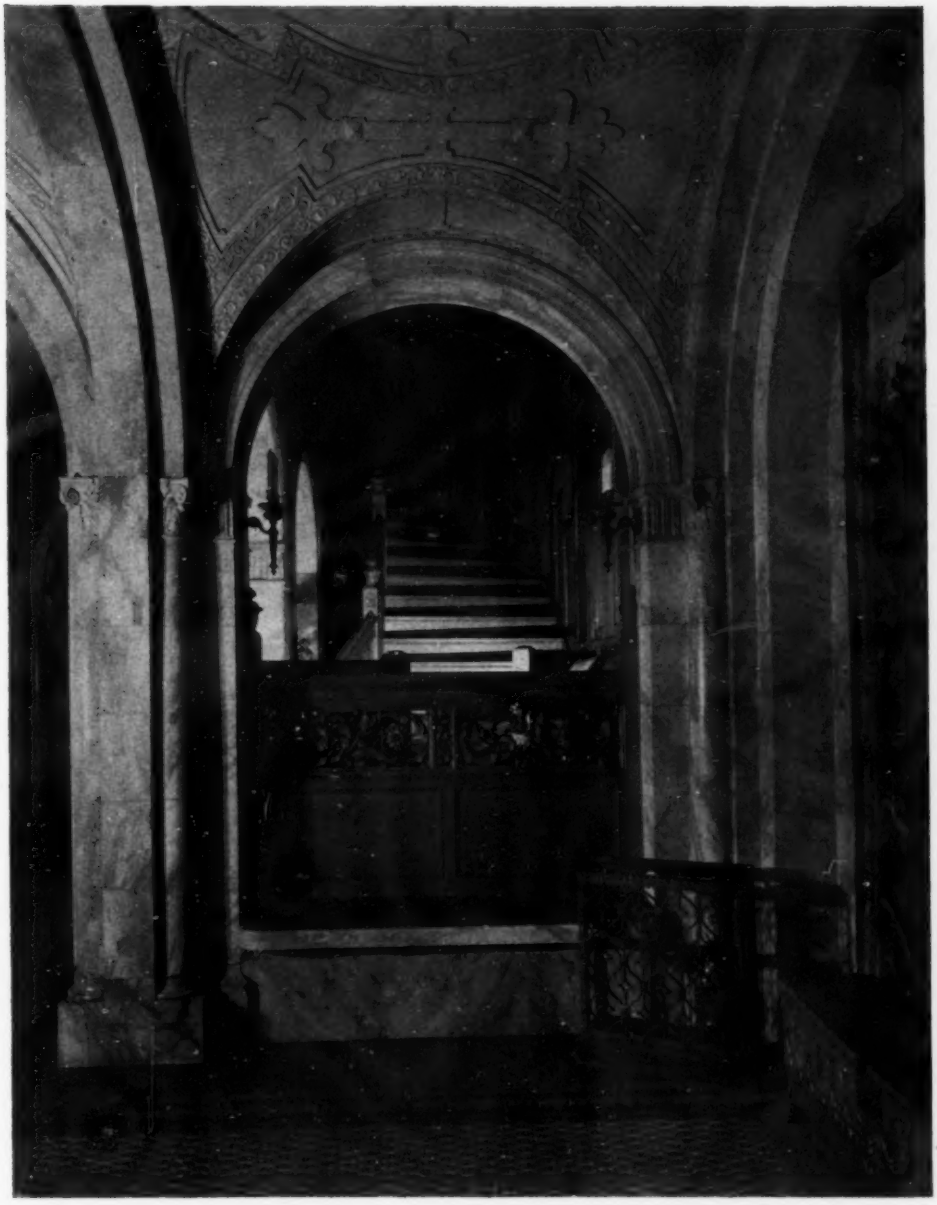

Stairway leading to second floor. (Photo by M. E. Hewitt.)

The new home of the American Institute of Physics is situated in what is known to real estate brokers as a protected area. All around it are developments which preclude the possibility of the neighborhood's becoming a blighted area for some time. Close by are Rockefeller Center, Fifth Avenue, Grand Central Station, Park Avenue, and Central Park, all guarantees of high land values in that section. All these developments have risen within the past one hundred years. Fifth Avenue which a century ago was called Middle Road above Forty-Second Street, has changed from country land, to fashionable residential street, to fashionable business avenue. Park Avenue which covers a double-deck railroad yard to a point near Fifty-Ninth Street did not become synonymous with luxury until after the first World War, when it was dis-

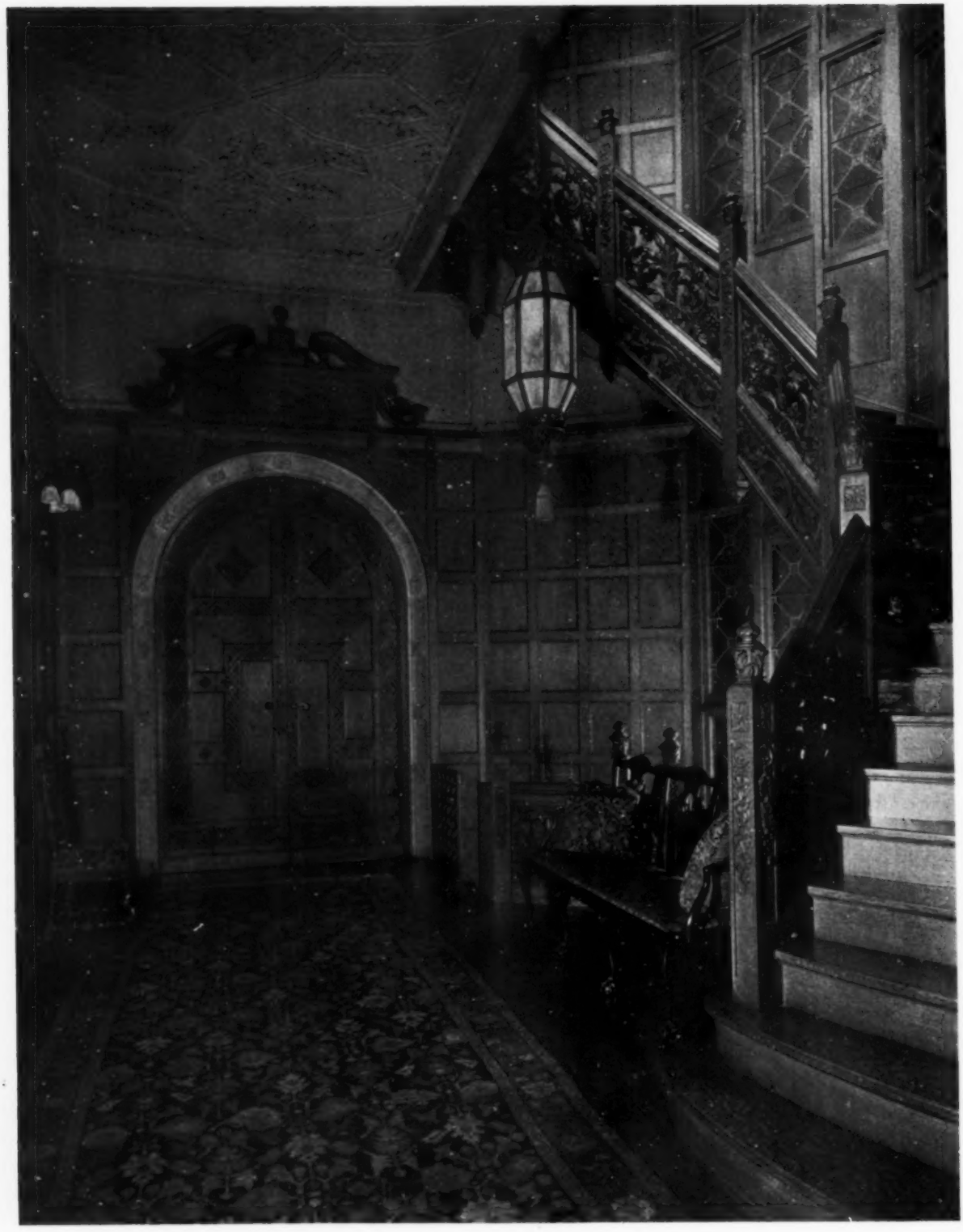

Staircase leading from second to third floors. (Photo by M. E. Hewitt.)

Typical third floor room which the late Mr. Erdmann used as a study. (Photo by M. E. Hewitt.)

covered that tall apartment buildings could be made free from vibration of railroads by anchoring them to the rocks far below the tracks. Rockefeller Center, begun in 1930 as an example of urban planning for the future, necessitated the tearing down of two hundred-odd buildings on its site. Grand Central Terminal was opened in 1871 in its present location, and Central Park has lent prestige to the north-central section of Manhattan since its construction in 1857. The house at 57 East 55th Street located close to the center of this favored area benefits by the proximity of these great investments. That section of Manhattan has been described as "a quarter of old mansions, air-conditioned apartments, exclusive clubs, luxurious hotels, fabulous penthouses; of great churches and museums; of art galleries, antique shops and specialty stores; of high priced cafes, cocktail lounges, night clubs."[7]

As the national headquarters for American Physicists, the former Erdmann Residence, after having been vacant for seven years, assumes a new and important role. With its distinguished past and promising future, it should remain an interesting and prominent landmark for many decades.

[7] Federal Writers Project, *New York City Guide*, page 233.

Frictional Phenomena. XVI

BY ANDREW GEMANT

The Detroit Edison Company, Detroit, Michigan

Chapter XVI. Technical Applications of External Friction of Solids

Abstract

THE following technical applications are dealt with in this chapter: (1) belt drives, (2) clutches, (3) brakes, (4) vibration dampers, such as the Lanchester damper, (5) self-excited vibrations, such as shaft whipping and sound production in a violin, and (6) grinding and crushing. In most cases a brief outline of the mechanism of operation is given, followed—in the first three of the above-mentioned applications—by principles of design, chief types of construction, and necessary numerical data on friction coefficients.

59. Belt Drives

In the application involving the belt drive as in the other cases of application that follow, the mechanical principles concerned will be discussed only briefly, the main point being to show how solid friction is utilized in these appliances.

The principle of a belt drive for power transmission is shown in the diagram, Fig. 150. The

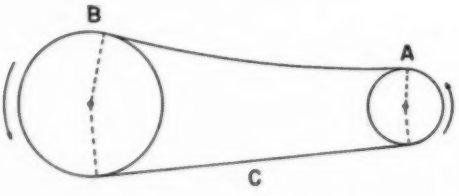

FIG. 150. Diagram of belt drive.

pulley A, called "driver pulley," is driven by a motor, not shown in the figure. The pulley B, called "driven pulley," is connected with a machine (not shown) to be driven by the motor. The connection between the two pulleys is established by means of the belt C.

When A rotates, the belt is carried along by means of friction forces active between the two surfaces. The belt originally has a certain tension when at rest, which is the same at every point. However, because of the frictional force acting on the belt when moving, the tension on the lower portion of the belt will be greater than that on the upper portion, the difference between the two tensions being identical with the frictional force. Because of this difference in tension the lower portion of the belt will be tighter than the upper portion. The former—characterized by its movement toward the driver pulley—is called the tight side of the belt, the latter—characterized by movement away from the driver pulley—is called the slack side.

The moving belt grips the driven pulley, again by means of friction active between them, and rotation of pulley B will be the result.

The power input or output W is then given by the equation:

$$W=\frac{(T_1-T_2)v}{33{,}000}, \qquad (171)$$

where T_1 = tension on the tight side, T_2 = tension on the slack side, in lb.; hence (T_1-T_2) = total frictional force, and v = velocity of surface of pulley in ft./min. W is then given in hp. In case of slip between the belt and one of the pulleys v for the two pulleys will differ. According to whether v measures the velocity of the driver or of the driven pulley, W from Eq. (171) will give the input or the output powers.

The power transmitted depends on two factors, v and (T_1-T_2). The first depends on the rotational speed and the diameter of the pulleys, both being limited by design considerations. High values of v are unwanted because the centrifugal force acting on the belt decreases its ability to transmit power by decreasing the normal pressure and, hence, the frictional force and because side-to-side riding and flapping of the belt result from high speeds. It follows that the frictional force has to be kept as large as is feasible. The maximum frictional force two

bodies can sustain without allowing slipping to take place—and slipping obviously limits the performance of the belt—is given by Eq. (167), the product of load times static friction coefficient. As the third section of the curve in Fig. 147 shows, this is the maximum obtainable frictional force. In our particular case the normal pressure P is represented by the tension of the belt.

The formula giving the maximum frictional force (T_1-T_2) as a function of T_1 can be found easily by means of Fig. 151. Here one of the

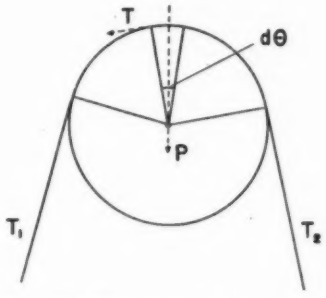

FIG. 151. Forces acting on pulley.

pulleys and part of the belt are shown diagrammatically. Consider an angle $d\theta$ of the circumference at the left side of which the belt-tension T has the direction shown. At the right side of the angle the tension (not shown in the figure) acts to the right. These two tensions differ by an amount dT, corresponding to the angle $d\theta$. The component of T in the radial direction, shown by P, is $T \sin (d\theta/2)$, or approximately $Td\theta/2$, and the same amount is added from the other side of $d\theta$, making a total of $Td\theta$, and this is the normal load P acting upon the arc $d\theta$. The difference in tension, corresponding to the arc $d\theta$, namely, dT, as mentioned above, originates from the frictional force over this portion of the surface. Substituting into Eq. (167), we obtain

$$dT=\mu T d\theta \tag{172}$$

and integrating over the total angle of contact θ between belt and pulley, we obtain

$$T_1/T_2=e^{\mu\theta} \tag{173}$$

or:

$$T_1-T_2=T_1(1-e^{-\mu\theta}) \tag{174}$$

in which the frictional force (T_1-T_2) is represented as a function of the maximum belt tension T_1. Equation (174) is analogous to (167), the expression in the bracket standing instead of μ.

Returning to Eq. (171), expressing the power that can be transmitted by a belt-pulley system, it is now seen that this power depends on the tension of the belt T_1, the friction coefficient μ, and the angle of contact θ.

As to the value of T_1, it is limited by the tensile strength of the belt material. Best leather belts have a strength of 4000 lb. per sq. in. and a minimum strength of 3000. Using a safety factor of 10, the working stress of belts is considered to be 300 lb. per sq. in. With b = width and t = thickness in inches of the belt T_1 will be limited by

$$T_1=300\ bt. \tag{175}$$

As to the angle of contact θ, its value changes with the ratio between diameters of the pulleys. If the two pulleys employed are different in size, which is usually the case, θ for the smaller pulley is less than 180° and that for the larger pulley is greater. In this case, according to Eq. (174), the smaller pulley will limit the frictional force because, as soon as this limit is reached, slipping between the belt and the smaller pulley will take place, and the frictional force cannot increase further. In order to increase θ on the smaller pulley, a third, so-called idler pulley (Fig. 152)

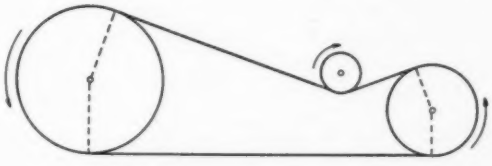

FIG. 152. Effect of idler on angle of contact.

is often connected between the two others. It can be seen from the figure how the idler, which is kept in position either by an additional weight or a spring, increases the angle on the smaller pulley to a value of around 230°. The idler should always be located at the slack side of the belt.

The value of the static friction coefficient is a further decisive factor that limits the power transmission: the higher the value of μ, the larger T_1-T_2, and, from Eq. (171), the larger the value of W. Table XXI gives the value of μ for various belt-pulley combinations.[1]

TABLE XXI. Friction coefficient μ, for various belt-pulley combinations.

Belt	Pulley					
	Steel, greasy	Steel, dry	Wood	Compressed paper	Leather	Rubber
Leather (oak tanned)	0.15	0.25	0.30	0.33	0.38	0.40
Leather (chrome tanned)	0.22	0.35	0.40	0.45	0.48	0.50
Canvas	0.12	0.20	0.23	0.25	0.27	0.30
Cotton	0.12	0.22	0.25	0.28	0.27	0.30
Rubber		0.30	0.32	0.35	0.40	0.42
Balata		0.32	0.35	0.38	0.40	0.42

It can be seen that leather and rubber, used both as belt and pulley-face materials, yield the highest coefficient, up to 0.50. Tanning with chromic acid yields better results than tanning with oak (chiefly digallic acid). Galloway[2] discusses improvements obtainable by reversing leather belts so that hair side comes in contact with pulleys. Burger[3] compares properties and proper treatments of belts made of various materials. Woven camel hair used as belt material also provides high friction coefficients.

A widely used method of increasing the effective friction coefficient of belts is the use of so-called V belts, shown in diagram in Fig. 153.

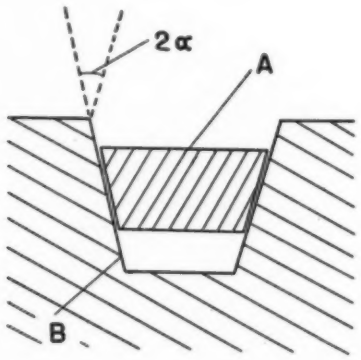

FIG. 153. Diagram of V belt and groove.

The belt A is pressed against the side walls of the groove B. It can be shown that the previous equations are valid if the effective coefficient μ_e is substituted for μ, μ_e being:

$$\mu_e = \mu/\sin\alpha, \tag{176}$$

where 2α is the groove angle. Nishihara and coworkers[4] investigated the fatigue properties of V belts. The dimensions of the grooves are standardized for various requirements.

As can be seen from the figures given, the coefficient μ does not allow a wide variation of the frictional force. In practice a more important factor is the width and thickness of the belt, as evidenced by Eq. (175). With increasing belt dimensions the pulley dimensions also must be increased; otherwise the limited flexibility of the belt would cause a dangerous drop of the contact angle θ. These considerations have led to standardized belt and pulley dimensions which must be consulted in designing belt drives.

Finally it should be added that, apart from the friction coefficient, the elastic modulus of the belt material also has to be considered. Even if conditions are such that no slippage of the belt over the pulley should take place, a small amount of slippage is unavoidable, owing to the elasticity of the belt material. This will result in a small difference in the velocities v of the driving and driven pulleys and, according to Eq. (171), the input power will be slightly higher than the output power. The efficiency of the transmission (ratio of output to input) is given by the formula

$$1-(T_1-T_2)btE \tag{177}$$

with E = Young's modulus and b and t the same as in Eq. (175). The loss in efficiency is of the order of 1 to 2 percent. Jagger and Sykes,[5] investigating this point, found an efficiency less than that obtainable from (177).

60. *Clutches*

Clutches, used for coupling the shaft of a driving machine to that of a driven machine, are frequently built upon the friction principle, in automobiles, for instance. A brief description of this mechanism should further illustrate the technical usage of external friction.

A disk clutch is shown diagrammatically in Fig. 154. A is the driving and B the driven shaft. A pair of friction disks C, made of suitable material, are mounted on the plate D, rigidly fixed to the driving shaft, and on the plate E, the latter being free to move along the driven shaft in opposition to the spring F. Normally, during driving, the clutch faces touch, owing to a certain pressure exerted by the spring, and during

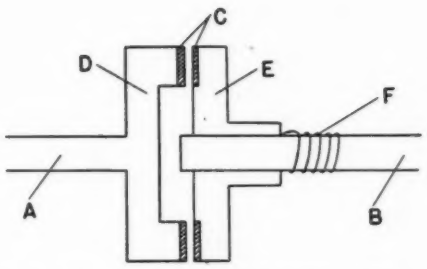

FIG. 154. Diagram of plate friction clutch.

disengagement the plate E is moved away from D by some mechanical device.

If the total pressure exerted upon the clutch is P, then the frictional force acting in a tangential direction during rotation is μP, and the friction torque is

$$T = \mu P r_m, \tag{178}$$

where r_m = mean radius of the circular disk.

The clutch is so designed that normally the two faces adhere to each other, without a relative motion taking place. In this case the friction force may assume any value up to the static friction value as a maximum. During the engagement period the resistance to motion of shaft B usually causes the clutch faces to slide against each other. This slippage, in its turn, causes μ to decrease [see Section 58 (2)] to a value less than the maximum.

With respect to the three factors in Eq. (178), which determine the torque and hence the power to be transmitted, r_m will be limited by space considerations, μ by the material chosen for the clutch face and its condition (whether dry or oily), and P by the spring pressure. The limiting factor in this latter value will be determined by the wearing properties of the face material in the following manner.

In Section 59 (2) abrasion as an accompanying process in friction was considered. The chipping off of protuberances is part of the total work spent when two surfaces slide against each other. Without a detailed knowledge of the mechanism of abrasion (see also Section 64) it is customary to assume the rate of wear w as being proportional to the total frictional work:

$$w = k\mu P v \tag{179}$$

(v = slipping velocity, k = constant). Wear will take place during the engagement periods which are characterized by a finite slipping velocity and, in order to keep its value low, P also will have to be kept at a low value.

Experience has shown the safe pressure values for the different clutch facings. Table XXII[1]

TABLE XXII. Friction coefficient and working pressure for clutch and brake-facing material.

Material	Friction coefficient		Pressure, lb. per sq. in.
	dry	oily	
Steel on cast iron	0.30	0.10	40–60
Leather on cast iron	0.50	0.15	10–12
Cork on cast iron	0.35	0.30	1– 2
Wood on cast iron	0.30	—	25–50
Asbestos on asbestos	0.40	0.25	30–60

contains both friction coefficients and tolerable pressures for a number of facing materials.

In the following paragraphs a few of the most frequent clutch types are summarized.

In recent years the *plate* or *disk* clutch (Fig. 154) is usually of the multiple-disk type, there being several pairs of friction surfaces, arranged somewhat similarly to opposite plates in electrical condensers. By this means the total torque is multiplied, although radius of clutch and pressure are not increased.

The theory of the disk clutch is based on the plausible assumption that wear must be uniform over the whole area. If at any point of the area wear is less than elsewhere, the pressure at this point is automatically increased because of the protruding surface, and the wear becomes equalized. Since the velocity at any point is proportional to the radius, Eq. (179) will yield

$$w = k\mu p v_0 r, \tag{180}$$

with w = local wear rate, p = local unit pressure, v_0 = angular velocity. Should w be constant over the area, then p must satisfy the condition:

$$p = K/r \tag{181}$$

with K = constant. This relation is automatically maintained owing to the condition of uniform wear.

From (181) and integration over the whole area bounded by the outer radius r_0 and the inner radius r_i of the circular disk, one obtains

$$P = 2\pi K(r_0 - r_i). \tag{182}$$

The total torque also can be obtained by an integration over the whole area with the result

$$T=\pi\mu K(r_0^2-r_i^2). \tag{183}$$

If Eq. (178) is then used for design calculations, r_m must be given the value

$$r_m=(r_0+r_i)/2, \tag{184}$$

an equation that follows if (182) and (183) are substituted into (178).

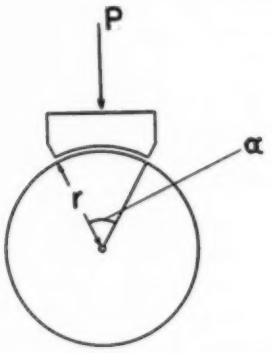

FIG. 155. Diagram of block clutch.

A *cone* clutch is essentially similar to the plate clutch with the difference that the faces are conical instead of plane. It requires a smaller pressure to produce a given torque than the plate clutch. This is because the total normal pressure is $1/\sin\alpha$ times larger than the axial force P_a if α is the angle between a cone element and the axis. Consequently one has instead of Eq. (178)

$$T=\mu P_a r_m/\sin\alpha. \tag{185}$$

A *block* clutch consists of one or several blocks that are pressed against the outer surface of a cylinder, the latter being coaxial with the shaft. Figure 155 shows in diagram one block pressed against the cylinder. An equation such as (178) is approximately valid for this case, too, if r_m is replaced by r, the radius of the cylinder. When the angle of contact, α, is large, the equation has to be modified, because the unit pressure is less near the edges of the block than near the center. The pressure distribution is calculated on the basis that wear in the direction of the applied force is uniform. This assumption is reasonable, since it implies tight fit of block and cylinder at all points. From this characteristic of the wear the pressure distribution is known, and by integration over the contact area both the total pressure P and the torque T are computed. The two equations then yield the relation:

$$T=\frac{4\mu Pr\sin(\alpha/2)}{\alpha+\sin\alpha}. \tag{186}$$

It can be seen that for small values of α the equation is reduced to the form of (178).

In addition, the *expanding ring* clutch, in which a ring inside a hollow cylinder is forced by expansion against the inner wall of the cylinder, should be mentioned. The inner ring consists either of two separate sections or of a single piece, in which latter case its elastic resistance against stretching has to be considered for design purposes. The *band* clutch consists essentially of a flexible steel band that is pulled tight against the outer wall of a drum. In all these various designs the basic principle by means of which external friction is utilized for coupling two members of a machine is the same.

For further details the reader is referred to the technical literature. Fundamental principles and various designs are dealt with by Rutledge.[6] Humphrey[7] discusses industrial friction clutches and the care and maintenance of them. A paper by Stubbings[8] deals with various clutch types and characteristics.

61. Brakes

As a third mechanical appliance utilizing external friction, a brief discussion of brakes, in particular automobile brakes, will be given. Figure 156 is a diagram of the simplest type of

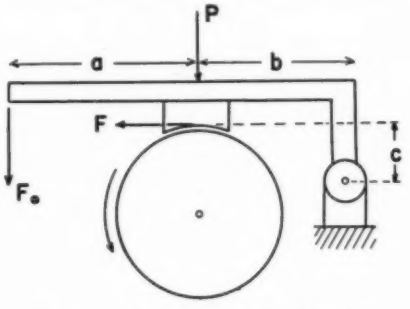

FIG. 156. Diagram of block brake.

brake: the block brake. It has essentially the same mechanism as that of a block clutch but its purpose is different. While the clutch makes

part of a machine run by connecting this part to the generator, the brake makes a running part of the machine stop or slow down. A relative motion between the two surfaces of a brake takes place during the whole braking action, with the result that considerable heat is generated. The temperature resistance of the facing material is just as important in this case as are the friction coefficient and the wearing property.

If the force F_0 is applied to the brake rod, the normal pressure P is exerted between the block and the drum of the wheel. Thereby, because of the lever action:

$$F_0=(b/(a+b))P. \qquad (187)$$

The friction force then retards the rotation of the drum, the torque being given by the same equation (Eq. 186) as that which applies for clutches.

One peculiar action, called self-application, and often encountered with certain types of brakes, can be seen from the diagram. The frictional force, as always, acts in a direction opposing the relative speed; thus, with respect to the drum, toward the right, and, with respect to the block, toward the left. This force F produces a moment Fc about the fulcrum, acting in an anticlockwise direction. It can be seen that this moment increases the pressure P acting on the brake block, again increasing the moment, and so on. Hence the slightest pressure P will be increased automatically until the drum stops. In certain cases, as mentioned, use is made of such automatic action. Since the latter depends upon the magnitude of the brake arm c, the action can be eliminated by making the length of this arm zero.

The torque produced by a brake will be proportional to μ, the friction coefficient, and the unit pressure. The latter is limited by the allowable wear. Design figures for brake facings can be taken from Table XXII as given in the previous section for clutches. Besides, Figs. 157 and 158 (after Vallance) show the coefficient μ for woven and molded facings as a function of sliding speed and pressure. There is a slight decrease with speed in keeping with what was said in Section 58 (2). Although μ is usually found to be independent of the pressure [Section 58 (1)], the data given here indicate a slow decrease with increasing pressure.

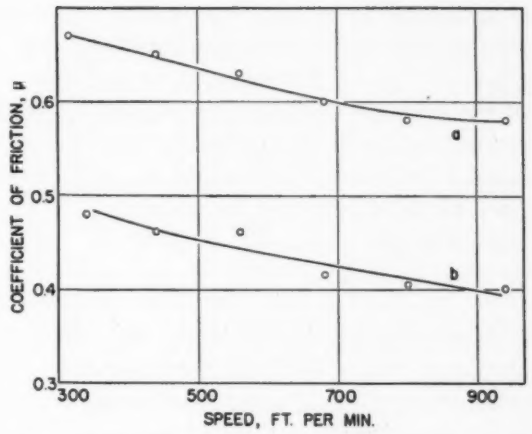

FIG. 157. Coefficient of friction *vs.* sliding speed for brake-lining materials at 50 lb. per sq. in. pressure; a = woven, b = molded material (after Vallance).

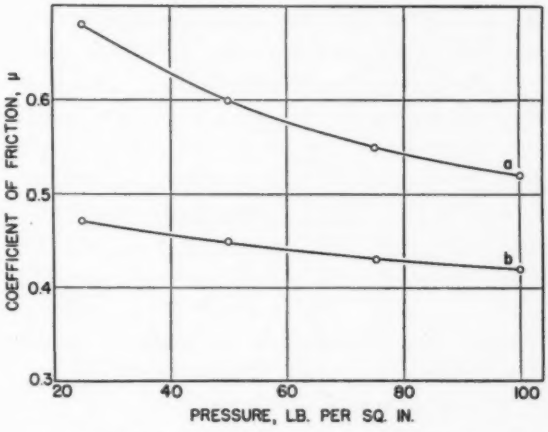

FIG. 158. Coefficient of friction *vs.* pressure for brake-lining materials at a speed of 630 ft. per min.; a = woven, b = molded material (after Vallance).

A further essential design factor, as stated, is the temperature resistance of the facing. The heat generating rate is given by

$$H=1.28\times10^{-3}\mu Spv \text{ B.t.u./min.}, \qquad (188)$$

if p is expressed in lb. per sq. in., S (area) in sq. in., and v in ft. per min. Obviously the effect of heat will have to be considered chiefly for those types of brakes that operate nearly continuously, as with mine hoists and the like. In cases of intermittent operation, as with automobiles, this point is of less importance.

Since the product pv is decisive with regard to the heat generated, its value should not exceed

certain limits. This limit varies from 20,000 to 80,000, increasing with decreasing frequency of operation and with increasing heat radiation.

In machines of nearly continuous brake operation the power W of the machine is transferred by the brake into heat. If q is the so-called load factor, being the ratio of the time of brake operation to the period of a cycle, then

$$H=42qW \text{ B.t.u./min.}, \tag{189}$$

if W is expressed in hp. This heat will raise the temperature of the facings, until the heat dissipated equals that of the heat generated. The heat dissipated H' is given by

$$H'=ktS, \tag{190}$$

where k = radiation factor, t = temperature difference in deg. F between the brake and surroundings, and S = total free surface in sq. in. The value of the constant k in Eq. (190) is 6 to 9×10^{-4} B.t.u. per sq. in. per F per min. Equating (189) and (190), the surface required to keep the temperature below certain specified limits, which depends upon the heat resistance of the brake material, is obtained. This limit is 150°F for leather or wood, and 350°F for asbestos on cast iron.

Among the different brake types, the *block* brake has already been discussed. A brief description of two further types follows.

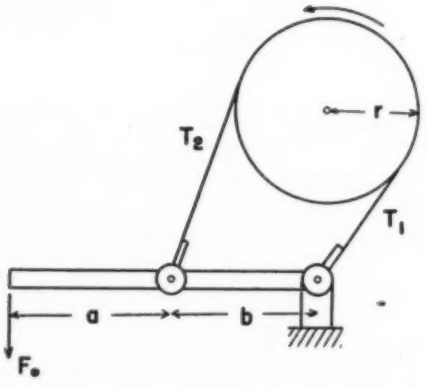

FIG. 159. Diagram of band brake.

The *band brake* is shown in Fig. 159. It consists of a belt or metal band that is pulled tight around the drum by applying the force F_0. The tension of the band is different for the two sides, Eq. (173) applying for this case, too. Hence, with rotation of the drum as shown, the left side has the smaller tension and the force F_0 is given by

$$F_0=(b/(a+b))T_2.$$

In case the drum should rotate in the opposite direction, the larger of the two band tensions would have to be compensated by the applied external force.

The band width required is given by the maximum safe working pressure p_{max} (see Table XXII) of the facing material. In Section 59 it was shown that the radial pressure acting upon the angle $d\theta$ of the circumference is

$$P=T_1 d\theta$$

as applied to the high tension side of the band. Writing dl/r (arc by radius) for $d\theta$ and $p_{max}\cdot dl\cdot b$ for P (b = width), one obtains:

$$b=T_1/rp_{max}.$$

The *internal shoe brake* as used in automobiles is sketched in Fig. 160. The external force F_0

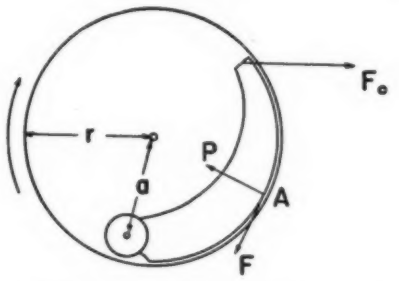

FIG. 160. Diagram of internal shoe brake.

acting upon the shoe presses the latter against the inner surface of the drum. The pressure P of the drum acting on the shoe is shown at the point A of the latter. The friction force acting on the shoe at the same point is shown as F. The three corresponding moments acting on the anchor pin of the shoe should be denoted by M_0, M_p, and M_f. The figure will show that M_f acts in the same direction as M_0, while M_p acts in the opposite direction. Thus

$$M_0+M_f=M_p. \tag{192}$$

Since the friction moment helps to lock the shoe, the construction is called self-energizing. In case M_f becomes equal to or larger than M_p, the external force becomes unnecessary for locking

and the brake will be self-locking. This action is obviously not wanted for automobiles, and this implies that the ratio M_f/M_p must be kept below unity. The ratio depends on the value of the friction coefficient (Table XXII), on the distance a of anchor pin and drum center, and on the angle of contact θ. It is given by $(\mu/2a)$ times a certain function of r and θ. These four quantities have to be designed in such a manner as to make the ratio M_f/M_p not larger than 0.7.

Concerning the technical literature on brakes, a paper by Taylor and Holt[9] on an automatic machine for measuring friction coefficients and wear of lining material should be mentioned. A brake-testing laboratory for automobile and industrial friction material is described by Humphreys;[10] properties, performance, and testing of brake-drum material are dealt with by Smalley.[11]

62. Vibration Dampers

In Section 52 the damping of crank-shaft vibrations by means of internal friction was discussed. It was mentioned, however, that this contribution to damping is generally not large and that artificial devices, based on external friction, are frequently used. Here we illustrate this principle briefly by explaining the mechanism of the so-called Lanchester damper which is used to reduce the amplitude of torsional shaft vibrations.

Figure 161 shows a diagram of this device. A

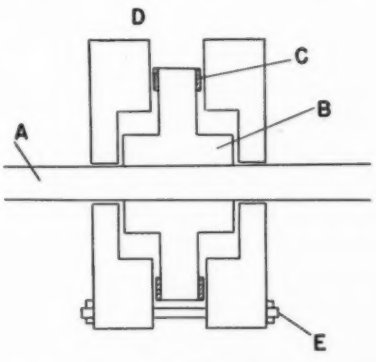

FIG. 161. Diagram of Lanchester damper.

is the shaft upon which is mounted rigidly the hub B, having brake linings C as shown. Two disks D are arranged so as to rotate freely by means of bearings not shown. The damper is attached to a part of the shaft that has a large torsional amplitude. With the aid of screws like E the pressure between the brake lining of the hub and the disks can be adjusted.

Concerning the constant rotation of the shaft, the disks will follow by means of the frictional torque, and any vibrational motion will simply be superimposed upon the steady motion of the disks.

It can be seen that there must be a medium range of frictional force (hence pressure between hub and disk) at which dissipation will be a maximum. For too small forces the slip between disk and hub during vibrations is considerable, but the frictional work is little. For too large forces the slip will be small; hence the frictional work again is little. It is obvious that some medium value for the slip is required for effective damping action. If the amplitude of the shaft (and the hub) is β_h, and that of the disk β_d, and if we have the relation

$$\beta_d = k\beta_h, \tag{193}$$

then a medium value (around 0.5) for k will give the best results. The amplitude of the relative motion is $(1-k)\beta_h$.

In order to bring about an amplitude β_d of the disk, a friction torque $M = Id^2\beta_d/dt^2$ is required, if I = inertia of the disks. If the motion is approximately sinusoidal, the second differential quotient is given by $\omega^2\beta_d$ ($\omega = 2\pi$ times frequency), hence

$$M = Ik\omega^2\beta_h. \tag{194}$$

The work dissipated per cycle is $4M(\beta_h - \beta_d)$, or

$$W = 4M(1-k)\beta_h, \tag{195}$$

an equation characteristic for dry friction in which the force (or torque) is approximately constant during the whole vibration. It was shown in Section 58 (2) that for not too high velocities the friction force is constant. Accordingly the work done during each quarter of a cycle is $M(1-k)\beta_h$, and four times this amount is the heat dissipated per cycle. Combining (194) with (195) one obtains:

$$W = 4k(1-k)I\omega^2\beta_h^2. \tag{196}$$

As has already been mentioned the numerical factor in Eq. (194) that gives the torque required for optimum dissipation is about 0.5. A more

rigorous computation[12] shows the correct factor to be 0.45. Similarly the numerical factor in (196) is $4k(1-k)$, or approximately 1.0. Again the more rigorous value of this factor is 1.27.

In other types of dampers liquid viscosity instead of external solid friction is utilized; such a type is described, for instance, by Wente and Mueller.[13]

63. *Self-Excited Vibrations*

In this section two cases of self-excited vibrations, as caused by external friction, will be described.

In Section 53 it was briefly explained how self-excitation takes place. An example, the whirl of rotating shafts as caused by internal friction, was discussed in some detail. Here an analogous case, so-called shaft whipping, due to external friction will be described. Here, as there, frictional forces act just like external forces, maintaining a vibrational motion. Because of the great simplicity of this case, it is particularly instructive.

Figure 162 shows the cross section of a shaft

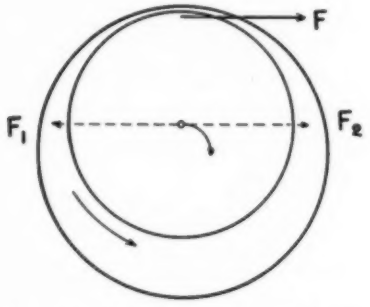

FIG. 162. Diagram of shaft whipping.

rotating anticlockwise in a loose bearing. If, for any reason, the shaft is thrown toward one side (here to the top), a frictional force F originates, acting to the right upon the shaft circumference. The effect of this force can be best seen by adding two opposite forces, both of magnitude F, acting on the center of the shaft. Forces F and F_1 form a couple that will retard the rotation of the shaft. Thus, this component of the friction force acts in the usual damping manner upon the original motion. The other component, F_2, however, will throw the shaft to the right along the bearing. Since the relation of shaft to bearing will remain essentially the same as the shaft is thrown to the right, the force F, its direction rotating, will whirl the shaft all along the wall in a clockwise direction. Hence, this component of the friction force acts as the driving force for a whipping motion. The power of maintaining it comes, of course, from the rotating motion of the shaft that has to be kept up by an external couple.

Such whipping might lead to trouble in practical cases. It is also observed on thrust bearings, resulting in a whirl of the collar. Flexible bearing supports that tend to prevent non-uniform pressures acting on the bearing, in spite of an angular deviation of the shaft, will prevent a whirl in this case.

The other case to be mentioned in this section is the setting up of vibrations by means of a unidirectional motion; the effect of the bow upon the violin string is a typical example. The fundamental process underlying the effect in question was discussed in detail in Section 59 (1), describing the stick-slip process. There is only little difference between the two cases. In Bowden's experiment the elastically supported body had a high natural frequency and was strongly damped. Each time a slip occurred, natural vibrations of a high frequency were introduced (visible in some of his oscillograms), which decayed rapidly while the next "stick" phase started.

The same process, however, with two factors changed, might lead to self-excited vibrations of constant amplitude. First the damping of the elastic body has to be low. Second the velocity of the continuous motion must be of the same order of magnitude as that of the oscillations of the vibrating body. If the velocity of the continuous motion is much smaller, as in Bowden's experiment, the relative speed between the two bodies is high, the frictional force is low, and no sticking takes place, until the natural vibrations have practically died out.

If, on the other hand, the two velocities are commensurate, then, as soon as the vibrating body moves in the same direction as the continuously moving body, the relative speed will be low, the friction force large, and sticking will take place. The stick-slip process as seen in Fig. 148, for instance, will then occur in the frequency of the natural vibrations of the elastic body.

The necessity of the two velocities being commensurate can also be deduced in the following manner with special reference to the violin. If t is the period of the stick-slip process, a the amplitude of the string, and v_b the velocity of the bow, then

$$a = tv_b.$$

If this process should merge with the oscillations of the string with frequency ν, then t must be of the order of $1/\nu$, thus:

$$a\nu \sim v_b.$$

But $a\nu$ is of the order of v_s, the vibrational velocity of the string, hence

$$v_s \sim v_b. \tag{197}$$

Vibrations known as chatter, such as that of the cutting tool of a lathe, are caused by a similar mechanism, also noises like the squeaking of doors. Liquid lubrication will eliminate these noises, replacing external friction by viscous forces that do not have a negative characteristic. The positive and the negative work done on the vibrating body during the two opposite phases of motion are then equal in magnitude; hence the total work done is zero and no vibration can build up.

64. *Grinding and Crushing*

In Section 59 (2) mention was made of wear that accompanies friction. This is an exception to the general rule that work against friction is used up as heat, because part of the work in this case is spent in the chipping off of particles or, what amounts to the same thing, into surface energy. There are chiefly two industrial applications that make use of such a process. One is the grinding of metals by means of abrasive cutting tools, and the other is the crushing of materials into smaller particles by means of rolls or balls.

Grinding consists of shaping an object (in technical language the "work") by means of abrasion of its surface in a controlled manner. The most usual tool is the grinding wheel the active surface of which is covered with finely graded abrasive grains, held together by a bond. This wheel is rotated against the object, a certain pressure acting between the two. Apart from a frictional force between the surfaces, the grains, which have sharp cutting edges, plough into the object to a small depth and cut out thin threadlike chips off the surface. This operation is carried out until the surface of the "work" attains the required shape. While the process is most important in the manufacture of metal objects, it is also extensively used with plastics.[14]

The abrasive grains used are brittle materials (high plastic flow resistance), having high mechanical strength and refractoriness. The materials most frequently used are feldspar, quartz, topaz, sapphire, and diamond.[15] All these have a large Young's modulus and large hardness numbers, 6 or more on Mohs' scale. Owing to the appreciable frictional forces the heat developed is considerable, so that the material may become red hot. These high temperatures are avoided by using copious amounts of coolants, either water or kerosene, yet it is essential that the abrasive used should be highly temperature-resistant. The bonding material is either of the silicate type or a plastic, rubber, or shellac. The bond must be sufficiently strong to hold the grains in position against the forces tending to dislodge them.

A complete theory that would allow the amount of work spent in producing the chips to be computed does not yet exist. Because of the importance of the problem, a few remarks indicating the way in which such a computation might be made will follow.

Figure 163 shows the mechanism of chip formation.[16] The grains have sharp cutting edges, often of triangular cross section, particularly if their orientation was promoted by electrification during the manufacture of the abrasive layer. Let us assume that the separation of neighboring grains is a cm, giving $1/a^2$ as the number of grains per cm^2.

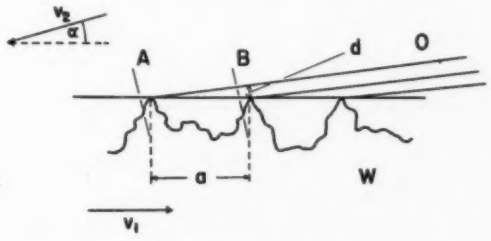

FIG. 163. Diagram of grinding of metal.

Although the grinding surface is usually cylindrical, and the object is too, in many cases, they can be represented diagrammatically as shown in the figure, where the lower portion W is the wheel with three neighboring grains having a separation a. The wheel rotates to the right with a tangential velocity v_1 and at the same time the object O moves relative to the wheel with a velocity v_2. This velocity is in a direction nearly parallel to v_1, differing from it by a small angle α. The object then has a velocity component towards the wheel of magnitude $v_2 \sin \alpha$. Because of this component each grain cuts into the surface of the object as shown by the slanting lines. Grain A will arrive at the point originally occupied by grain B after a time approximately a/v_1, valid for the usual case $v_1 \gg v_2$, and during this time the displacement of the object normal to the surface is

$$d = (av_2/v_1) \sin \alpha. \tag{198}$$

This distance is the cutting depth of the grains. It is plausible to assume that the chips will be threads of thickness of the order d. Microphotographs verify the threadlike shape of the chips.

The theory should proceed from here on, and lead to the computation of the force opposing the chipping off of particles. If the process of chip formation were an abrupt one, like failure under shearing or tensile stresses, then one might compute that force on the basis of the shearing strength and the known or assumed geometry of chips. Unfortunately this assumption is far from the reality. Chip formation is a process in which plastic flow plays an essential role, making a calculation as just suggested rather illusory. Several authors have set up various theories,[16] assuming, for instance, that the force each grain has to overcome is proportional to d^2 or d, but none of these can be considered as satisfactory.

The second application under consideration offers better possibilities for analysis. This is the *crushing* or pulverizing of materials. While in the previous procedure the cutting effect of abrasive was utilized, it is by applying pressure and consecutive compression that a subdivision of the material is accomplished in the present case. Here again, both frictional forces have to be overcome and free surface energies are produced. This latter process is effected by rupture under shearing conditions, so our analysis of the two forces in question is relatively simple.

Failure through shear occurs under a so-called angle of rupture, θ (Fig. 164), as shown on a

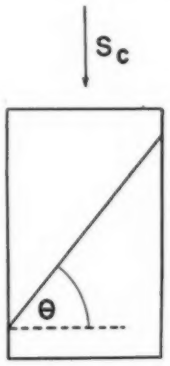

FIG. 164. Diagram of angle of rupture in crushing.

specimen of unit cross section under compression.[17] It is assumed that the pressure is S_c, the so-called crushing strength. Its component in the plane of gliding, which forms the angle θ with the horizontal, is $S_c \sin \theta$. This force must overcome both the shearing strength and the static frictional force. Let the shearing strength of the material be S_s; then the total strength over the plane of rupture is $S_s/\cos \theta$. The normal force on the plane is $S_c \cos \theta$ and the frictional force is $\mu S_c \cos \theta$. Hence

$$S_c \sin \theta = S_s/\cos \theta + \mu S_c \cos \theta. \tag{199}$$

Since S_s and μ are constants of the material, the relation shows the crushing strength as a function of θ. Obviously rupture will take place under an angle that corresponds to the smallest crushing force. Forming the differential quotient $dS_c/d\theta$ and equating to zero, an equation for θ is obtained. The result is

$$\theta = 0.5 \cot^{-1} (-\mu). \tag{200}$$

With a negligible frictional coefficient θ becomes 45°, the angle increasing with increasing μ.

Equation (200) was proved experimentally on a number of materials. For limestone, for instance, μ is 0.66 and the angle of rupture, computed from (200), is 61.7°. The observed angle of rupture is 62.2°. The assumption underlying Eq. (199), namely, that the two force components

act simultaneously, is somewhat hypothetical; the validity of Eq. (200) depends upon the correctness of this hypothesis.

The ratio of the frictional force to the force opposing rupture is, from Eq. (199) and (200),

$$\mu(1/(1+\mu^2))^{\frac{1}{2}}, \qquad (201)$$

indicating that the two forces are of the same order. In order to crush a material, the pressures must be of the same magnitude as the shearing forces, hence the frictional force is also of the same order as the shearing strength.

A different answer is obtained, however, if one asks for the *energy* expenditure for producing the new surfaces (overcoming the shearing strength) and for the production of frictional heat. The forces are equal, but the paths along which they are acting are very different. When the material fails, the shearing strength acts along molecular distances only. After the material is disrupted, the shearing force is used only for acceleration of the parts, the acquired kinetic energy being ultimately transformed into heat. The kinetic friction force, on the other hand, even if numerically less than the static, acts along the macroscopic path of gliding and produces heat during this process.

The correctness of this view is to be seen by looking into the numerical values of crushing strength. Take an average value such as 40,000 lb. per sq. in., or around 3.0×10^9 dynes per cm^2. Acting along the molecular distance of, say, $5A$, a work of 150 ergs is expended, and this figure is of the order of the surface energy per cm^2 of solids.

In writing down the energy balance for this case, therefore, it is found that only a small fraction of the work is actually used for a subdivision of the material, the largest part of the work being transformed into heat.

In closing this chapter, a recent application of external friction toward increasing the damping and eliminating chatter of electric relays should be mentioned, an idea exploited by the Westinghouse Electric Company. Parts are made hollow and partly filled with powder that will move about much in the same manner as the balls in a grinding mill. This mechanism has a damping effect, similar to that caused by internal friction of parts.

Bibliography for Chapter XVI

1. A. Vallance, *Design of Machine Members* (McGraw-Hill, New York, 1938).
2. D. F. Galloway, J. Inst. Prod. Eng. **20**, 139 (1941).
3. W. Burger, Fördertechnik **33**, 22 (1940).
4. T. Nishihara *et al.*, Trans. Soc. Mech. Eng. Japan **5**, 31 (1939).
5. J. G. Jagger and F. Sykes, J. Inst. Mech. Eng. **143**, 318 (1940).
6. L. T. Rutledge, Can. Mach. News **50**, 15 (1939).
7. K. B. Humphrey, Mill and Factory **26**, 67 (1940).
8. G. W. Stubbings, Mech. World **109**, 12 (1941).
9. R. H. Taylor and W. L. Holt, J. Research Nat. Bur. Stand. **24**, 531 (1940).
10. H. H. Humphreys, Roads and Bridges **79**, 89 (1941).
11. O. Smalley, Foundry Trade J. **64**, 387 (1941).
12. J. P. Den Hartog, *Mechanical Vibrations* (McGraw-Hill, New York, 1940).
13. E. C. Wente and A. H. Mueller, J. Soc. Mot. Pic. Eng. **37**, 406 (1941).
14. C. E. Holmes, Modern Plastics **20**, 76 (1942).
15. L. H. Milligan, Bull. Am. Ceram. Soc. **20**, 39 (1941).
16. A. H. Dall, Engineering **150**, 54 (1940).
17. M. O. Withey and J. Aston, *Materials of Construction* (Wiley, New York, 1939).

A Bibliography of Electron Microscopy

COMPILED BY

CLAIRE MARTON, *Division of Electron Optics, Stanford University, Stanford University, California*

AND

SAMUEL SASS, *In Charge of Physics and Astronomy Libraries, University of Michigan, Ann Arbor, Michigan*

THE first ten years of the development of electron microscopy being over, it seems worth while to look back and assemble the publications in this particular field. In every new field which is growing rapidly, there is very keen competition not only among different countries but often among laboratories located in the same country. As a consequence, it often happens that accounts of the development become decidedly one-sided, forgetting completely to mention what other groups or individuals accomplished in the same field.

This bibliography is an attempt to present the field as completely and impartially as possible. Due to wartime conditions, the desired completeness may not have been achieved and we invite, therefore, the users of this bibliography to notify us of any omissions. The bibliography contains only those papers which were published in scientific periodicals; semi-scientific and popular accounts have been omitted. Of papers dealing with general electron optics only those are included which have a direct bearing on electron microscopy.

The material is arranged in eight categories:

1. Books
2. Emission Microscopy
3. Transmission Type Microscope
4. Optics of the Transmission Type Electron Microscope
5. Image Defects
6. Electron Speeds Above 100 kv
7. Different Related Instruments
8. Applications of the Transmission Type Microscope

Within each group the arrangement is chronological and within each year alphabetical by author and title. Titles of articles which appeared in languages other than English have been translated. The abbreviations of the names of journals are those used in Science Abstracts, Chemical Abstracts, and Index Medicus.

The generous assistance of Professor L. Marton, of the Division of Electron Optics, Stanford University, is gratefully acknowledged.

May 31, 1943.

Addendum: Since the closing date of this bibliography a number of publications appeared in this country and quite a number of papers published abroad, principally in Germany, came to our knowledge. Our intention is to bring the bibliography up to date by publishing an addition some time later.

I. BOOKS

Brüche, E. and Scherzer, O. *Geometrische Elektronenoptik.* J. Springer, Berlin, 1934.

Marton, L. *Le microscope electronique et ses applications;* suivi de: **Henriot, E.,** *L'optique electronique des systèmes centrés.* Revue d'Optique, Paris, 1935.

Starks, H. J. H. The electron microscope. *Reports on progress in physics,* **2**, 283–291. Physical Society of London, 1935.

Brüche, E. and Henneberg, W. Geometrische Elektronenoptik. *Ergebnisse der exakten Naturwissenschaften* **15**, 365–421. J. Springer, Berlin, 1936.

Busch, H. and Brüche, E. *Beiträge zur Elektronenoptik.* J. A. Barth, Leipzig, 1937.

Klemperer, O. *Electron optics.* Cambridge University Press, Cambridge, 1939.

Myers, L. M. *Electron optics.* Chapman and Hall, London, 1939.

Ardenne, M. von. *Elektronen Übermikroskopie.* J. Springer, Berlin, 1940.

AEG Forschungs-Institut. *Jahrbuch.* Sonderheft: Übermikroskop. J. Springer, Berlin, 1940.

Klemperer, O. Electron microscopes of high magnification. *Reports on progress in physics* **7**, 107–129. Physical Society of London, 1940.

Borries, B. von and Ruska, E. Microscopy of high resolving power by means of fast electrons. *Ergebnisse der exakten Naturwissenschaften* **19**, 237–322. J. Springer, Berlin, 1941.

Brüche, E. and Recknagel, A. *Elektronengeräte, Prinzipien und Systematik.* J. Springer, Berlin, 1941.

Anderson, T. F. The study of colloids with the electron microscope. In Kraemer, E. O., ed. *Advances in colloid science,* Vol. 1, pp. 353–390. Interscience, New York, 1942.

Burton, E. F. and Kohl, W. H. *The electron microscope.* Reinhold, New York, 1942.

Marton, L. The electron microscope in biology. *Annual review of biochemistry*, Vol. 12, pp. 587–614. Annual Reviews Inc., Stanford University.

II. EMISSION MICROSCOPY

Brüche, E. and Johannson, H. Cinematography of oxide cathodes using the electron microscope. *Ann. d. Physik* **15**, 145–166 (1932).

Brüche, E. and Johannson, H. New investigations of cathodes with the electron microscope. *Phys. Zeits.* **33**, 898–899 (1932).

Knoll, M., Houtermanns, F. G., and Schulze, E. Emission distribution at glow cathodes with the magnetic microscope. *Zeits. f. Physik* **78**, 340–362 (1932).

Brüche, E. and Johannson, H. Crystallographic investigations with the electron microscope. *Zeits f. techn. Physik* **14**, 487–488 (1933).

Brüche, E. Electron microscopical reproduction by means of photoelectric electrons. *Zeits. f. Physik* **86**, 448–450 (1933).

Johannson, H. Electron optical immersion objective. *Ann. d. Physik* **18**, 385–413 (1933).

Knoll, M. and Lubszinsky, G. Electron microscope pictures with secondary electrons. *Phys. Zeits.* **34**, 671–674 (1933).

Richter, E. F. Electron microscope observations of the migration of emitting material on oxide cathodes. *Zeits. f. Physik* **86**, 697–709 (1933).

Ruska, E. Formation of pictures of surfaces irradiated by electrons in the electron microscope. *Zeits. f. Physik* **83**, 492–497 (1933).

Benham, W. E. Demonstration of low voltage electron microscope using electrostatic focusing. *I. E. E., J.* **75**, 388–390 (1934).

Calbick, C. J. and Davisson, C. J. Electron microscope. *Phys. Rev.* **45**, 764 (1934).

Brüche, E. The electron microscope and its application in particular to the study of thin layers on metals. *Kolloid Zeits.* **69**, 389–394 (1934).

Brüche, E. and Knecht, W. Electron-optical observation of the transformation of iron at temperatures between 500° and 1000°C. *Zeits. f. techn. Physik* **15**, 461–463 (1934).

Brüche, E. and Knecht, W. Note on attaining high resolution with the electron optical immersion objective. *Zeits. f. Physik* **92**, 462–466 (1934).

Johannson, H. Immersion objective for electron microscopes. *Ann. d. Physik* **21**, 274–284 (1934).

Knecht, W. Combined light and electron microscope. *Ann. d. Physik* **20**, 161–182 (1934).

Brüche, E. The electron-optical image of structures and its interpretation in the emission ratio of barium nickel cathodes. *Zeits f. Physik* **98**, 77–107 (1935).

Brüche, E. and Knecht, W. Electron-optical observation of the α-γ transformation in iron. *Zeits. f. techn. Physik* **16**, 95–98 (1935).

Brüche, E. and Mahl, H. On the emission image of thoriated tungsten and thoriated molybdenum. I. *Zeits. f. techn. Physik* **16**, 623–627 (1935).

Dosse, J. and Knoll, M. Electron distribution at focus of x-ray tubes with electron microscope. *Arch. f. Elektrot.* **29**, 729–730 (1935).

Kemnitz, G., Knoll, M., and Walcher, W. Electron concentration by concave hot cathode surfaces with the electron microscope. *Zeits. f. Physik* **96**, 612–619 (1935).

Mahl, H. Electron-optical image formation with emitting wires. *Zeits. f. Physik* **98**, 321–322 (1935).

Schenk, D. Distribution of emission over a crystalline heated cathode. *Ann. d. Physik* **23**, 240–254 (1935).

Behne, R. Characteristics of the immersion objective for image formation with fast electrons. *Ann. d. Physik* **26**, 372–384 (1936).

Behne, R. Contribution to the knowledge of the electron-optical immersion lens, II. *Zeits. f. Physik* **101**, 521–526 (1936).

Behne, R. Photography of foils with the electron-optical immersion objective. *Ann. d. Physik* **26**, 385–397 (1936).

Brüche, E. and Mahl, H. On the emission image of thoriated tungsten and thoriated molybdenum, II. *Zeits. f. techn. Physik* **17**, 81–84 (1936).

Brüche, E. and Mahl, H. On the emission image of thoriated tungsten and thoriated molybdenum, III. *Zeits. f. techn. Physik* **17**, 262–266 (1936).

Heinze, W. and Wagener, S. The processes in the activation of oxide cathodes. *Zeits. f. techn. Physik* **17**, 645–653 (1936).

Mahl, H. Influence of oxygen on glow emission investigated by the electron microscope. *Zeits. f. techn. Physik* **17**, 653–656 (1936).

Burgers, W. G. Direct observation of structural changes at high temperature with the electron microscope. *Zeits. f. Metallkunde* **29**, 250–251 (1937).

Burgers, W. G. and van Amstel, J. J. A. P. Electron-optical observation of metal surfaces. Parts I and II. *Physica* **4**, 5–22 (1937).

McMillen, J. H. and Scott, G. H. A magnetic electron microscope of simple design. *Rev. Sci. Instruments* **8**, 288–290 (1937).

Burgers, W. G. and van Amstel, J. J. A. P. Electron-optical observation of the transition of α- into β-zirconium. *Nature* **141**, 330 (1938).

Mahl, H. Electron-optical examination of electronic and ionic emission of wires. *Zeits. f. Physik* **108**, 771–776 (1938).

Meschter, E. An electron microscope for studying thermal and secondary electron emission. *Rev. Sci. Instruments* **9**, 12–15 (1938).

Scott, G. H. and Packer, D. M. The localization of minerals in animal tissues by the electron microscope. *Science* **89**, 227–228 (1938).

Scott, G. H. and Packer, D. M. The electron microscope as an analytical tool for the localization of minerals in biological tissues. *Anat. Rec.* **74**, 17–30 (1939).

Scott, G. H. and Packer, D. M. An electron microscope study of magnesium and calcium in striated muscle. *Anat. Rec.* **74**, 31–46 (1939).

Scott, G. H. An electron microscope study of calcium and magnesium in smooth muscle. *Proc. Soc. Exp. Biol. and Med.* **45**, 30–31 (1940).

Fox, G. W. and Bailey, F. M. Measurement of cathode emission by use of the electron microscope. *Phys. Rev.* **59**, 174–178 (1941).

III. TRANSMISSION TYPE MICROSCOPE

Knoll, M. and Ruska, E. The electron microscope, *Zeits. f. Physik* **78**, 318–339 (1932).

Marton, L. and Nuyens, M. Geometrical electron optics. *Wis-én Natuurkundig Tijdschrift* **6**, 159–170 (1933).

Marton, L. Electron microscopy of biological objects. I. *Bull. Acad. Roy. de Belg., Cl. des Sciences* **20**, 439–446 (1934).

Ruska, E. Advances in building and performance of the magnetic electron microscope. *Zeits. f. Physik* **87**, 580–602 (1934).

Ruska, E. Magnetic objective for the electron microscope. *Zeits f. Physik* **89**, 90–128 (1934).

Sommerfeld, A. and Scherzer, O. Description of an electron microscope. *Munch. Med. Wochenschr.* **81**, 1859–1860 (1934).

Knoll, M. The electron microscope. *Zeits. f. Ärztl. Fortbild.* **32**, 644–678 (1935).

Marton, L. Electron microscopy of biological objects. III. *Bull. Acad. Roy. de Belg., Cl. des Sciences* **21**, 606–617 (1935).

Fritz, R. The electron microscope. *Rev. Gen. des Sciences* **47**, 338–342 (1936).

Martin, L. C., Whelpton, R. V., and Parnum, D. H. A new electron microscope. *Journ. Sci. Instruments* **14**, 14–24 (1937).

Borries, B. von and Ruska, E. Development and present efficiency of the electron microscope. *Wiss. Veröffent. Siemens-Werken* **17**, 99–106 (1938).

Nuttall, A. K. An electron microscope for high magnifications. *Metro-Vickers Gaz.* **17**, 256–259 (1938).

Ardenne, M. von. An electrostatic high voltage lens of short focal distance. *Naturwiss.* **27**, 614–615 (1939).

Ardenne, M. von. Single crystal fluorescent screens for supermicroscopy. *Zeits. f. techn. Physik* **20**, 235–239 (1939).

Borries, B. von and Ruska, E. Development and efficiency of the Siemens ultramicroscope. *Z. f. wiss. Mikroskop.* **56**, 317–333 (1939).

Borries, B. von and Ruska, E. An electron supermicroscope for research institutes. *Naturwiss.* **27**, 577–582 (1939).

Brüche, E. and Haagen, E. A new simple supermicroscope and its application to bacteriology. *Naturwiss.* **27**, 809–811 (1939).

Burton, E. F., Hillier, J., and Prebus, A. A report on the development of the electron microscope at Toronto. *Phys. Rev.* **56**, 1171–1172 (1939).

Mahl, H. The electrostatic electron microscope. *Zeits. f. techn. Physik* **20**, 316–317 (1939).

Martin, L. C. The electron microscope. *J. Roy. Microscop. Soc.* **59**, 217–231 (1939).

Martin, L. C., Parnum, D. H., and Speak, G. S. Report on experimental work on the development of the electron microscope. *J. Roy. Microscop. Soc.* **59**, 203–216 (1939).

Prebus, A. and Hillier, J. Construction of a magnetic electron microscope of high resolving power. *Canad. J. of Research* **17**, 49–63 (1939).

Ardenne, M. von. Results of a new electron ultramicroscope. *Naturwiss.* **28**, 113–127 (1940).

Ardenne, M. von. Stereo-ultramicroscopy with the universal electron microscope. *Naturwiss.* **28**, 248–252 (1940).

Ardenne, M. von. A universal electron microscope for bright field, dark field and stereoscopic use. *Zeits. f. Physik* **115**, 339–368 (1940).

Borries, B. von, and Ruska, E. The effect of the potential difference on the super-microscopic image. *Zeits. f. Physik* **116**, 249–256 (1940).

Kinder, E. and Pendzich, A. A new magnetic lens of short focal length. *Jahrbuch AEG-Forsch., Sonderheft, Übermikroskop* **7**, 23–26 (1940).

Kinder, E. A new high-potential ultramicroscope. *Zeits. f. techn. Physik* **21**, 222–223 (1940).

Mahl, H. The electrostatic electron ultramicroscope. *Jahrbuch AEG-Forsch., Sonderheft, Übermikroskop* **7**, 43–56 (1940).

Martin, L. C. Ultraviolet and electron microscopy. *Nature* **146**, 288–292 (1940).

Marton, L. A new electron microscope. *Phys. Rev.* **58**, 57–60 (1940).

O'Daniel, H. and Radczewski, O. E. Electron microscopy and electron-diffraction study on the same specimen of highly dispersed minerals. *Naturwiss.* **28**, 628–630 (1940).

Marton, L., Banca, M. C., and Bender, J. F. A new electron microscope. *RCA Rev.* **5**, 232–243 (1940).

Prebus, A. Improved pole piece construction of the objective lens of a magnetic electron microscope. *Canad. J. of Research* **18**, 175–177 (1940).

Ruska, E. Electron diffraction patterns recorded in the supermicroscope. *Wiss. Veröffentl. Siemens-Werken, Werkstoff-Sonderheft* 372–379 (1940).

Ruska, H. Supermicroscopy. *Ned. T. Natuurk.* **7**, 179–191 (1940).

Zworykin, V. K. An electron microscope for the research laboratory. *Science* **92**, 51–53 (1940).

Ardenne, M. von. Electron ultramicroscopy with accessory probe for production of electron diffraction diagrams with very limited field of view. *Zeits. f. Physik* **117**, 515–523 (1941).

Hillier, J. and Vance, A. W. Recent developments in the electron microscope. *Proc. Inst. Radio Engrs.* **29**, 167–176 (1941).

Hughes, A. L. The magnetic electron lens. *Amer. J. Phys.* **9**, 204–207 (1941).

Vance, A. W. Stable power supplies for electron microscopes. *RCA Rev.* **5**, 293–300 (1941).

Zworykin, V. K., Hillier, J., and Vance, A. W. An electron microscope for practical laboratory service. *Trans. Am. Inst. Elect. Engrs.* **60**, 157–162 (1941).

Ardenne, M. von, Schiebold, E., and Gunther, F. Fine beam electron diffraction in the universal electron microscope. *Zeits. f. Physik.* **119**, 352–365 (1942).

Ardenne, M. von. Further development of the universal electron microscope. *Phys. Zeits.* **43**, 11–15 (1942).

Bachman, C. H. and Ramo, S. Simplified electron microscope. *Phys. Rev.* **62**, 494 (1942).

Hillier, J., Baker, R. F., and Zworykin, V. K. A diffraction adapter for the electron microscope. *J. of Applied Physics* **13**, 571–577 (1942).

Bachman, C. H. and Ramo, S. Electrostatic electron microscopy. I. *J. of Applied Physics* **14**, 8–18 (1943).

Bachman, C. H. and Ramo, S. Electrostatic electron microscopy. II. *J. of Applied Physics* **14**, 69–76 (1943).

Bachman, C. H. and Ramo, S. Electrostatic electron microscopy. III. *J. of Applied Physics* **14**, 155–160 (1943).

Bachman, C. H. Simplified electron microscopy. *Electronics* **16**, 78–81; 195–200 (1943).

Zworykin, V. K. Electron microscope: most recent research tool. *Electronics* **16**, 146–147; 254 (1943).

IV. OPTICS OF THE TRANSMISSION TYPE ELECTRON MICROSCOPE

Davisson, C. J. and Calbick, C. J. Electron lenses. *Phys. Rev.* **38**, 585 (1931).

Davisson, C. J. and Calbick, C. J. Electron lenses, *Phys. Rev.* **42**, 580 (1932).

Knoll, M. and Ruska, E. Contribution to geometrical electron optics. I. *Ann. d. Physik* [5] **12**, 607–640 (1932).

Knoll, M. and Ruska, E. Contribution to geometrical electron optics. II. *Ann. d. Physik* [5] **12**, 641–661 (1932).

Ruska, E. and Knoll, M. The magnetic concentration coil for fast electrons. I. *Zeits. f. techn. Physik* **12**, 389–399 (1932).

Ruska, E. and Knoll, M. The magnetic concentration coil for fast electrons. II. *Zeits. f. techn. Physik* **12**, 448 (1932).

Henneberg, W. The resolving power of the electron microscope for transparent objects. *Zeits. f. Instrumentenk.* **55**, 300–305 (1935).

Stabenov, G. Magnetic electron lens without image rotation. *Zeits. f. Physik* **96**, 612–619 (1935).

Boersch, H. On the primary and secondary image in the electron microscope. I. *Ann. d. Physik* **26**, 631–644 (1936).

Boersch, H. On the primary and secondary image in the electron microscope. II. *Ann. d. Physik* **27**, 75–80 (1936).

Marton, L. Some considerations concerning the resolving power in electron microscopy. *Physica* **3**, 959–967 (1936).

Ardenne, M. von. The image errors of the electron microscope caused by electron scattering in the object and their relation to each other. *Zeits. f. Physik* **11**, 152–157 (1938).

Ardenne, M. von. Limits of the resolving power of the electron microscope. *Zeits. f. Physik* **108**, 308–338 (1938).

Borries, B. von, and Ruska, E. Image formation in the supermicroscope. *Zeits. f. techn. Physik* **19**, 402–407 (1938).

Ardenne, M. von. Chromatic errors in the electron microscopes. *Zeits. f. Physik* **113**, 257–259 (1939).

Ardenne, M. von. Intensity and resolving power of the electron microscope. *Zeits. f. Physik* **112**, 744–753 (1939).

Borries, B. von, and Ruska, E. Properties of the supermicroscopical image formation. *Naturwiss.* **27**, 281–287 (1939).

Borries, B. von, and Ruska, E. The resolving power of the supermicroscope. *Zeits. f. techn. Physik* **20**, 225–235 (1939).

Hillier, J. Effects of chromatic error on the electron microscope. *Canad. J. of Research*, **A17**, 64–69 (1939).

Ardenne, M. von. Determination of the resolving power of electron microscopes. *Phys. Zeits.* **42**, 72–74 (1941).

Ardenne, M. von. Testing of short focus electron lens. *Zeits. f. Physik* **117**, 602–611 (1941).

Hillier, J. A discussion of the fundamental limit of an electron microscope. *Phys. Rev.* **60**, 743–745 (1941).

Marton, L. and Schiff, L. I. Determination of object thickness in electron microscopy. *J. of Applied Physics* **12**, 759–765 (1941).

Ruska, E. Lenses for electron microscopes of high resolving power. *Archiv. f. Elektrotechn.* **36**, 431–454 (1942).

Schiff, L. I. Ultimate resolving power of the electron microscope. *Phys. Rev.* **61**, 721–722 (1942).

V. IMAGE DEFECTS

Busch, H. Calculation of the trajectory of cathode rays in electromagnetic fields of axial symmetry. *Ann. d. Physik* **81**, 974–993 (1926).

Busch, H. On the action of the concentration coil in Braun-tubes. *Arch. f. Elektrot.* **18**, 583–594 (1927).

Picht, J. Theory of geometrical optics for electrons. *Ann. d. Physik* **15**, 926–964 (1932).

Glaser, W. Geometrical optics of electron rays. *Zeits. f. Physik* **80**, 451–464 (1933).

Glaser, W. Geometrical electron optics of the axial symmetrical electromagnetic field. *Zeits. f. Physik* **81**, 647–686 (1933).

Glaser, W. Optical imagery by mechanical systems and the optics of nonhomogeneous isotropic media. *Ann. d. Physik* **18**, 557–586 (1933).

Glaser, W. Theory of the electron microscope. *Zeits. f. Physik* **83**, 104–122 (1933).

Johannson, H. and Scherzer, O. Electric electron condensing lens. *Zeits. f. Physik* **80**, 183–192 (1933).

Posener, L. Theory of the electron microscope. *Zeits f. Physik* **80**, 813–818 (1933).

Scherzer, O. Theory of electric electron condensing lenses. *Zeits. f. Physik* **80**, 193–202 (1933).

Diels, K. and Knoll, M. Proof of the aberrations of an electron lens by point imagery. *Zeits. f. techn. Physik* **16**, 621–623 (1935).

Glaser, W. Theory of image defects of an electron microscope. *Zeits. f. Physik* **97**, 171–201 (1935).

Wallauschek, R. and Bergmann, P. Theory of electron microscope using purely magnetic fields. *Zeits. f. Physik* **94**, 329–347 (1935).

Scherzer, O. On some defects of electron lenses. *Zeits. f. Physik* **101**, 593–603 (1936).

Scherzer, O. The weak electric single lens of least spherical aberration. *Zeits. f. Physik* **101**, 23–26 (1936).

Diels, K. and Wendt, G. Eight third-order aberrations of magnetic electron lenses. *Zeits. f. techn. Physik* **18**, 65–69 (1937).

Rebsch, R. and Schneider, W. Spherical aberration of weak electron lenses. *Zeits. f. Physik* **107**, 138–143 (1937).

Rogowski, W. Defects in electron images. *Arch. f. Elektrot.* **31**, 555–593 (1937).

Rebsch, R. Theoretical resolving power of the electron microscope. *Ann. d. Physik* **31**, 551–560 (1938).

Scherzer, O. The theoretically attainable resolving power of the electron microscope. *Zeits. f. Physik* **114**, 427–434 (1939).

Voit, H. Third-order electron-optical aberrations. *Zeits. f. Instrumentenk.* **59**, 71–82 (1939).

Glaser, W. Chromatic aberration in electron lenses. *Zeits. f. Physik* **116**, 56–67 (1940).

Glaser, W. On a magnetic field free from spherical aberration. *Zeits. f. Physik* **116**, 19–33 (1940).

Rebsch, W. and Glaser, W. Aperture error of electron lenses. *Zeits. f. Physik* **116**, 729–735 (1940).

Dosse, J. Optical constants of strong electron lenses. *Zeits. f. Physik* **117**, 722–753 (1941).

Dosse, J. Precise computation of unsymmetrical field form $H = H_0/1+(z/a)^2$. *Zeits. f. Physik* **117**, 316–321 (1941).

Glaser, W. Precise computation of magnetic lenses with the field form $H = H_0/1+(z/a)^2$. *Zeits. f. Physik* **117**, 285–315 (1941).

Kompfner, R. On a method of correcting the spherical error of electron lenses, especially those employed with electron microscopes. *Phil. Mag.* **32**, 410–416 (1941).

Recknagel, A. Theory of electrical electron microscope which is self-illuminating. *Zeits. f. Physik* **177**, 689–708 (1941).

Plass, G. N. Electrostatic electron lenses with a minimum of spherical aberration. *J. of Applied Physics* **13**, 49–55 (1942).

Ramberg, E. G. Variation of the axial aberrations of electron lenses with lens strength. *J. of Applied Physics* **13**, 582–594 (1942).

VI. ELECTRON SPEEDS ABOVE 100 KV

Marton, L. The electron microscope in biology. *Acta Union Internat. Contre Cancer* **4**, 221–238 (1939).

Ardenne, M. von. 200-kv universal electron microscope with an object screen. *Zeits. f. Physik* **117**, 657–688 (1941).

Müller, H. O. and Ruska, E. A supermicroscope for 220-kv beam potential. *Kolloid Zeits.* **95**, 21–25 (1941).

Zworykin, V. K., Hillier, J., and Vance, A. W. A preliminary report on the development of a 300-kv magnetic electron microscope. *J. of Applied Physics* **12**, 738–742 (1941).

VII. DIFFERENT RELATED INSTRUMENTS

Johnson, R. P. and Shockley, W. Investigation of thermionic filaments with a simple electron microscope. *Phys. Rev.* **48**, 973 (1935).

Wehnelt, A. and Schilling, W. Electron microscope examination of the electron emission of cold metals. *Zeits. f. Physik* **98**, 286–287 (1935).

Johnson, R. P. and Shockley, W. An electron microscope for filaments: emission and adsorption by tungsten single crystals. *Phys. Rev.* **49**, 436–440 (1936).

Muller, E. W. Electron microscopical observations of field emittors. *Zeits. f. Physik* **106**, 541–550 (1937).

Ardenne, M. von. The electron scanning microscope. *Zeits. f. techn. Physik* **19**, 407–416 (1938).

Ardenne, M. von. Electron scanning microscope—theoretical fundamentals. *Zeits. f. Physik* **109**, 553–573 (1938).

Johnson, R. P. Simple electron microscopes. *J. of Applied Physics* **9**, 508–516 (1938).

Boersch, H. The electron shadow microscope. I. *Zeits. f. techn. Physik* **20**, 346–350 (1939).

Zworykin, V. K., Hillier, J., and Snyder, R. L. A scanning electron microscope. *A. S. T. M. Bull.* **117**, 15–23 (1942).

VIII. APPLICATIONS OF THE TRANSMISSION TYPE MICROSCOPE

Borries, B. von, and Ruska, E. Images of films in transmission by means of the electron microscope. *Zeits. f. Physik* **83**, 187–193 (1933).

Marton, L. The electron microscope; first attempts at its application to biology. *Ann. et Bull. de la Soc. Roy. des Sciences Med. et Nat. de Bruxelles* [5–6] **92**, 106 (1934).

Marton, L. Electron microscopy of biological objects. *Phys. Rev.* **46**, 527–528 (1934).

Marton, L. Electron microscopy of biological objects. *Nature* **133**, 911 (1934).

Borries, B. von, and Ruska, E. Electron microscope and its uses. *V. D. I.* **79**, 519–524 (1935).

Driest, E. and Müller, H. O. Electron micrographs of chitin substances. *Z. f. wiss. Mikroskop.* **52**, 53–55 (1935).

Marton, L. The electron microscope and its applications. *Rev. d'Optique* **14**, 129–145 (1935).

Marton, L. The electron microscope and its applications especially in biology. *2ème Congrès Nat. d. Sciences, Bruxelles* **2**, 928–933, 1935.

Marton, L. Electron microscopy of biological objects. II. *Bull. Acad. Roy. de Belg., Cl. des Sciences* **21**, 553–564 (1935).

Saupe, E. Use of electron microscope and diffraction in biology and pathology. *Frankfurt. Z. f. Path.* **47**, 485–516 (1935).

Krause, F. Electron-optical pictures of diatoms with the magnetic electron microscope. *Zeits. f. Physik* **102**, 417–422 (1936).

Marton, L. The electron microscope. *Rev. Microbiol. Appl.* **3**, 117–124 (1936).

Marton, L. Electron microscopy of biological objects. IV. *Bull. Acad. Roy de Belg., Cl. des Sciences* **22**, 1336–1344 (1936).

Beischer, D. and Krause, F. Electron microscope in colloid investigations. *Naturwiss.* **25**, 825–829 (1937).

Krause, F. The electron microscope and its use in biology. *Naturwiss.* **25**, 817–825 (1937).

Luft, F. Practical uses of electron optics. *Röntgenpraxis* **9**, 384–394 (1937).

Marton, L. Electron microscopy of biological objects. V. *Bull. Acad. Roy. de Belg., Cl. des Sciences* **23**, 672–678 (1937).

Beischer, D. Determination of size of crystals in metal and metal oxide smokes by means of Röntgen- and electron-diffraction diagrams and electron photomicrographs. *Zeits. Elektrochem.* **44**, 375–385 (1938).

Borries, B. von, Ruska, E., and Ruska, H. Bacteria and virus as seen in the ultramicroscope, with introduction to technology of ultramicroscopy. *Klin. Wochenschr.* **17**, 921–925 (1938).

Borries, B. von, Ruska, E., and Ruska, H. Photographs of bacteria with the supermicroscope. *Wiss. Veröffent. Siemens-Werken* **17**, 107–111 (1938).

Borries, B. von, Ruska, E., and Ruska, H. Status of the supermicroscope. *V. D. I.* **82**, 937–941 (1938).

Eitel, W. H., Müller, H. O., and Radczewski, O. E. Examination of clay minerals with the ultramicroscope. *Ber. Deut. Keram. Ges.* **20**, 165–180 (1938).

Krause, F. Examination of viruses by the electron microscope. *Naturwiss.* **26**, 122 (1938).

Marton, L. A note on the article: "Practical uses of electron optics," by Fritz Luft. *Röntgenpraxis* **10**, 352–353 (1938).

Beischer, D. and Krause, F. The electron microscope in colloid chemistry. *Angew. Chem.* **51**, 331–334 (1938).

Ruchardt, E. New developments in electron microscopy and their results. *Münch. Med. Wochenschr.* **85**, 1832–1837 (1938).

Ardenne, M. von. Possibility of examining living substances with electron microscopes. *Zeits. f. techn. Physik* **20**, 239–242 (1939).

Frank, F. and Ruska, H. Examination of the bluestructure of bird feathers with the electron microscope. *Naturwiss.* **27**, 229–230 (1939).

Friess, H. and Müller, H. O. Smokes and dusts in the electron microscope. *Gasmaske* **11**, 1–9 (1939).

Kausche, G. A., Pfankuch, E., and Ruska, H. Examination of plant viruses with the high power electron microscope. *Naturwiss.* **27**, 292–299 (1939).

Kausche, G. A. and Ruska, H. The structure of the "crystalline aggregates" of tobacco mosaic virus proteins. *Biochem. Z.* **303**, 221–230 (1939).

Kausche, G. A. and Ruska, H. Supermicroscopic investigation of the adsorption of metal colloids on proteins. *Kolloid Zeits.* **89**, 21–26 (1939).

Krause, F. Use of the electron microscope in biology and medicine. *Arch. Exp. Zellforsch.* **22**, 668–672 (1939).

Marton, L. On the sensitivity of photographic emulsions for electrons between 50 and 100 kv. *Phys. Rev.* **56**, 290 (1939).

Müller, H. O. The supermicroscope in medicine. *Med. Klinik* **35**, 1041–1043 (1939).

Piekarski, G. and Ruska, H. Supermicroscopic pictures of bacterial flagellae. *Klin. Wochenschr.* **18**, 383–386 (1939).

Piekarski, G. and Ruska, H. Supermicroscopical investigations of bacteria with particular reference to the so-called nucleoids. *Arch. Mikrobiol.* **10**, 302–321 (1939).

Radczewski, O. E., Müller, H. O., and Eitel, W. The hydration of tricalcium aluminate. *Naturwiss.* **27**, 837–838 (1939).

Radczewski, O. E., Müller, H. O., and Eitel, W. Supermicroscopical investigation of the hydration of lime. *Zement* **28**, 693–697 (1939).

Radczewski, O. E., Müller, H. O., and Eitel, W. The hydration of tricalcium silicate. *Naturwiss.* **27**, 807 (1939).

Ruska, H. Supermicroscopic demonstration of organic structure. *Arch. Exp. Zellforsch.* **22**, 673–680 (1939).

Ruska, H., Borries, B. von, and Ruska, E. The importance of the supermicroscope in virus research. *Arch. Ges. Virusforsch.* **1**, 155 (1939).

Wolpers, C. and Ruska, H. Structural investigations of the clotting of blood. *Klin. Wochenschr.* **18**, 1077–1111 (1939).

Ardenne, M. von. Analysis of the structure of highly and very highly illuminated silver bromide grains with the universal electron microscope. *Z. Angew. Photogr.* **2**, 14–20 (1940).

Ardenne, M. von, and Beischer, D. Examination of the fine structure of high-molecular compounds with the universal electron microscope. I. The structure of β-polyoxymethylene crystals. *Zeits. f. phys. Chem.*, [B] **45**, 465–473 (1940).

Ardenne, M. von, and Beischer, D. Examination of the fine structure of high-molecular compounds with the universal electron microscope. II. The morphology of rubber and Buna. *Kautschuk* **16**, 55–60 (1940).

Ardenne, M. von, Endell, K., and Hoffmann, E. Examination of finest fractions of bentonite and cement with the universal electron microscope. *Ber. Deut. Keram. Ges.* **21**, 209–227 (1940).

Ardenne, M. von. Images of minute particles, especially of molecules, by means of the universal electron microscope. *Zeits. f. phys. Chem.* [A]**187**, 1–12 (1940).

Ardenne, M. von, and Beischer, D. Investigation of catalysts with the universal electron microscope. *Angew. Chem.* **53**, 103–107 (1940).

Ardenne, M. von, and Beischer, D. Investigation of metal oxide smokes with the universal electron microscope. *Zeits. Elektrochem.* **46**, 270–277 (1940).

Ardenne, M. von. Occurrence of black lines in electron microscope images of crystal lamellae. *Zeits. f. Physik* **116**, 736–738 (1940).

Ardenne, M. von. Stage vibrator for electron microscopes. *Kolloid Zeits.* **93**, 158–163 (1940).

Borries, B. von, and Kausche, G. A. Determination of the size and shape distribution of colloidal gold by means of the supermicroscope. *Kolloid Zeits.* **90**, 132–141 (1940).

Borries, B. von, and Ruttmann, W. Metallographic investigations of steel, cast iron, and brass by means of the supermicroscope. *Wiss. Veröffentl. Siemens-Werken, Werkstoff-Sonderheft* 342–362 (1940).

Borries, B. von. Higher resolving power at the formation of images of surfaces by the supermicroscope. *Zeits. f. Physik* **116**, 370–378 (1940).

Burton, E. F., Hillier, J., and Prebus, A. Contribution of the electron microscope to medicine. *Canad. M. A. Jour.* **42**, 116–119 (1940).

Columbian Carbon Company Research Laboratories. The particle size and shape of colloidal carbon as revealed by the electron microscope. *Columbian Colloidal Carbons* **2**, 5–53 (1940).

Eitel, W. and Schusterius, C. The determination of the efficient surfaces of clay particles with the supermicroscope. *Chem. Erde* **13**, 322–335 (1940).

Eitel, W. and Schusterius, C. The interpretation of electron microscope pictures for the determination of clay grain distribution. *Naturwiss.* **28**, 300–303 (1940).

Eitel, W. and Radczewski, O. E. The characteristics of the clay mineral montmorillonite as shown by the supermicroscope. *Naturwiss.* **28**, 397–399 (1940).

Eitel, W. and Gotthardt, E. Stereophotographic measurement of the thickness of very small crystals by electron microscope observation. *Naturwiss.* **28**, 367 (1940).

Frühbrodt, E. and Ruska, H. Research on the structure of bacteria, especially of bacterium membranes and capsules. *Arch. Mikrobiol.* **11**, 137–154 (1940).

Husemann, E. and Ruska, H. Making glycogen molecules visible. *J. Prakt. Chem.* **156**, 1–10 (1940).

Husemann, E. and Ruska, H. Making visible the molecules of *p*-iodobenzoyl-glycogen. *Naturwiss.* **28**, 534 (1940).

Jakob, A. and Mahl, H. Application of the supermicroscope in bacteriology, especially for experiments with capsules. *Jahrbuch AEG-Forsch., Sonderheft, Übermikroskop* **7**, 77–87 (1940).

Jakob, A. and Mahl, H. Structure of bacteria, in particular capsulation of anaerobiae by means of the electrostatic supermicroscope. *Arch. Exp. Zellforsch.* **24**, 87–104 (1940).

Kausche, G. A. and Ruska, H. The identification of tobacco mosaic virus molecules in the chloroplast of virus-infected plants. *Naturwiss.* **28**, 303 (1940).

Kausche, G. A. Investigations on the problem of biological characterization of phytopathogenic virus proteins. *Arch. Ges. Virusforsch.* **1**, 362–372 (1940).

Kausche, G. A. The mechanism of the gold-sol reaction of the protein of tobacco mosaic and potato-*X*-virus. *Biol. Zentr.* **60**, 179–199 (1940).

Kausche, G. A. and Ruska, H. The problem of the structure of the chloroplast. *Naturwiss.* **28**, 303–304 (1940).

Kausche, G. A. Results and problems of experimental plant virus research. *Ber. Deut. Botan. Ges.* **58**, 200–222 (1940).

Koch, L. and Lehmann, A. Supermicroscopical investigation of rolled aluminum surfaces. *Wiss. Veröffentl. Siemens-Werken, Werkstoff-Sonderheft* 363–371 (1940).

Lembke, A., Ruska, H., and Christophersen, J. Comparative microscopical and supermicroscopical observations on the infective agent of tuberculosis. *Klin. Wochenschr.* **19**, 217–220 (1940).

Mahl, H. Application of the supermicroscope in colloid chemistry and metallurgy. *Jahrbuch AEG-Forsch., Sonderheft, Übermikroskop* **7**, 67–76 (1940).

Mahl, H. Determination of the orientation of single crystals of aluminum by means of the supermicroscope. *Metallwirtschaft* **19**, 1082–1085 (1940).

Mahl, H. The electrostatic electron microscope and some applications in colloid chemistry. *Kolloid Zeits.* **91**, 105–117 (1940).

Mahl, H. Metallurgical researches with the electrostatic ultramicroscope. *Zeits. f. techn. Physik* **21**, 17–18 (1940).

Mahl, H. A plaster-cast method for supermicroscopical investigation of metal surfaces. *Metallwirtschaft* **19**, 488–491 (1940).

Meldau, R. Fine dusts in the submicroscopic field. *V. D. I.* **84**, 103–106 (1940).

Middel, V., Reichmann, R., and Kausche, G. A. Supermicroscopic investigation of the structure of bentonites. *Wiss. Veröffentl. Siemens-Werken, Werkstoff-Sonderheft* 334–341 (1940).

Pfankuch, E. and Kausche, G. A. Ultramicroscopic examination of bacteriophages. *Naturwiss.* **28**, 46 (1940).

Radczewski, O. E., Müller, H. O., and Eitel, W. Supermicroscopic investigation of the beginning of precipitation of calcium carbonate from aqueous solutions. *Zentr. Mineral. Geol.* 8–19 (1940).

Ruska, H. Making visible the bacteriophage lysis in the supermicroscope. *Naturwiss.* **28**, 45–46 (1940).

Ruska, E. and Müller, H. O. Progress in reproduction of electron irradiated surfaces. *Zeits. f. Physik* **116**, 366–369 (1940).

Ruska, H. The structure of cellulose fibers. *Kolloid Zeits.* **92**, 276–285 (1940).

Ruska, H. and Wolpers, C. The structure of "liquor-fibrin." *Klin. Wochenschr.* **19**, 695 (1940).

Ruska, H. and Kretschmer, M. Supermicroscopic investigation of the degradation of cellulose fibers. *Kolloid Zeits.* **92**, 163–166 (1940).

Ruska, H. and Frühbrodt, E. Supermicroscopy as a method of investigation. *Biologe* **9**, 69–75 (1940).

Ruska, H. Visibility of bacteriophage cultures in the ultramicroscope. *Naturwiss.* **28**, 45–46 (1940).

Trurnit, H. and Friedrich-Freksa, H. The electronmicroscopical investigation of "tomato mosaic virus Dahlem 1940." *Biol. Zentr.* **60**, 546–556 (1940).

Zahn, H. Experiments on the supermicroscopy of wool. *Melliand Textilberichte* **21**, 505–508 (1940).

Anderson, T. F. and Stanley, W. M. A study of the reaction between the tobacco mosaic virus and its antiserum by means of the electron microscope. *J. Biol. Chem.* **139**, 339–344 (1941).

Ardenne, M. von. Electron microscopy of living tissue. *Naturwiss.* **29**, 521–523 (1941).

Ardenne, M. von, and Friedrich-Freksa, H. Germination of the spores of the bacillus vulgatus from photographs in the 200-kv universal electron microscope. *Naturwiss.* **29**, 523–528 (1941).

Barnes, R. B. and Burton, C. J. Metallic smokes as test objects in electron microscopy. *Ind. Eng. Chem.*, News Ed. **19**, 965–967 (1941).

Beischer, D. Newer methods for investigating the structure of colloidal systems. *Kolloid Zeits.* **96**, 127–135 (1941).

Borries, B. von, and Janzen, S. Image of finely machined technical surfaces in the supermicroscope. *V. D. I.* **85**, 207–211 (1941).

Hall, C. E. and Schoen, A. L. Application of the electron microscope to the study of photographic phenomena. *J. Opt. Soc. Am.* **31**, 281–285 (1941).

Hass, G. and Kehler, H. Investigations on the electrolytically-produced and annealed layers of aluminum oxide by means of electron interferences and measurements in the supermicroscope. *Kolloid Zeits.* **97**, 27–35 (1941).

Hass, G. and Kehler, H. On a temperature resistant and durable carrier for electron interference and electron-microscope investigations. *Kolloid Zeits.* **95**, 26–29 (1941).

Humbert, R. P. and Shaw, B. Studies of clay particles with the electron microscope. *Soil Science* **52**, 481–487 (1941).

Knoll, M. Evidence for built-up layers of iron oxide with the electron microscope. *Phys. Zeits.* **42**, 120–122 (1941).

Kregel, E. A. et al. A technique for electron-microscopic examination of encapsulated bacteria. *Science* **94**, 592 (1941).

Marton, L. The electron microscope. *J. Bact.* **41**, 397–413 (1941).

Marton, L., McBain, J. W., and Vold, R. D. Electron microscope study of curd fibres of sodium laurate. *J. Am. Chem. Soc.* **63**, 1990–1993 (1941).

Mehl, R. F. The structure and rate of formation of pearlite. *Trans. Am. Soc. Metals* **29**, 813–862 (1941).

Menke, W. Investigations of the fine structure of protoplasm with the universal electron microscope. *Protoplasma* **35**, 115 (1941).

Morton, H. E. and Anderson, T. F. Electron-microscopic studies of biological reactions. I. Reduction of potassium tellurite by Coryne-bacterium diphteriae. *Proc. Soc. Exp. Biol. Med.* **46**, 272–276 (1941).

Mudd, S. and Anderson, T. F. Demonstration by the electron microscope of the combination of antibodies with flagellar and somatic antigens. *Journ. of Immunology* **42**, 251–266 (1941).

Mudd, S., Polevitzky, K., Anderson, T. F., and Chambers, L. A. Bacterial morphology as shown by the electron microscope. *J. Bact.* **42**, 251–264 (1941).

Mudd, S. and Lackman, D. B. Bacterial morphology as shown by the electron microscope. *J. Bact.* **41**, 415–420 (1941).

Mudd, S. The electron microscope. *Frank. Inst. J.* **231**, 496–498 (1941).

Müller, F. H. Fiber production, fiber characteristics, and molecular structure. *Phys. Zeits.* **42**, 123–129 (1941).

Schmieder, F. Electron microscopic investigation of the relation between covering quality and grain size of pigments. *Kolloid Zeits.* **95**, 29–33 (1941).

Shaw, B. T. and Humbert, R. P. Electron micrographs of clay minerals. *Soil Sci. Soc. Am. Proc.* **6**, 146–149 (1941).

Stanley, W. M. and Anderson, T. F. A study of purified viruses with the electron microscope. *J. Biol. Chem.* **139**, 325–338 (1941).

Wallner, F. E. and Schiebold, E. Contribution to the interpretation of supermicroscopical pictures of fibrous specimens. *Kolloid Zeits.* **97**, 36–37 (1941).

Wesch, L. Electron-optical properties of Lenard phosphors. *Ann. d. Physik* **40**, 249–294 (1941).

Zworykin, V. K. and Ramberg, E. G. Surface studies with the electron microscope. *J. of Applied Physics* **12**, 692–695 (1941).

Anderson, T. F. and Richards, A. G. Electron microscope studies of some structural colors of insects. *J. of Applied Physics* **13**, 748–758 (1942).

Ardenne, M. von. Reaction-chamber supermicroscopy by means of the universal electron microscope. *Zeits. f. phys. Chemie*, [B] **52**, 61–71 (1942).

Baker, R. F., Ramberg, E. G., and Hillier, J. The photographic action of electrons in the range between 40 and 212 kilovolts. *J. of Applied Physics* **12**, 450–456 (1942).

Barnes, R. B. and Burton, C. J. The electron microscope and its uses. *A. S. T. M. Bull.* **116**, 34–41 (1942).

Brown, O. J., Jr. and Smith, W. R. Relation of paint properties to surface areas of carbon black. *Ind. and Eng. Chem.* Ind. Ed. **34**, 352–355 (1942).

Burton, C. J., Barnes, R. B., and Rochow, T. G. The electron microscope: calibration and use at low magnifications. *Ind. and Eng. Chem.* Ind. Ed. **34**, 1429–1436 (1942).

Clark, G. L., Bernays, P. M., and Tordella, J. P. Progress in lime investigation with x-rays and electron microscope. *Nat. Lime Assoc. Proc. 24th Annual Convention*, May 1942.

Clark, G. L., Barnes, M. R., and Baylor, E. R. A study of lampbrush chromosomes by the electron microscope. *Science* **95**, 250 (1942).

Eisenhut, O. and Kuhn, E. Light microscopic and electron microscopic investigations of native and artificial cellulose fibers. *Angew. Chem.* **55**, 198–206 (1942).

Frampton, L. V. The size and shape of the tobacco mosaic virus protein particle. *Science* **95**, 232–233 (1942).

Green, R. H., Anderson, T. F., and Smadel, J. E. Morphological structure of the virus of vaccinia. *J. Exp. Med.* **75**, 651–656 (1942).

Hall, C. E., Jakus, M. A., and Schmitt, F. O. Electron microscope observations of collagen. *J. Am. Chem. Soc.* **64**, 1234 (1942).

Hamly, D. H and Watson, J. H. L. Electron and optical microscope interpretation of the wall of pleurosigma angulatum. *J. Opt. Soc. Am.* **32**, 433–442 (1942).

Heidenreich, R. D. Electron reflections in MgO crystals with the electron microscope. *Phys. Rev.* **62**, 291–292 (1942).

Hillier, J. and Baker, R. F. The observation of crystalline reflections in electron microscope images. *Phys. Rev.* **61**, 722–723 (1942).

Luria, S. E. and Anderson, T. F. The identification and characterization of bacteriophages with the electron microscope. *Proc. Natl. Acad. Sci.* **28**, 127–130 (1942).

Marshall, C. E., Humbert, R. P., Shaw, B. T., and Caldwell, O. G. Studies of clay particles with the electron microscope. II. The fractionation of beidellite, nontronite, magnesium bentonite, and attapulgite. *Soil Science* **54**, 149–157 (1942).

Marton, L. Applications of the electron microscope in colloid chemistry. *Jour. Phys. Chem.* **46**, 1023–1032 (1942).

Marton, L. and McBain, J. W. The electron microscope and its developments. *Chemical Products* **5**, 61–67 (1942).

Morton, H. E. and Anderson, T. F. Some morphologic features of the Nichols strain of treponema pallidum as revealed by the electron microscope. *Am. J. Syph. Gono. and Ven. Dis.* **26**, 565–573 (1942).

Mudd, S., Polevitzky, K., Anderson, T. F., and Kast, C. Bacterial morphology as shown by the electron microscope. III. Cell wall and protoplasm in a strain of fusobacterium. *J. Bact.* **44**, 361–366 (1942).

Mudd, S., Polevitzky, K., and Anderson, T. F. Bacterial morphology as shown by the electron microscope. IV. Structural differentiation within the bacterial protoplasm. *Arch. Path.* **34**, 199–207 (1942).

Mudd, S. and Anderson, T. F. Selective staining for electron microscopy: the effects of heavy metal salts on individual bacterial cell. *J. Exp. Med.* **76**, 103–108 (1942).

Mueller, H. and Sakmann, B. W. Electro-optical properties of colloids. *J. Opt. Soc. Am.* **32**, 309–317 (1942).

Picard, R. G. Studies on the structure of thin metallic films by means of the electron microscope. Dissertation, U. of Michigan, 1942. (Manuscript)

Richards, A. G., Jr. and Anderson, T. F. Electron micrographs of insect tracheae. *J. N. Y. Ento. Soc.* **50**, 147–167 (1942).

Richards, A. G., Jr. and Anderson, T. F. Electron microscope studies of insect cuticle with a discussion of the application of electron optics to this problem. *J. Morph.* **71**, 135–183 (1942).

Richards, A. G., Jr. and Anderson, T. F. Further electron microscope studies on arthropod tracheae. *J. N. Y. Ento. Soc.* **50**, 245–247 (1942).

Richards, A. G., Jr., Anderson, T. F., and Hance, R. T. A microtome sectioning technique for electron microscopy illustrated with sections of striated muscle. *Proc. Soc. Exp. Biol. and Med.* **51**, 148–152 (1942).

Rosenblatt, M. B., Fullam, E. F., and Gessler, A. E. Studies of mycobacteria with the electron microscope. *Amer. Rev. of Tuberculosis* **46**, 587–598 (1942).

Schaefer, V. J. New methods for preparing surface replicas for microscopic observation. *Phys. Rev.* **62**, 495–496 (1942).

Schaefer, V. J. and Harker, D. Surface replicas for use in the electron microscope. *J. of Applied Physics* **13**, 427–433 (1942).

Schmitt, F. O., Hall, C. E., and Jakus, M. A. Electron microscope investigations of the structure of collagen. *J. Cell. and Comp. Physiol.* **20**, 11–53 (1942).

Scott, G. H. and Anderson, T. F. A study of connective tissue with the electron microscope. *Anat. Rec.* **82**, 445 (1942).

Sears, G. R. and Kregel, E. A. Application of the electron microscope to the problems of the pulp, paper and paperboard industry. *Paper Trade Jour.* **114**, 43–49 (1942).

Sharp, D. G., Taylor, A. R., Beard, D., and Beard, J. W. Electron micrography of the western strain equine encephalomyelitis virus. *Proc. Soc. Exp. Biol. and Med.* **51**, 206–207 (1942).

Sharp, D. G., Taylor, A. R., Beard, D., and Beard, J. W. Study of the papilloma virus protein with the electron microscope. *Proc. Soc. Exp. Biol. and Med.* **50**, 205–207 (1942).

Shaw, B. T. The nature of colloidal clay as revealed by the electron microscope. *Jour. Phys. Chem.* **46**, 1032–1043 (1942).

Stanley, W. M. and Anderson, T. F. Electron micrographs of protein molecules. *J. Biol. Chem.* **146**, 25–30 (1942).

Taylor, A. R., Sharp, D. G., Beard, D., and Beard, J. W. Electron micrography of the eastern strain equine encephalomyelitis virus. *Proc. Soc. Exp. Biol. and Med.* **51**, 332–334 (1942).

Umbreit, W. W. and Anderson, T. F. A study of thiobacillus thiooxidans with the electron microscope. *J. Bact.* **44**, 317–320 (1942).

Wergin, W. What does electron microscopy reveal regarding the structure of cellulose fibers? *Kolloid Zeits.* **98**, 131–141 (1942).

Wiegand, W. B. and Ladd, W. A. Colloidal carbon as revealed by the electron microscope. *Rubber Age* **50**, 431–436 (1942).

Wile, U. J., Picard, R. G., and Kearny, E. B. The morphology of spirochaeta pallida in the electron microscope. *J. Am. Med. Assoc.* **119**, 880–881 (1942).

Alexander, L. T., Faust, G. T., Hendricks, S. B., Isley, H., and McMurdie, H. F. Relationships of the clay minerals halloysite and endellite. *Am. Miner.* **28**, 1–18 (1943).

Barnes, R. B. and Burton, C. J. The electron microscope and cellulose. *Ind. and Eng. Chem.* Ind. Ed. **35**, 120–125 (1943).

Chambers, L. A. and Henle, W. Studies on the nature of the virus of influenza: I. The dispersion of the virus of influenza A in tissue emulsions and in extra-embryonic fluids of the chick. *J. Exp. Med.* **77**, 251–264 (1943).

Chambers, L. A., Henle, W., Lauffer, M. A., and Anderson, T. F. Studies on the nature of the virus of influenza: II. The size of the infectious unit in influenza A. *J. Exp. Med.* **77**, 265–276 (1943).

Heidenreich, R. D. and Peck, V. G. Fine structure of metallic surfaces with the electron microscope. *J. of Applied Physics* **14**, 23–29 (1943).

Mahl, H. and Stranski, J. N. The behavior of aluminium in metallographic etching. *Naturwiss.* **31**, 12–17 (1943).

Plotz, H., Smadel, J. E., Anderson, T. F., and Chambers, L. A. Morphological structure of Rickettsiae. *J. Exp. Med.* **77**, 355–358 (1943).

Richards, A. G., Jr., Steinbach, H. B., and Anderson, T. F. Electron microscope studies of squid giant nerve axoplasm. *J. Cell. and Comp. Phys.* **21**, 129–137 (1943).

Zworykin, V. K. Electron microscope in chemistry. *Electronics* **16**, 190–196 (January, 1943).

Calendar of Meetings

October

7– 9 Optical Society of America, Pittsburgh, Pennsylvania
16 American Physical Society, New England Section, New London, Connecticut
18–23 American Welding Society, Chicago, Illinois
23 American Physical Society, Metropolitan Section, New York, New York
29–30 Society of Rheology, New York, New York

November

6 American Physical Society, New York State Section, Ithaca, New York
12–13 American Physical Society, Evanston, Illinois
15–16 American Institute of Chemical Engineers, Pittsburgh, Pennsylvania
26–27 Central Association of Science and Mathematics Teachers, Chicago, Illinois

January

13–15 American Physical Society, New York, New York
13–15 American Association of Physics Teachers, New York, New York

Here and There

The Physical Society: Charles Chree Medal and Prize

The Charles Chree Medal and Prize are provided by the income from a fund given to the Physical Society in 1939 by Miss Jessie S. Chree of Edinburgh in memory of her brother Dr. Charles Chree, a former President of the Society and Superintendent of the Kew Magnetic Observatory. The prize and medal are awarded biennially in recognition of distinguished research in terrestrial magnetism, atmospheric electricity, or cognate subjects, in which Dr. Chree was especially interested. The Council of the Society made the first award to Professor Sydney Chapman in 1941 for his work in the first of these fields. The Medal and Prize for 1943 are awarded to Professor (now Brigadier) Basil F. J. Schonland, F.R.S., Director of the Bernard Price Institute of Geophysics, Johannesburg, in recognition of his valuable researches in the second field.

Schonland's work on atmospheric electricity has been primarily concerned with thunderstorm phenomena: first his investigations of the "polarity" of thunderclouds in South Africa, and his measurement of the discharge from a small tree, which clearly established the importance of point discharges in maintaining the earth's negative charge; secondly, his use of a rotating-lens camera of the Boys type in a spectacularly successful series of systematic experiments which elucidated the rather complicated succession of discharges forming what is known as a "stroke" of lightning; and thirdly, his work on the nature of atmospherics and the part played by the ionosphere in determining their structure.

The presentation was made at a meeting of the Society at the Royal Institution on Friday, July 16, when Brigadier Schonland delivered the Second Charles Chree Address, taking as his subject "Thunderstorms and their Electrical Effects."

★

International Series in Pure and Applied Physics

The McGraw-Hill Book Company announces a change in title and an enlargement in the scope of its International Series in Physics. Because of the rapid advances in the field of applied physics, the International Series will henceforth be known as the International Series in Pure and Applied Physics. An active effort will be made to include in the series in the future important volumes in the growing field of applied physics and, in addition, will continue to include distinguished contributions in the field of pure physics.

The International Series began in 1929 with the late Professor F. K. Richtmyer as Consulting Editor. Throughout its entire history it has published many volumes which have been outstanding contributions to the applied physics field. The importance of the applications of physics has grown greatly during recent years, a trend which has been accelerated by the war. Thus, new developments in the field of electricity, radio, acoustics, thermodynamics, biophysics, and other fields have emphasized again the great contributions which developments in physics have made and will continue to make to modern life. It is, therefore, necessary to recognize the growing importance of these applications more specifically, but at the same time to recognize that there is no sharp dividing line between pure and applied physics. Both of these objectives will be accomplished by incorporating volumes in both pure and applied physics in the International Series through the present enlargement in the scope of this series.

Dr. L. A. DuBridge will remain as Consulting Editor of this series, and associated with him will be an advisory editorial committee, which will assist in the selection and review of manuscripts for the series. The membership of this advisory committee may be enlarged from time to time, but the initial members will be Dr. E. U. Condon, Associate Director, Research Laboratories, Westinghouse Electric and Manufacturing Company; Dean George R. Harrison, Massachusetts Institute of Technology; Professor Elmer Hutchisson, University of Pittsburgh; and Dr. K. K. Darrow, Bell Telephone Laboratories.

★

Honors and Awards

Dr. George D. Birkhoff, Perkins Professor of Mathematics at Harvard University, has been elected an honorary fellow of the Royal Society of Edinburgh.

Frank H. Shaw, President of the Shaw Insulator Company of Irvington, New Jersey, received the John Wesley Hyatt Award, a gold medal and $1000 for distinguished achievement in plastics during 1942 in recognition of his invention and development of transfer moulded plastics. The presentation was made on June 17th at a dinner in the Waldorf-Astoria, New York, by Dr. Per K. Frolich, President of the American Chemical Society and a member of the award committee. The award was established in 1941 by the Hercules Powder Company.

The Society of Chemical Industry has awarded the Chemical Industry Medal for 1943 to Dr. John J. Grebe, Director of the Physical Research Laboratory at the Dow Chemical Company, Midland, Michigan. The presentation will be made next November.

★

News Notes

The appointment of Ralph J. Cordiner as Assistant to the President of the General Electric Company has been announced by Gerard Swope, President.

Dr. John G. Albright, of Case School of Applied Science, has been appointed head of the Physics Department at the Rhode Island State College, Kingston, Rhode Island.

Innovations in Instruments

High Speed Electronic Light Equipment

Photographs with an exposure of but one millionth of a second, brief enough to stop a rifle bullet or any fast moving object, can now be made by a new high speed electronic light equipment developed by engineers in General Electric's laboratory.

This device, using a small mercury lamp no bigger than a cigarette, consists of a small portable box, 10 inches square and weighing less than 20 pounds. On the front is the light source, resembling a small auto headlight, which can be operated manually by means of a push button, or automatically by electrical contacts or a photo-tube and preamplifier. It will illuminate 20 square feet of area with sufficient intensity to photo the fastest moving objects, in fact in tests has "stopped" a wheel revolving at 70,000 revolutions per minute.

Fastest camera shutters of the usual type, with blades moving between the lens elements, ordinarily operate at a minimum of 1/300 second. Focal plane shutters, consisting of slits in a curtain moving immediately in front of the film, cut this down to 1/1200 second. Recently published high speed photographs of athletes have been made with a lamp giving exposures of 1/30,000 second, but 1/33 as fast as the new G-E unit.

The new device uses standard and easily replaceable electrical parts and a single electronic tube, with a 100-watt Mazda mercury lamp as the light source. Such a lamp is now used as a high intensity light for illuminating airports, television and motion picture studies, and for other purposes. Its brightness in such installations is one-fifth of that of the sun's surface.

The ordinary 115-volt a.c. household lighting circuit is used to operate the unit. The current is rectified by an electronic tube and then used to charge a capacitor, really an electrical storage tank. In three seconds enough power is accumulated to operate the lamp at full flash intensity.

Ohmite Tandem Rheostat Assemblies

The tandem unit (illustrated) consists of eight Ohmite Model U, 1000-watt, 12-inch diameter rheostats mounted in a sturdy steel frame. It is controlled by a single hand wheel and is one of the largest units of this type ever assembled. Although this unit utilizes eight of the largest size rheostats, there are many other tandem assemblies that can be made up of two, three, or more rheostats ranging in power rating from 25 watts to 1000 watts and in diameter from $1\frac{9}{16}$ inches to 12 inches. Rheostats in tandem are insulated from each other so that they may be used for simultaneous control of several circuits of phases of a circuit by means of one knob.

Two rheostats can be separately controlled by means of concentrically located knobs. This may be done to conserve panel space or where it may be desired to use one rheostat as a vernier for another. In this type of unit two

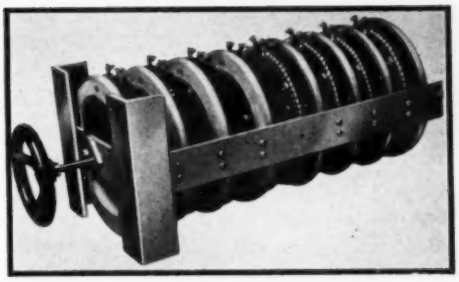

rheostats are mounted in tandem with the shaft of the rear unit extending through the hollow shaft of the front unit. For increased capacity, the front or back units can consist of several rheostats connected together. Tandem rheostats are also available in taper winding and the same range of resistance values as individual units.

New Instrument Booklets

Photovolt Corporation at 95 Madison Avenue, New York 16, New York, has published a booklet on their Lumetron Photoelectric Colorimeter Model 402-E, which is designed to cover a wide field of application in chemical and color analysis by photoelectric measurements. Equipped with 100-cp light source and mirror galvanometer, the instrument has ample sensitivity for use with color filters isolating wave bands approximately 30 millimicrons wide. There are 14 monochromatic filters of this spectral width available to be employed in the instrument. These filters cover, in approximately even steps, the whole visible spectrum, giving Model 402-E the character of a spectrophotometer by permitting complete spectral transmission and reflection curves to be plotted.

A great variety of sample holders can be used with the instrument. It accommodates plane-parallel absorption cells up to 15-mm light path as well as microcells, microtubes, and standard test tubes (14 pages).

Photovolt Corporation has also published another booklet on their Photoelectric Glossmeter. The Glossmeter is designed for measuring the gloss of paints and varnishes, ceramics, plastics, paper, and machined or polished metallic or non-metallic surfaces. It is also suited to register changes in gloss as a result of age, wear, abrasion, exposure to moisture, heat, light, vapors, or sprays.

The Glossmeter comprises the instrument proper and the search unit which is connected to it by a flexible cable. The search unit may be placed on the sample to be tested. Or the search unit may be positioned with the opening pointing upwards so that the sample is placed on top of it. The unit may, furthermore, be turned with the opening sideways for convenient measurement of vertical surfaces. Samples can be of any size and may be measured in rapid succession.

A new General Electric publication, designated as GET-1173, *Electric Instruments, Principles of Operation*, presents a concise discussion of the characteristics of instruments, their operation, and their individual limitations. Among the instruments included are: direct-current permanent-magnet moving-coil instruments such as ammeters, millivoltmeters, and voltmeters; alternating-current instruments of dynamometer type such as voltmeters, ammeters, wattmeters, and compensated wattmeters; alternating-current instruments of magnetic-vane type, induction type, rectifier type, and thermocouple type. Copies of the booklet can be obtained from the Company at Schenectady, New York (19 pages).

Sound Advances, July, 1943, presents an article on their Model PS High Speed Graphic Recorder, which was developed as a machine of considerable versatility, and one that is simpler, more compact, and less expensive than their PL High Speed Graphic Recorder.

A material mechanical simplification resulted from limiting the machine to a single paper speed and a single writing speed. The feature of interchangeable potentiometers was retained in the new design because though there are many users who need only one potentiometer scale, one paper speed and one writing speed, the users' needs differ from each other particularly as to the type of potentiometer. They differ also, though perhaps to a less important degree, as to the speeds required. Because of this, the user may within certain limits specify on his order what paper speed and writing speed he wants built into the machine. In order to retain as much as possible of the simplifications realizable in the new design, the range of possible speeds is limited to those given in the specifications. A detailed discussion of the various types of potentiometers available is also given. The booklet is published by Sound Apparatus Company, New York (6 pages).

Recent Applications of Physics

Application of Mass Spectrometer in Synthetic Rubber Production

The "mass spectrometer" will soon accelerate wartime chemical research in synthetic rubber plants. Dr. John A. Hipple, physicist at the Westinghouse Research Laboratories, developed the mass spectrometer in a form to analyze swiftly and precisely many of the complicated gases formed in making butadiene, the principal ingredient of several types of synthetic rubber. In 15 minutes this spectrometer will dissect a complicated gas molecule a twenty-five-millionth of an inch long and can be arranged to produce automatically an autograph that tells the chemist the composition of the gas.

Butadiene molecules are carefully built up from carbon and hydrogen atoms according to definite chemical patterns. As the molecule is being put together in a butadiene plant, its composition must be checked at intervals to make certain that the chemical pattern is being followed. Present methods of determining the molecular structure are so slow that a batch of butadiene has often gone through the various treatments of the process before the analysis is completed. If there is an error in the molecular design, the butadiene has to be reprocessed, causing lost production time.

Gyro-Stabilizer for Tank Guns

A new aiming device, known as a gyro-stabilizer, to increase by several hundred percent the shooting accuracy of new Army tanks while in motion, was developed by the Westinghouse Electric and Manufacturing Company in answer to a request made by the Army Ordnance Department. The stabilizer enables gunners in American tanks to fire accurately even while racing at full speed over the shattered terrain of a battlefield, according to L. H. Campbell, Jr., Chief of Ordnance, Army Service Forces.

"Not only do the high-velocity 75-mm guns in our M-3 medium tanks far and away outrange the best the Germans have, but we can fire this high velocity 75-mm gun when the M-3 tank is in motion. We fire our main armament in tanks when the tanks are in motion, regardless of speed, and we hit the target. Despite the pitch of the tank, the stabilizer keeps the gun barrel at a fixed elevation and the target within focus of the gunner's telescopic sight. The gunner can fire quickly and effectively, making only slight manual adjustments when necessary."

"The advantage in striking force gained by America's tanks is clear. The Germans have won their smashing blitzkrieg victories by a skillful combination of fire and movement. Progressing in groups in a zigzag advance, they cover each other's advance by alternating at firing from standing positions. This in effect immobilizes one half the tanks participating in an offensive while the other half is advancing. American tanks equipped with the stabilizer are able to advance simultaneously and fire with greatly improved accuracy. The new control gives American tanks still another great advantage. A tank that must come to a dead stop to fire accurately itself becomes an excellent target for enemy airplanes and artillery. Since American tanks can be always in motion, they make difficult targets."

The stabilizer, in effect, places the tank gun on a floating mount so that the gun barrel remains at a fixed elevation regardless of the dipping and bucking of the tank. It overcomes violent upward bucks and downward pitches as tanks race over rough ground.

Contributed Original Research

Harmonic Analysis by Photographic Method

ARCHIE W. STRAITON AND GEORGE K. TERHUNE
Texas College of Arts and Industries, Kingsville, Texas
(Received August 9, 1943)

This paper describes a method for determining Fourier series coefficients from area measurements on photographs of the function to be analyzed with the graph sheet formed into a series of semi-cyclinders.

THE Fourier coefficients for the interval $0<x<2\pi$ are given by

$$b_n=\frac{1}{\pi}\int_0^{2\pi} f(x)\sin nx dx$$

and

$$a_n=\frac{1}{\pi}\int_0^{2\pi} f(x)\cos nx dx$$

where n has the values 1, 2, 3, $\cdots$.

The value of the expression

$$\int_0^{2\pi} f(x)\sin nx dx$$

for a given value of n may be obtained as follows:

1. Place the graph sheet on a form made up of a series of tangent semi-cylinders alternately convex and concave whose diameters are each equal to $2/n$ with the y axis lying along a line of tangency between two cylinders.

2. Obtain a projection of the curve thus formed by photographing it from sufficient distance to reduce the distance distortion to a desired value.

3. Measure with a planimeter the area between the curve and the x axis as projected onto the photograph over $2n$ semi-cylinders, reversing the sense of the area measurement each time a new semi-cylinder is reached.

4. Determine the value of b_n from the area measurement by correcting for the scale of the photograph and dividing by π.

The proof of the correctness of the procedure outlined above is as follows:

Figure 1 represents the cross section of a form

FIG. 1.

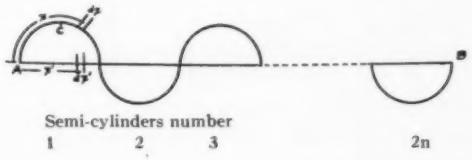

used. The graph sheet would follow the contour of the form with the x axis perpendicular to the semi-cylinder elements. The lines $x=0$ and $x=2\pi$ would pass through A and B respectively, falling along elements of the semi-cylinders. Then $\sin nxdx=dx'$ for semi-cylinders 1, 3, 5, $\cdots$ $(2n-1)$ and $\sin nxdx=-dx'$ for semi-cylinders 2, 4, 6, $\cdots 2n$. Also

$$\int_0^{2\pi} f(x)\sin nxdx=\int_0^{2/n} f(x')dx'-\int_{2/n}^{4/n} f(x')dx'$$

$$+\int_{4/n}^{6/n} f(x')dx'-\cdots-\int_{2(2n-1)/n}^{4} f(x')dx'.$$

The values of the integrals may be obtained with a planimeter giving the negative sense to the area measurements on the even numbered semi-cylinders.

The value of the expression

$$\int_0^{2\pi} f(x)\cos nxdx$$

may be determined in a similar manner with the y axis moved to fall along a semi-cylinder element through a maximum of the form cross section, such as the point C of Fig. 1.

Form models were made up from cylindrical cardboard cartons with the top half of alternate ones removed. In order to determine b_1 for the saw-tooth curve shown in Fig. 2, a graph sheet

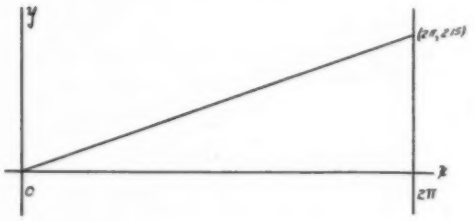

FIG. 2.

containing the curve was placed in a form with semi-cylinder diameters of two and with the y axis along a line of tangency. The photograph of the projected curve and the area measurement are shown in Fig. 3.

Photographs for obtaining a_1, b_2, a_2, b_3, and a_3 are shown in Figs. 4 through 8. The values of the coefficients thus obtained are compared in the table with the values determined analytically.

	a_1	b_1	a_2	b_2	a_3	b_3
Photographically	0.02	−0.66	−0.01	−0.35	0.02	−0.23
Analytically	0.00	−0.68	0.00	−0.34	0.00	−0.23

The photographs were made with a Crown view camera, using a 9-inch focal length lens from a distance of 30 feet. The prints were inked and washed in a solution of potassium ferricyanide to remove shadows.

Acknowledgment is made to Dr. S. L. Brown, of The University of Texas, for his helpful comments and suggestions.

FIG. 3.

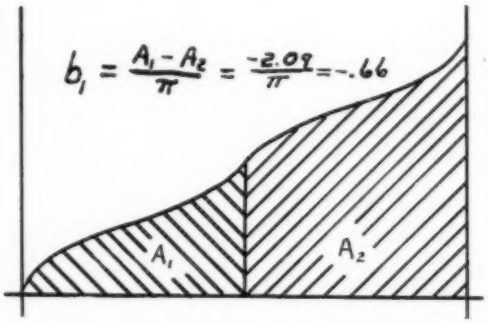

FIG. 4.

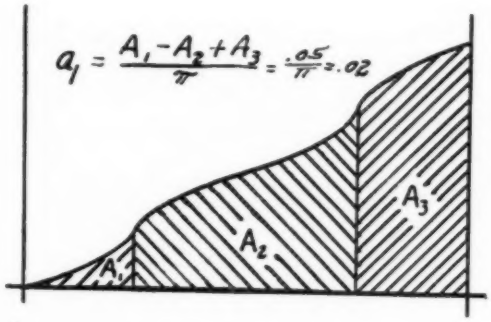

FIG. 5.

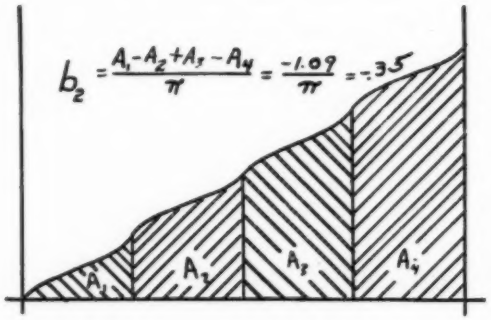

FIG. 6.

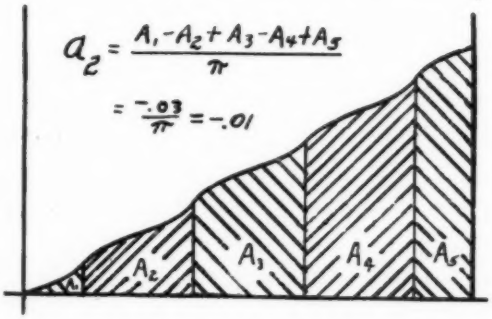

FIG. 7.

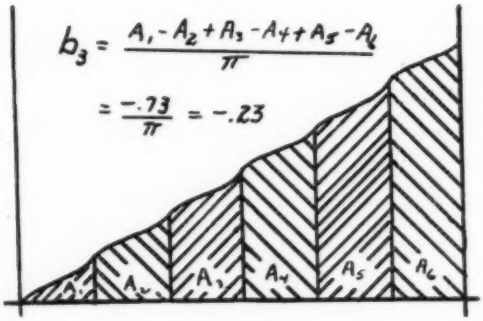

FIG. 8.

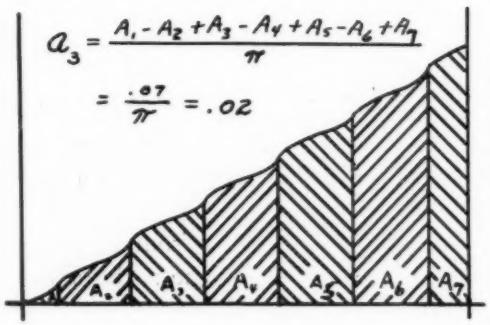

The Radiation Field of Long Wires, with Application to Vee Antennas

CHARLES W. HARRISON, JR.
Cruft Laboratory, Harvard University, Cambridge, Massachusetts
(Received August 4, 1943)

The analysis previously made for the current distribution along a symmetrical center-driven antenna of non-vanishing radius, and radiation field thereof, is extended to include long wire center-driven antennas. The results of this investigation are then applied to obtain an approximate solution for the field of a long wire resonant vee antenna.

INTRODUCTION

THE general problem of the antenna may be divided conveniently into three parts. The first part deals with the transmitting antenna as a circuit element; the second part involves the calculation of the electromagnetic field; and the third part is concerned with the question of the magnitude of voltage that may be developed across a given load impedance at the receiving station. In a classic paper, Hallén[1] has treated specifically the first and third parts of the antenna problem for the case of a symmetrical center-driven or center-loaded antenna of finite radius. In a series of recent papers[2–6] his analysis has been greatly extended, and a treatment of the distant field of a center-driven wire added.

In analyzing the transmitting or receiving antenna as a circuit element, a knowledge of the impedance of the antenna is required. This implies an accurate determination of the quadrature components of current existing along the antenna, specialized to the input terminals. From a precise analytical description of the distribution of current, it is a simple process to calculate the radiation field of the antenna, at least in principle.

The present paper is concerned chiefly with the question of the distribution of current on long wire center-driven antennas, and the radiation fields of such antennas. It is hoped that at a later date the long wire symmetrically loaded receiving antenna may be investigated, particularly with regard to its complex effective length.

THE DISTRIBUTION OF CURRENT ALONG A SYMMETRICAL CENTER-DRIVEN ANTENNA

The cylindrical center-driven antenna, when analyzed as a boundary value problem, leads to an integral equation involving the unknown current distribution under the integral sign. The solution of this equation, as carried out by Hallén, is based on a method of successive approximations. Unhappily, only a first-order correction is available in terms of known functions, for the simple sine distribution of current ordinarily assumed in antenna work. It is apparent, therefore, that the more precise theory is least accurate whenever the simple sine wave theory predicts sharp zeros of current along the antenna. This occurs at $h-|z|=n\lambda/2$. If $h=n\lambda/2$, a zero occurs at the input terminals, hence large errors in impedance calculations are to be expected under these conditions.

The zeroth- and the first-order terms in the solution for the current are

$$I_z=\frac{j2\pi V_0^e}{\Omega R_c}\times\left[\frac{\sin\beta(h-|z|)+(1/\Omega)[M_1^I+jM_1^{II}]}{\cos\beta h+(1/\Omega)[A_1^I+jA_1^{II}]}\right]. \quad (1)$$

Here V_0^e is the applied voltage.

[1] E. Hallén, Nova Acta (Uppsala) [IV] Vol. 11, No. 4, 1–44 (1938).
[2] R. King and F. G. Blake, Jr., Proc. I. R. E. **30**, 335–349 (1942).
[3] R. King and C. W. Harrison, Jr., "The distribution of current along a symmetrical center-driven antenna," accepted for publication in Proc. I. R. E.
[4] C. W. Harrison, Jr., and R. King, "The radiation field of a symmetrical center-driven antenna of finite cross section," accepted for publication in Proc. I. R. E.
[5] R. King and C. W. Harrison, Jr., "The receiving antenna," accepted for publication in Proc. I. R. E.
[6] C. W. Harrison, Jr. and R. King, "The receiving antenna in a plane-polarized field of arbitrary orientation," submitted for publication in Proc. I. R. E.

$\Omega = 2 \ln 2h/a$, a being the radius of the antenna wire.

R_c is the characteristic resistance of space ($\approx 120\pi$ ohms).

$$\beta = 2\pi/\lambda.$$

λ is the wave-length; h is the antenna half-length.

z is the distance along the wire measured from the indefinitely close together input terminals, to the point where the current is computed.

The factors M_1^I, M_1^{II}, A_1^I, and A_1^{II} are defined in the appendix.

The complete formula for the distribution of current (as originally derived by Hallén) consists of the sum of a series involving powers of $1/\Omega$. It has been generally assumed that for values of Ω as small as 10, the correction terms of order $1/\Omega^2$, $1/\Omega^3$, etc., contribute a negligible amount to the final result. Thus the Hallén method is entirely satisfactory in practical problems for long wire antennas of moderate radii.

In sketching out the distribution of current on a long wire center-driven radiator, a considerable amount of labor is saved if points are chosen at intervals of $\pi/2$ for the calculation of the quadrature components of current. This was actually done in computing the curves shown in Figs. 1 and 2. For Fig. 1, $h = 6\lambda$ and $\Omega = 25$. In Fig. 2, $h = 6\lambda$ and $\Omega = 10$. The distribution of current along only one-half of the antenna is shown.

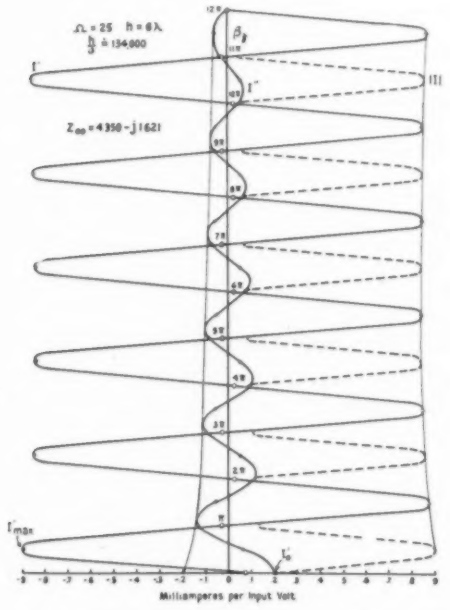

FIG. 1. The distribution of current along one-half of a symmetrical center-driven antenna for $\Omega = 25(h/a \doteq 134{,}000)$ and $h = 6\lambda$.

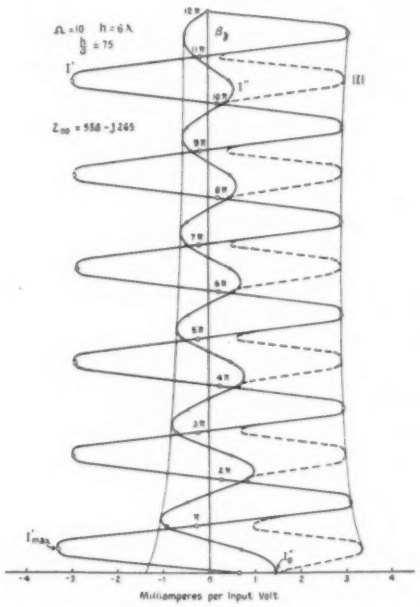

FIG. 2. The distribution of current along one-half of a symmetrical center-driven antenna for $\Omega = 10(h/a \doteq 75)$ and $h = 6\lambda$.

It is of interest to observe in Fig. 1 that the component of current I'_{max} in quadrature with the driving electromotive force, is essentially sinusoidally distributed, and that the in-phase component of current, I_0'', is approximately cosinusoidally distributed, and linearly damped along the antenna. However, an obvious condition is that both components must become zero at the end of the wire. There is also some tendency for the magnitude of the current to decrease from the driving point along the antenna and then to increase near the outer extremity of the wire. This phenomenon has been verified experimentally, and certainly would have to be contained within an adequate antenna theory.

Of further interest is the fact that I_0'' increases with increasing length for fixed values of Ω. This is shown by Fig. 3, where the ratio of the quadrature component of current $\lambda/4$ removed from the input terminals to the in-phase component of current occurring at the input terminals for $\Omega = 25$, is plotted.

THE DISTANT FIELD OF A SYMMETRICAL CENTER-DRIVEN LONG WIRE ANTENNA

In an as yet unpublished paper[6] an expression is derived for the complex effective length of a receiving antenna in a plane-polarized field of arbitrary orientation. By means of the reciprocity theorem the relation between the magnitude of this effective length, and the radiation field of the same antenna when driven is pointed out. Thus a more rigorous expression for the distant field of a symmetrical center-driven antenna of non-vanishing radius is obtained than heretofore available. This equation is

$$E_\theta^r = j60I_0\frac{e^{-j\beta R_0}}{R_0}\left[\frac{j2\pi Z_{00}}{\Omega R_c \sin\theta}\right]\left[\frac{(\cos(\beta h\cos\theta)-\cos\beta h)+(1/\Omega)[m_1^I(0)+jm_1^{II}(0)]}{\cos\beta h+(1/\Omega)[A_1^I+A_1^{II}]}\right]. \tag{2}$$

In (2) E_θ^r is the electric field in the distant or radiation zone of the antenna.

I_0 is the complex current at the driving point.

R_0 is the distance from the point of field calculation in the distant zone to a convenient reference origin 0 at the center of a center-driven antenna or at the base of a vertical base-driven antenna over a perfectly conducting infinite plane.

Z_{00} is the self-impedance of the antenna, as obtainable from the curves of King and Blake.[1]

θ is the angle between the axis of the antenna wire, and the line drawn from the center of phase out to the point in the radiation zone where the field is calculated.

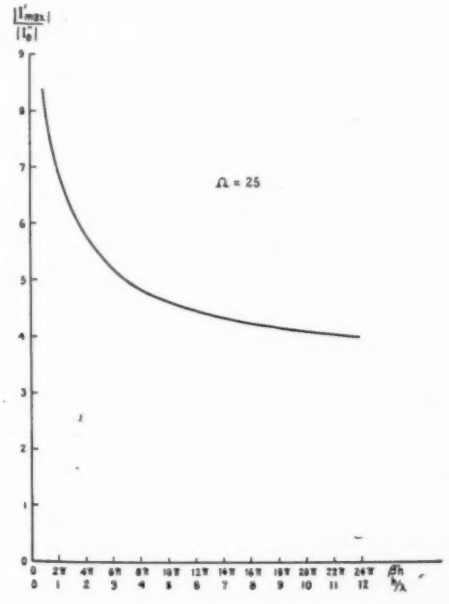

FIG. 3. The ratio I'_{max}/I_0'' as a function of βh for $\Omega=25$, I'_{max} and I_0'' being computed at the points $\beta z=\pi/2$ and $\beta z=0$, respectively.

The factors $m_1^I(0)$ and $m_1^{II}(0)$ are defined in the Appendix.

Equation (2) is the complete and accurate formula for the radiation field of a center-driven antenna of finite radius for which terms in $1/\Omega^2$ are negligible. Its use in conjunction with the "field characteristic" of an antenna array may be used to give correctly the distant field of the array, if it is proved that the existence of mutual impedance does not significantly alter the distribution of current in the individual radiators. Inasmuch as the current disappears at the opposite ends of a symmetrical center-driven antenna, (2) has no application, for example, to the case of the resonant vee antenna, where the component of current in phase with the driving voltage is a maximum at the input terminals of the vee.

In Fig. 4 is shown a plot of the magnitude of (2) (scale adjusted) for an antenna of half-length $h=0.625\lambda$ when $\Omega=10$, 20, 30, and ∞. This figure shows that the shape of the field pattern may be calculated with reasonable accuracy by assuming $\Omega=\infty$, i.e., that the simple sine distribution of current is a reasonable approximation. It is to be observed, however, that sharp zeros are rounded off more as Ω decreases in value.

In the limit as $\Omega\to\infty$ $(a\to 0)$,

$$Z_{00}=-j60\Omega\cot\beta h. \tag{3}$$

Using (3) with (2)

$$E_\theta^r = j60I_0 \frac{e^{-j\beta R_0}}{R_0}\left[\frac{\cos(\beta h\cos\theta)-\cos\beta h}{\sin\theta\sin\beta h}\right]. \quad (4)$$

The latter is the familiar equation given in the literature for the distant electric field of a doublet antenna.

In calculating the radiation field of a long-wire center-driven antenna, (2) may be used to give accurate results, though the labor involved will be very great, as numerous points are required. An alternative procedure is to represent the quadrature components of current as closely as possible by analytical expressions of simple form, and calculate the distant fields due to these components. Inasmuch as the currents are in quadrature in the antenna, the individual fields will be in quadrature, and hence the magnitude of the field will be the square root of the sum of the squares of the field components.

In the case of Fig. 1, the current distribution along the antenna may be approximated closely by the formula

$$I_z = I_z'' + jI_z' = \frac{I_0''(h-|z|)}{h}\cos(\beta|z|+\zeta) + jI'_{\max}\sin\beta(h-|z|). \quad (5)$$

Here I_0'' is the amplitude of the component of current in phase with the driving voltage at the input terminals.

$I'_{\max}$ is the maximum value of the sinusoidally distributed component of current in quadrature with the driving voltage.

ζ is the phase angle at the origin of the component I_0'' with respect to a cosine curve. Close examination of Figs. 1 or 2 indicates that ζ changes slowly along the wire. However, since it will be shown later that the whole contribution of the I_0'' component of current to the distant field is very small, this variation of ζ may be considered inconsequential.

The radiation field for the quadrature component of current is given by (4), where $I'_{\max}$ is to be written for $I_0/\sin\beta h$. The field due to the tapered cosinusoidally distributed component of current must be calculated directly. For this purpose, the following well-known formula is of use:

$$E_\theta^r = j30\beta\frac{e^{-j\beta R_0}}{R_0}\int_{-h}^{+h} I_z' e^{j\beta z'\cos\theta}\sin\theta\, dz'. \quad (6)$$

In this relation

I_z' is the complex current amplitude in amperes flowing in the element dz'.

z' is the distance from the reference origin at the center of the antenna to the element dz'.

It might be well to mention in passing that (1) used with (6) leads to (2), though to obtain (2) by carrying out the necessary integration would be well nigh impossible.

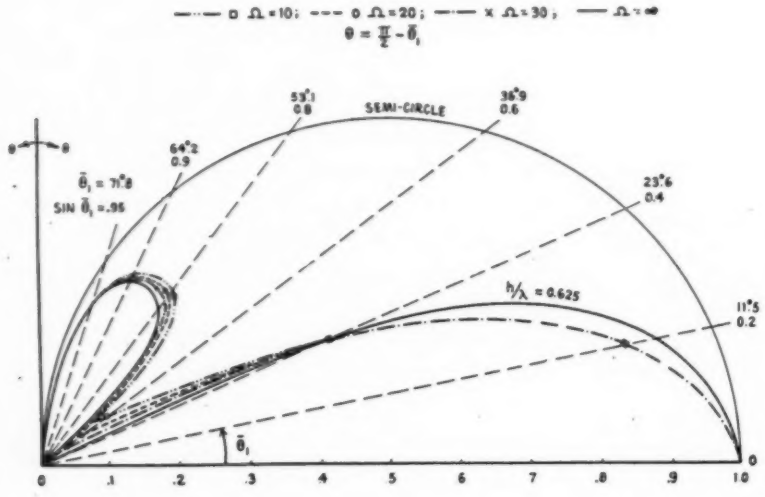

FIG. 4. The radiation field of a base-driven vertical antenna over a perfectly conducting plane of infinite extent, for $h=0.625\lambda$ and $\Omega=10$, 20, 30, and ∞.

For the specific field to be calculated, one has

$$E_\theta' = j30\beta \frac{e^{-j\beta R_0}}{R_0} \sin\theta \int_{-h}^{+h} \frac{I_0''(h-|z|)}{h} \times \cos(\beta|z|+\zeta) e^{j\beta z' \cos\theta} dz'$$

$$= \frac{j60 I_0'' e^{-j\beta R_0}}{R_0 \beta h \sin^3\theta} [(1+\cos^2\theta) \times (1-\cos\beta h \cos(\beta h \cos\theta)) \cos\zeta - (\beta h \sin^2\theta + 2\cos\theta \cos\beta h \times \sin(\beta h \cos\theta)) \sin\zeta]. \quad (7)$$

This formula is restricted for simplicity to the case $\sin\beta h = 0$, i.e., $h = n\lambda/2$. The combination of (4) with (7) is conveniently accomplished by the introduction of a factor

$$C = I_0''/I'_{\max}$$

the reciprocal of which is given very closely by Fig. 3, for $\Omega = 25$.

For a practical long-wire antenna for which $h = 6\lambda$, $f = 12$ megacycles/sec. and $\Omega = 25$ ($a = 0.112$ cm), it is seen from Fig. 1 that ζ is a small angle. If one sets $\zeta = 0$ degrees, then (4) and (7) predict absolute nulls in the field pattern, since the factor $[1-\cos\beta h \cos(\beta h \cos\theta)]$ occurs in both equations. Hence it is reasonable to suppose that for this case (2) would predict extremely small minimum fields. Figure 5 is a sketch of the field pattern for a symmetrical center-driven antenna for the case $h = 6\lambda$, $\Omega = 25$, $\zeta = 0$ degrees, and $C = 0.224$.

For the thicker antenna (implied by $\Omega = 10$), the approximate representation of the quadrature components of current using (5) becomes much less accurate, and one would expect the null positions in the distant field to be rounded off significantly. An investigation of this problem requires an application of (2) if precise results are to be obtained. Even so, it is doubted if the degree of refinement thus achieved, as compared to that available from the simplified analysis, is commensurate with the great labor involved.

THE DISTANT FIELD OF END-DRIVEN ANTENNA SECTIONS

To calculate the field of an end-driven antenna Section (6) is applicable, provided the lower limit of integration is changed from $-h$ to 0. As an illustration, assume an antenna section carrying the current distribution shown in Fig. 1. For the quadrature component of current

$$E_\theta' = j30 I'_{\max} \frac{e^{-j\beta R_0}}{R_0 \sin\theta} \times (e^{j\beta h \cos\theta} - \cos\beta h - j\cos\theta \sin\beta h). \quad (8)$$

This formula applies to an end-driven wire of any length. For the component of current in phase with the driving voltage

$$E_\theta' = j \frac{30 I_0'' e^{j\beta R_0}}{R_0 \beta h \sin^3\theta} \times [((1+\cos^2\theta)(1-\cos\beta h e^{j\beta h \cos\theta}) - j\beta h \sin^2\theta \cos\theta) \cos\zeta - (\beta h \sin^2\theta + j2\cos\theta - j2\cos\theta \times \cos\beta h e^{j\beta h \cos\theta}) \sin\zeta]. \quad (9)$$

In (9) the length of the wire is restricted to $h = n\lambda/2$. It is readily verified that when (8) and

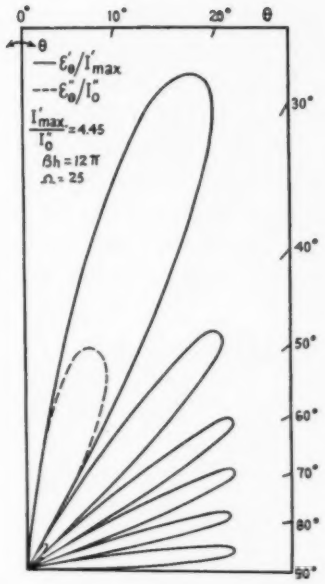

FIG. 5. The radiation fields due to the components of current $I'_{\max}$ and I_0'' along a base-driven vertical antenna over a perfectly conducting half-space for $h = 6\lambda$, $\Omega = 25$, and $\zeta = 0$ degrees. In combining the individual fields in quadrature E_θ'', as plotted, must be multiplied by the reduction factor $C = 0.224$. The resulting pattern is thus substantially the same as that given by E_θ'.

(9) are combined in quadrature, due account being taken of the ratio factor $C=I_0''/I'_{max}$, (9) contributes but little to the field, except when (8) passes through a zero which occurs for certain values of h. Thus the shape of the field pattern is given for all practical purposes by (8), the nulls being rounded off by the contribution of (9). A plot of the field of an antenna section for which $h=6\lambda$, $\zeta=0°$, and $\Omega=25$ is given in Fig. 6.

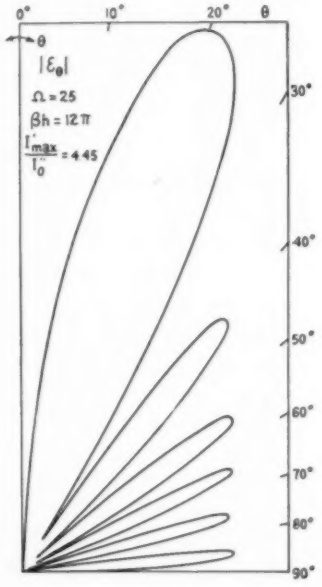

FIG. 6. The radiation field of an end-driven antenna section without image for $h=6\lambda$, $\Omega=25$, and $\zeta=0$ degrees. Absolute nulls in the field pattern are entirely absent.

Since the in-phase component of current provides but a slight correction to the field, it follows immediately from the principle of superposition that the field of an array composed of such sections can differ but slightly from that determined by assuming a sine distribution of current in all elements, provided the distribution of current is not significantly altered in the individual radiators by the existence of mutual impedance.

THE RESONANT VEE ANTENNA

P. S. Carter, C. W. Hansell, and N. E. Lindenblad[7] have developed equations for the distant field of a resonant vee antenna. These writers presupposed that an end-driven vee antenna may be represented by two symmetrical antennas oriented appropriately so as to form a vee. The validity of this assumption, in the absence of published data regarding the distribution of current on the legs of the long wire antenna, was certainly open to question at the time their treatment appeared. The basic objection to the prior work on vee antennas is that the input impedance to the vee must necessarily be infinite, regardless of the leg length, inasmuch as the current disappears at each end of a symmetrical antenna element. A true picture of the radiation field is available from Carter's analysis only when $\sin \beta h=0$, i.e., for a so-called "antiresonant" vee. Whereas it is true that the radiation field for vee antennas fulfilling this requirement could be corrected for the existence of the component of current I_0'' by calculating the radiation field due to this component, and properly combining with the previously published result, it is impossible to correct the field of a vee antenna satisfying the condition $\cos \beta h=0$, i.e., for a "resonant" vee. In the latter case, the component of current I'_{max} has a large value at the input terminals, and a more basic analysis for the vee antenna problem is desirable.

A rigorous analysis has been given above for the distribution of current along a symmetrical center-driven antenna of finite radius, when the antenna dimensions are such that terms in $1/\Omega^2$ are negligible. On the other hand, the distribution of current along an open-ended transmission line of zero dissipation is

$$I_z=jE_s \sin \beta(h-z)/Z_c \cos \beta h. \qquad (10)$$

Here E_s is the voltage maintained by the generator across the input terminals, and Z_c is the characteristic impedance of the line. The current I_z is seen to be in quadrature with the applied voltage E_s. In the case of a transmission line with small dissipation, the inphase component of current, while not zero, is very small. If then one imagines the antenna folded into a parallel wire line, the component of current I_0'' along the antenna ultimately becomes negligible in value. The vee antenna lies within these limits, and thus it can be assumed with confidence that proximity

[7] P. S. Carter, C. W. Hansell, and N. E. Lindenblad, Proc. I. R. E. 19, 1773–1842 (1931).

of the wires cannot cause an increase in I_0'' above that given by (1) for a center-driven long wire.

It has been shown that little is to be gained by correcting the field for the I_0'' component of current in the case of end-driven long wire antenna sections. Accordingly, it is a legitimate procedure to analyze the radiation field of a vee antenna on the basis of the assumption of a sine distribution of current. Thus the field calculations made by the previous investigators give satisfactory results, since the addition or subtraction of a section $\lambda/4$ in length makes little difference in the field pattern when one is dealing with very long wire antennas.

Expressions have been derived for the fields of isolated vee antennas having leg lengths any multiple of $\lambda/4$ for any direction of radiation. These relations, it is thought, cannot be expressed in a very compact form. Accordingly, formulae will be given here only for the radiation field in the "horizontal" and "vertical" planes.

Using a method developed by Dr. S. A. Schelkunoff,[8] and used in a recent paper by the writer,[9] it is readily shown that the field in the plane $y=0$ for a vee antenna of arbitrary leg length oriented in the plane $z=0$ with the positive x axis bisecting the angle formed by the wires at the origin of a right-hand coordinate system is

$$K^2=\frac{4I_0^2\sin^2\eta}{\beta^2\sin^2\beta h\sin^4\psi_1}\{1-\cos\psi_1\sin\beta h\times[2\sin(\beta h\cos\psi_1)-\cos\psi_1\sin\beta h]-\cos\beta h[2\cos(\beta h\cos\psi_1)-\cos\beta h]\}. \quad (11)$$

In (11), K^2 is defined as the "radiation function." (The field strength is proportional to K.)

2η is the angle formed by the wires.

I_0 is the amplitude of the sinusoidal current at the input terminals to the antenna, this component being in quadrature with the driving electromotive force.

(θ, ϕ) are the spherical coordinates of a typical point anywhere in the far zone of the antenna, θ being measured from the positize z axis, and ϕ from the positive x axis.

For the selected antenna orientation and considering that the radiation is being calculated in the plane $y=0$, $\cos\psi_1=\sin\theta\cos\eta$ when $\phi=0$ degrees, and $\cos\psi_1=-\sin\theta\cos\eta$ when $\phi=180$ degrees. The field pattern in the vertical plane in either the forward, or backward direction is obtained for $0\leqq\theta\leqq+90$ degrees.

For the directional characteristic in the plane $z=0$ for $\sin\beta h=0$,

$$K^2=\frac{2I_{\max}^2}{\beta^2\sin\psi_1\sin\psi_2}\left\{\frac{1}{\sin\psi_1\sin\psi_2}(\sin^2\psi_2-\sin\psi_1\sin\psi_2+\sin^2\psi_1+\cos\beta h\times[(\sin\psi_2-\sin\psi_1)(\sin\psi_1\cos(\beta h\cos\psi_2)-\sin\psi_2\cos(\beta h\cos\psi_1))])-\cos[\beta h(\cos\psi_2-\cos\psi_1)]\right\}. \quad (12)$$

Here $\psi_1=\phi-\eta$, and $\psi_2=\phi+\eta$. $I_{\max}$ is the maximum value of the sinusoidal current along the antenna wires. This current is in quadrature with the applied voltage.

For the directional characteristic in the plane $z=0$ for $\cos\beta h=0$,

$$K^2=\frac{I_0^2}{\beta^2\sin\psi_1\sin\psi_2}\left\{\frac{1}{\sin\psi_1\sin\psi_2}(\sin^2\psi_2+\sin^2\psi_1+\sin 2\eta\sin\beta h[\sin 2\eta\sin\beta h-2\sin\psi_2\sin(\beta h\cos\psi_1)+2\sin\psi_1\sin(\beta h\cos\psi_2)])-2\cos[\beta h(\cos\psi_2-\cos\psi_1)]\right\}. \quad (13)$$

Equations (11), (12), and (13) apply to isolated vee antennas. The effect of the earth may be taken into account in the usual way. For antennas located over an earth of finite constants, currents flowing along the surface of the earth have quadrature components which probably affect the distant field a great deal more than the field due to the component of current in-phase with the driving voltage ordinarily neglected in antenna calculations.

An expression has been obtained for the field pattern in the plane $y=0$ due to the component of current in-phase with the driving voltage.

[8] S. A. Schelkunoff, Proc. I. R. E. **27**, 660–666 (1939).
[9] C. W. Harrison, Jr., Proc. I. R. E. **31**, 362–364 (1943).

Upon combining this field with (11), the conclusion previously drawn, that the assumption of a sine distribution of current is adequate for vee antenna calculations, was again verified.

CONCLUSION

For the calculation of field patterns of antenna arrays, the assumption of a sine distribution of current is entirely adequate, except in instances where the mutual impedance appreciably alters the distribution of current in the individual radiators, provided it is understood that complete nulls in the field pattern are absent. A more advanced theory is unnecessary unless the fields so calculated are being used in the Poynting vector method for determining the power radiated.

For the case of the vee antenna it is considered extremely unlikely that the mutual impedance of the wires alters the basic premise that the assumption of the simple distribution of current is satisfactory.

It is a pleasure to thank Dr. Philippe LeCorbeiller of the Cruft Laboratory staff for his discussion of the conclusions drawn in this paper.

APPENDIX

The factors M_1^I, M_1^{II}, A_1^I, A_1^{II}, $m_1^I(0)$, and $m_1^{II}(0)$, while defined in references 3, 5, and 6, are reproduced collectively for the convenience of the reader.

$$M_I^I+jM_I^{II}=F_1(z)\sin\beta h-F_1(h)\sin\beta|z| +G_1(h)\cos\beta z-G_1(z)\cos\beta h, \quad (14)$$

$$A_1^I+jA_1^{II}=F_1(h). \quad (15)$$

Neglecting ohmic resistance

$$\begin{aligned}F_1(z)=&-(\cos\beta z-\cos\beta h)\ln(h^2-z^2)/h^2\\&+\tfrac{1}{2}\cos\beta z[\langle Ci\rangle 2\beta(h+z)+\langle Ci\rangle 2\beta(h-z)\\&+jSi2\beta(h+z)+jSi2\beta(h-z)]\\&-\tfrac{1}{2}\sin\beta z[Si2\beta(h+z)-Si2\beta(h-z)\\&-j\langle Ci\rangle 2\beta(h+z)+j\langle Ci\rangle 2\beta(h-z)]\\&-\cos\beta h[\langle Ci\rangle\beta(h+z)+\langle Ci\rangle\beta(h-z)\\&+jSi\beta(h+z)+jSi\beta(h-z)], \quad (16)\end{aligned}$$

$$\begin{aligned}G_1(z)=&-(\sin\beta|z|-\sin\beta h)\ln(h^2-z^2)/h^2\\&-\tfrac{1}{2}\cos\beta z[Si2\beta(h+z)+Si2\beta(h-z)\\&-2Si2\beta|z|-j\langle Ci\rangle 2\beta(h+z)\\&-j\langle Ci\rangle 2\beta(h-z)+j2\langle Ci\rangle 2\beta z]\\&-\tfrac{1}{2}\sin\beta z[\langle Ci\rangle 2\beta(h+z)-\langle Ci\rangle 2\beta(h-z)\\&+jSi2\beta(h+z)-jSi2\beta(h-z)-j2Si2\beta z]\\&-\tfrac{1}{2}\sin\beta|z|[4\ln|z|/(h+|z|)\\&-2\langle Ci\rangle 2\beta z]-\sin\beta h[\langle Ci\rangle\beta(h+z)\\&+\langle Ci\rangle\beta(h-z)+jSi\beta(h+z)\\&+jSi\beta(h-z)]. \quad (17)\end{aligned}$$

$F_1(h)$ and $G_1(h)$ are obtained from (16) and (17), respectively, by setting $z=h$.

$$m_1^I(0)+jm_1^{II}(0)=F_1(0)\cos qh-F_1(h) +S_1(h)-S_1(0)\cos\beta h. \quad (18)$$

Neglecting ohmic resistance,

$$\begin{aligned}S_1(z)=&-(\cos qz-\cos qh)\ln(h^2-z^2)/h^2\\&+\tfrac{1}{2}\cos qz[\langle Ci\rangle(\beta+q)(h+z)\\&+\langle Ci\rangle(\beta+q)(h-z)+\langle Ci\rangle(\beta-q)(h+z)\\&+\langle Ci\rangle(\beta-q)(h-z)+jSi(\beta+q)(h+z)\\&+jSi(\beta+q)(h-z)+jSi(\beta-q)(h+z)\\&+jSi(\beta-q)(h-z)]-\tfrac{1}{2}\sin qz\\&\times[Si(\beta+q)(h+z)-Si(\beta+q)(h-z)\\&-Si(\beta-q)(h+z)+Si(\beta-q)(h-z)\\&-j\langle Ci\rangle(\beta+q)(h+z)+j\langle Ci\rangle(\beta+q)(h-z)\\&+j\langle Ci\rangle(\beta-q)(h+z)-j\langle Ci\rangle(\beta-q)\\&\times(h-z)]-\cos qh[\langle Ci\rangle\beta(h+z)\\&+\langle Ci\rangle\beta(h-z)+jSi\beta(h+z)\\&+jSi\beta(h-z)]. \quad (19)\end{aligned}$$

Here

$$q=\beta\cos\theta. \quad (20)$$

$S_1(0)$ and $S_1(h)$ are obtained from (19) by setting $z=0$, and $z=h$, respectively. $F_1(0)$ is the value of (16) when $z=0$.

$$Si(x)=\int_0^x(\sin u/u)du, \quad (21)$$

$$Ci(x)=\int_0^x(\cos u/u)du, \quad (22)$$

$$\langle Ci\rangle(x)=\int_0^x[(1-\cos u)/u]du =0.5772+\ln(x)-Ci(x). \quad (23)$$

For large arguments,

$$Si(x)=\pi/2-\cos x/x; \quad Ci(x)=+\sin x/x \quad (24)$$

and

$$\langle Ci\rangle(x)=0.5772+\ln(x)-\sin x/x.$$

Dosimetry and Local Distribution of Energy in the Electric High Frequency Field[1]

K. S. Lion
Massachusetts Institute of Technology, Cambridge, Massachusetts
(Received July 8, 1943)

The principles of a short wave dosimetry method, based upon measuring of the electric field strength distribution, are explained. The applicability of this method for measurements outside and inside of the body to be treated is discussed. Measurements in some typical field arrangements are presented.

I

THE electric field arising between the two plates of a condenser which are connected to a high frequency generator has been of special interest in many ways within the last few years. The physicist and chemist are interested chiefly in the interaction between high frequency fields and matter. The dielectric behavior of any substance in such fields depends upon the polar character of the molecules and can, therefore, be used conversely for investigations of the molecular structure.

Further interest arises from the field of insulation research, since the applicability of technical materials, such as used for insulation at short waves, is limited by the absorption of energy in the electric high frequency field. It may be interesting to note that a major effort of this research is devoted to the development of new insulation materials with low losses, while the reduction of losses by suitable shaping of the electric fields has been of relatively little interest.

The main technical application of the electrical high frequency field has been the production of heat inside of dielectric bodies, as for instance, in medical diathermy or short wave treatment. Originally a "biological technique" this technique has found industrial applications on a large scale, e.g., for the dehydration or drying of tobacco and wood, for polymerization of plastics or glue, and for many other purposes. The high frequency field treatment is, of course, particularly efficient for semi-conducting substances, such as predominate in biological objects. This fact and the many other advantages of the short wave field treatment make its use especially adaptable to many more new problems. A further development in this field seems, therefore, very probable, provided that our knowledge of the action of the field and the technique, in particular the measuring technique, can be improved.

The medical short wave therapy technique has been developed on an empirical basis, and is practically applied without physical measurements or dosimetry. The technique used at the present (with few exceptions) leaves it up to the experience of the physician to estimate the dose, and the heat sensation of the patient is mostly used as subjective measure of the intensity of a treatment. It is obvious that a physical method is more desirable.

Besides the application of a dosimeter to prevent burns there are other reasons for the necessity of a physical measuring method. In comparing the results obtained by the different authors in treating bacteria or plants with ultrashort waves, one can observe a great discrepancy. For instance, while some authors report a stimulation of growth, others observe the killing of seeds or bacteria. Unquestionably a killing of biological objects can be produced on treatment with sufficiently high energy and for sufficient time. On the other hand we cannot explain the observed stimulation of growth on the grounds of experimental error or mistake. Even if we grant that a part of the discrepancy is caused by the biological variability of the objects (or even the different judgment of the authors), we have to assume that another, perhaps more important, reason for the differences results from the dif-

[1] Read in part at the 20th annual meeting of the Am. Acad. of Physical Med., October 16, 1942.

ferent intensity of the treatment, for which a measuring method does not exist. If in experiments with such simple objects as bacteria or seeds no uniform results can be obtained, the situation may be still more difficult in such complicated processes as therapeutical treatments, since here not only the biological variability is greater but also the interpretation is more difficult because of the absence of untreated control experiments. If a physical method were available for the absolute determination of the dose, we would be able to compare results obtained in different places and by different authors, and this would enable us to make reproducible experiments and to apply their results as a scientific basis for therapy.

There is a further reason for the necessity of dosimetry in each case of treatment: The observed effects of stimulation and killing of bacteria and seeds may permit us to assume something about the effect of short waves in biological objects; if we increase the time of the treatment or the intensity, or both, the stimulation will increase up to a certain point and then will decrease until, with large doses, the effect becomes negative. An effect of this kind has been observed by different authors, as well as in clinical works, and it is just the advantage of a short wave dosimetry to permit dosage of the intensity in the one or the other sense.

Some dosimeter methods have already been proposed. In the first place, the voltage applied to the electrodes has been used as measure for the intensity of a treatment (with condenser plates); but this voltage is not identical with the voltage on the object. Also, the current through the condenser and, therefore, through the object, does not give a measure of the physical-biological effect. The current is composed of a capacitive and an ohmic current, the capacitive current flowing through the object cannot produce any effect, however, because it is not accompanied by an absorption of energy. Much better are the types of the instruments which measure the total amount of power absorbed in the body. The objection to these types of dosimeters is that the influence of any kind of short wave field is a local function and varies from point to point. If one says that the power of 50 watts is absorbed in the human body this does not say anything about the influence or effect of the short wave field. If this power is distributed over the whole body no influence may be observed, but if it is absorbed in a space of one centimeter cube, it will result in burning. A power meter would indicate in both cases the same value. The distribution of energy, however, can be determined by measuring the intensity of the electric field in arrangements using the condenser electrodes.[2]

The distribution of the electric field strength can be illustrated by connecting all points at which the field strength has the same value (amount, not direction, since the effect is proportional to E^2). The resulting iso-field strength lines indicate where the same effect, in a homogeneous medium, can be expected.

Figure 1 shows such curves for a homogeneous and a non-homogeneous field. The iso-field strength lines, as it can be seen from Fig. 1, are not identical with the equipotential lines.

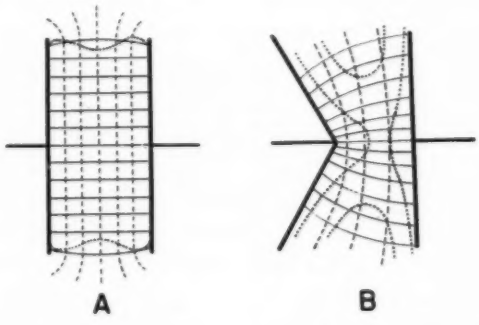

FIG. 1. Homogeneous and non-homogeneous fields. ——— force lines; - - - - - - equipotential lines; ..... iso-field strength lines.

II

According to the considerations mentioned above a measuring instrument applicable to short wave electric fields has been developed and has been described in a previous paper.[3,4] Its operation is based on the phenomenon of the electrodeless luminous discharge which arises in a small

[2] The method described here can be applied in some cases also when using coil fields. The present paper deals only with the condenser method; the application to coil fields will be described later.

[3] K. S. Lion, Rev. Sci. Inst. **13**, 338–341 (1942).

[4] K. S. Lion, Helv. Phys. Acta, **14**, 21–50 (1941).

tube filled with gas under reduced pressure if brought into an electric high frequency field. Under certain conditions (floating potential, spherical form of the discharge tube[5]) the brightness of the light emitted from the discharge vessel is a measure of the field strength. The discharge tube is connected to a photoelectric cell and amplifier, and the field strength at the point to be measured is directly indicated by a meter calibrated in volts per centimeter. The sensitivity of the dosimeter is sufficiently high to allow measurements outside and, under certain conditions, inside the body to be treated. The deflection of the meter is proportional to the field strength, except for field strengths so small that the discharge in the gas-filled vessel extinguishes.

The dosimeter is calibrated in a field in which the field strength can be calculated from the applied voltage and the physical dimensions of the condenser plates. The calibration constant depends on the wave-length and can be adjusted, if the wave-length of the short wave generator is known.

While measurements of the field outside the patient to be treated can be carried out in a simple way, there are some difficulties in conducting measurements inside the body, not so much because of insufficient sensitivity of the instrument as because there are no technical possibilities of making measurements inside the body to be treated, except inside the cavities of the body. The same is true in x-ray dosimetry in which case one measures the input intensity and determines the depth dose by means of tables or by calculation, or one contents oneself with the mere indication of the input intensity. This is permissible since the relation between depth dose and measured surface dose or input intensity is known and depends (at high voltages) only to a small extent on the "transparency" of the different tissues of the body. A relationship between field outside and inside the body to be treated exists also in electric short wave fields. With a given adjustment of condenser plates and short wave machine, the electric field strength distribution in the body (inside field) as well as the field in the space between body and condenser plates (outside field) is given by the electrical and geometrical properties of the body. For all clinical treatments in which the point to be treated is on the surface, the indication of the dosimeter can be used as measure of the field influence. In these cases (e.g., treatments of furuncles, etc.) measurements with the dosimeter not only furnish a relative measure for reproduction or comparison of treatments, but determine quantitatively the physical-biological effect. Measurements of the outside field by means of the dosimeter can serve to secure the quantitative reproduction of treatments or to compare different treatment also for the inner organs. Whether the reading of the dosimeter in the outside field furnishes a measure of the physical-biological effect in the inner organs can only be decided by experiment.

The practical way to study this question is to investigate, by means of the dosimeter, the field distribution in models. The aim of this investigation, however, is twofold: it should show if, from measurements with the dosimeter in the outside field, the field intensity in inner organs can be estimated with sufficient practical accuracy. If this is feasible, the mere measuring of the outside field could be used for dosage in therapy of the inner organs, as in x-ray therapy. Moreover, it might be of general interest to get some information about field distribution. This knowledge is of particular value for clinical application of short wave fields, enabling one to *control*, to a certain extent, the distribution of energy, to increase it at points at which higher energy is desirable, and to protect other points from too high field strengths.

Some of the field pictures which are shown below could be obtained by calculation. But calculations are only practicable in simple arrangements and are more time consuming than measurements.[6] For practical use in therapy calculations are not feasible. For predetermination of an intended field arrangement it is rather useful, therefore, to derive some general rules about field distribution which can be of use in the arrange-

[5] The known neon tube, used sometimes as tuning indicator, cannot be used for measuring the field strength.

[6] The field distribution pictures shown in this paper have been drawn by a semi-automatic method which allows plotting of an entire field curve in less than one hour.

ment of proper field distributions, and to determine quantitatively only the accessible parts of the field by means of the dosimeter.

It should be noted that the electric properties of the different tissues at high frequencies are known from the measurements of different authors.[7] The distribution of the different tissues, i.e., the anatomic structure of the part to be treated, is normally known with sufficient accuracy.

III

Figure 2 shows the field distribution between two parallel circular plates. Since the distance between the plates is of the same order of magnitude as the plates themselves, the field, as expected, is not homogeneous and is more concentrated towards the plates. Only in the middle a small area arises in which the field is approximately homogeneous. This space is the one used in therapy employing Schliephake distance electrodes. The field also is not homogeneous in the direction parallel to the plates. In immediate proximity of the plates the intensity is smaller in the middle and greater towards the edges. Along the vertical symmetry line, however, the field decreases from the center towards both sides, as expected. The maximum non-uniformity arises at the edges of the plates, the point of maximum field strength, however, is not directly on the plate edges but shifted more towards the horizontal symmetry line as indicated by an arrow. At this point the danger of burning (in a homogeneous medium) is a maximum. The ratio of minimum to maximum field strength in the space between the plates is about 1 : 3. If, therefore, this field should be applied for treatment of a homogeneous body, one part of this body, near the plates, would get nine times the dose of the center part.

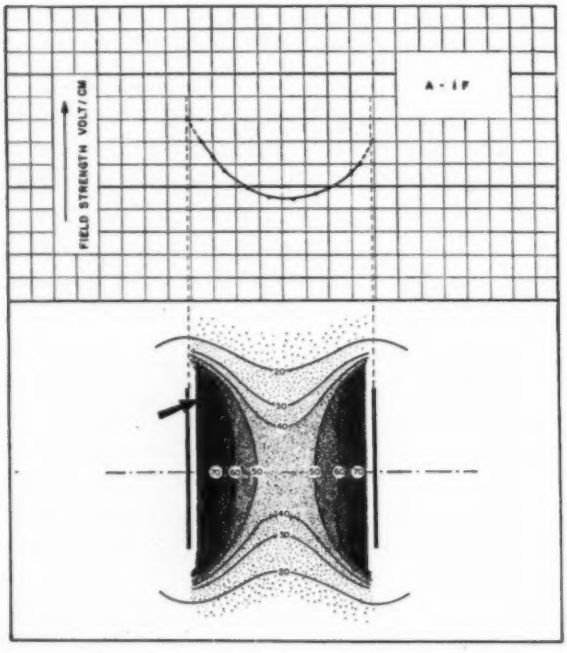

FIG. 2. Field distribution in a meridional plane between two parallel circular plates.

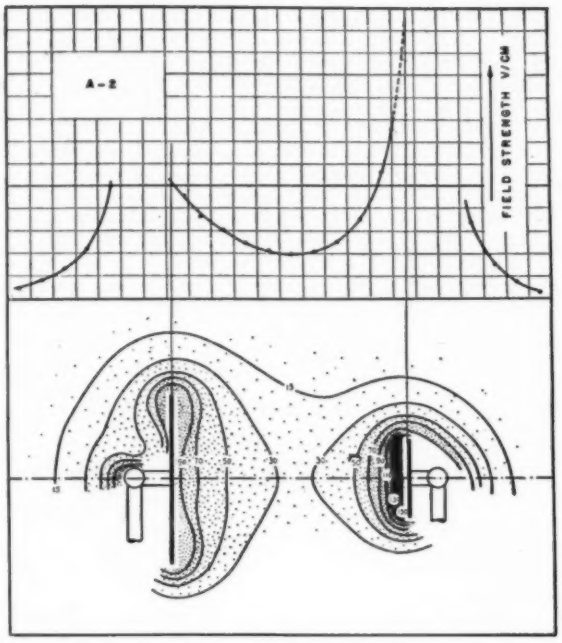

FIG. 3. Field strength between two circular plates of different size.

Figure 3 shows the field picture between two plates of different size. (Diameters of the plates are 15 cm and 7 cm, respectively; separation distance, 20.6 cm.) The field strength, as expected, is higher near the smaller electrode than near the larger one; the ratio of field strengths along the symmetry line is about 1 : 2.4 (extrapolated). One should generally expect, therefore, in treatments using two electrodes of different size that the greater effect would arise at the smaller electrode. It appeared, however, in one

[7] B. Rajewsky, *Ergebnisse der biophysikalischen Forschung* (G. Thieme, Leipzig, 1938), Vol. 1, Chapter 2, IV.

practical case, that the dosimeter showed a small reading at the smaller electrode while the field strength near the larger (so-called inactive) electrode was relatively high. This could be explained by the fact that the output circuit of the short wave generator was unsymmetrically grounded. The voltage between the smaller electrode and the (capacitively grounded) patient, therefore, was smaller than the one between the patient and the larger electrode. As a first approximation, the field form near one electrode can be determined without respect to the size and position of the other electrode, if the latter is sufficiently far away.

This becomes even more visible in Fig. 4, in which the smaller plate has been rotated through 45°. The field in the proximity of the smaller plate is nearly unchanged from the one in Fig. 3. At further distances from this plate, the field, of course, is deformed towards the other electrode. The field distribution in the middle between both electrodes is about the same as in Fig. 3. The high field strength in this case also is concentrated at the electrodes.

The effect of field concentration at the electrodes is undesirable for many practical applications. The maximum effect arises on the surface

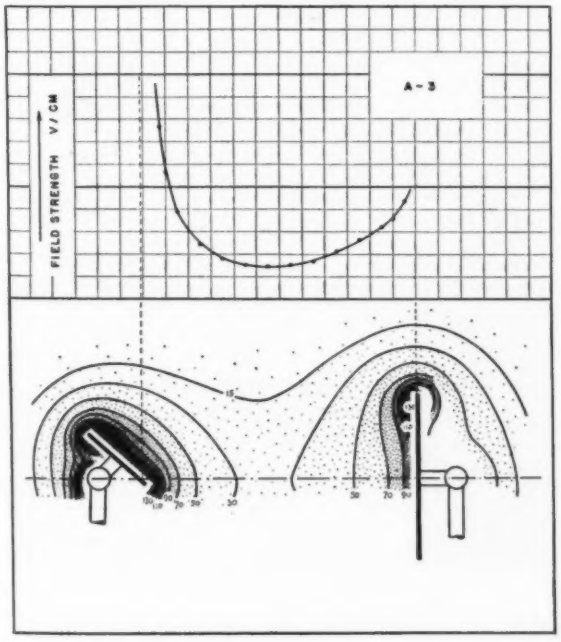

FIG. 4. Arrangement like Fig. 3, but position of one of the electrodes changed.

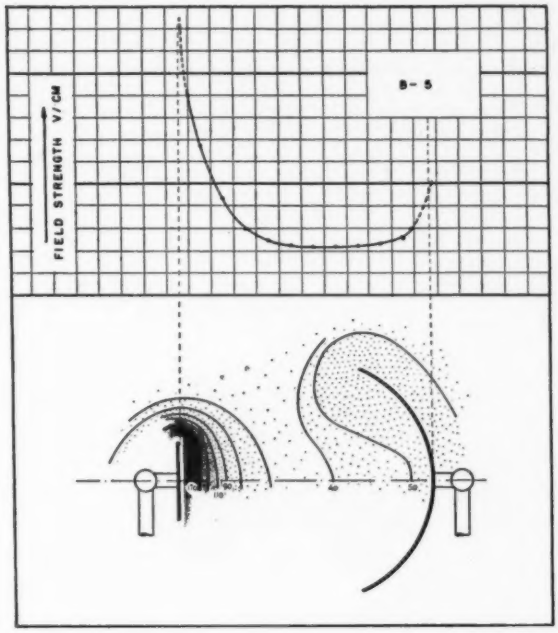

FIG. 5. Field form between one straight and one curved electrode.

(skin) of the body to be treated and limits the applicable energy. The field strength at the center of the field is smaller than on the plates, the relative depth effect is insufficient. By using distance electrodes, Schliephake increases the relative depth dose (ratio of depth dose to surface dose), however, at the expense of efficiency. In keeping the surface of the object at a certain distance from the electrodes he reduces the surface intensity and, therefore, obtains high relative depth dose. The strong field near the electrodes remains unused.

An arrangement which serves the same purpose of homogenizing the electric field, especially near the electrodes, by other means, is shown in Fig. 5. For comparison, the left electrode has the normal plate form, the right one is cylindrically curved, approaching the form of a Faraday cage. The field strength at the concave side of the curved electrode, therefore, is reduced and the field homogenized as can be seen from the upper curve of Fig. 5. Within 50 percent of the total space between the electrodes, the field strength does not vary more than ±6 percent (measured in the symmetry line). For comparison: in a similar arrangement with straight plates (e.g., Fig. 4) a homogeneity of 6 percent arises in less

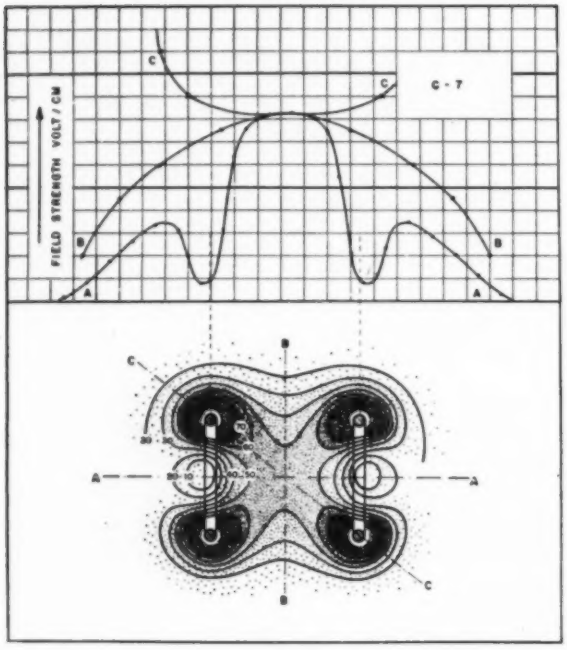

FIG. 6. Field strength distribution between two circular ring electrodes.

than 30 percent of the total space between the electrodes. Doubtless, an even better homogeneity can be obtained by curving also the other electrode of Fig. 5, in the proper way, preferably perpendicularly to the first one.

The problem of the depth dose, however, cannot generally be solved in this way. Relative depth doses greater than unity would require that the field strength in the middle of the area to be used for treatment be absolutely higher than the one in proximity to, or on, the electrodes. In principle, it may not be possible to obtain such a field in a homogeneous medium, by means of two electrodes, whatever their form may be. Field forms can be shown, however, in which the field intensity in certain spaces near the electrodes is reduced, while the field in the middle is relatively stronger.

An example of such a field which arises between two circular rings is shown in Fig. 6. (Diameter of the rings 10 cm, thickness 1 cm, distance 12.8 cm.) The three upper curves of Fig. 6 show the field strength along the three lines *AA*, *BB*, and *CC*. If one follows the symmetry line *AA* from the middle of one electrode, the field strength increases towards the center about 10 : 1 (!).

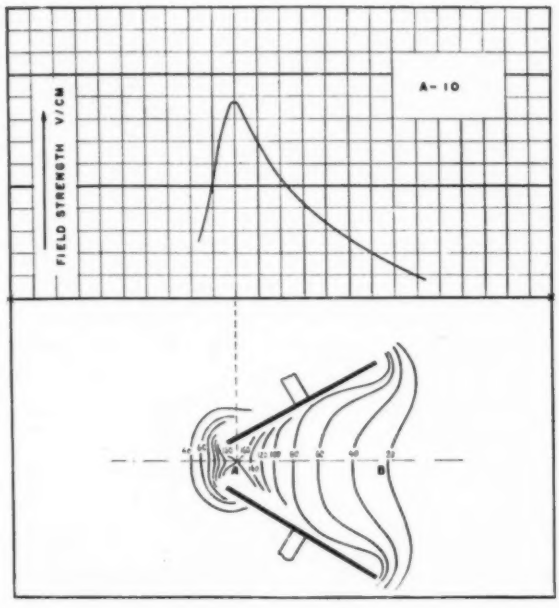

(a)

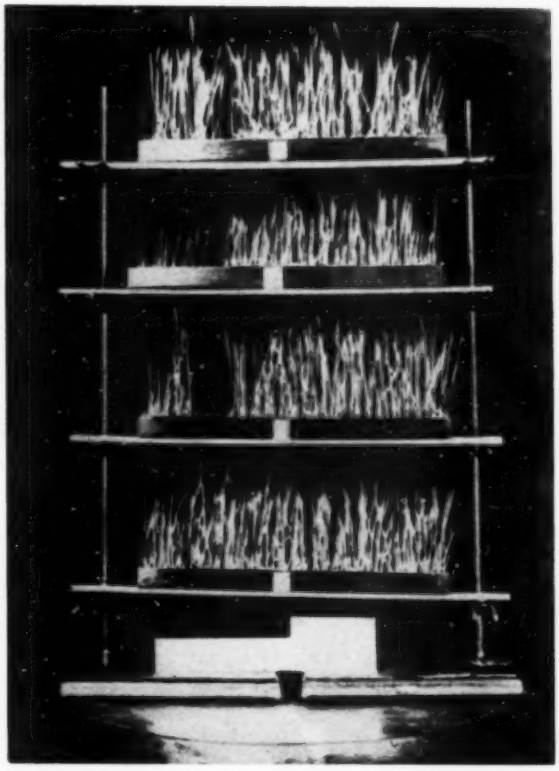

(b)

FIG. 7. (a) Non-homogeneous field. (b) Wheat seeds treated in this field for 1, 5, 15 minutes; untreated control.

Also in the direction *BB* a field concentration in the center of the field can be observed, but not in the direction *CC*, in which the field, as expected, decreases towards the center. In fact, a similar arrangement has already been used, for treatment of the extremities, by Leistner and Schaefer[8] (ring electrodes) and the authors emphasize the high depth effect of the arrangement which, from Fig. 6, can now be easily understood.

The field pictures shown here arise in air or in any non-conducting homogeneous and isotropic dielectric substance which fills up the whole area between the two electrodes. If a dielectric substance different from air does not fill up this whole space, a refraction of electric force lines will occur at the interphase of both dielectrics.[9]

Nevertheless, measurements of the empty field may serve, sometimes, as quantitative indications of processes that will occur inside of substances if brought into the electric field. An example of this is shown in Fig. 7a. The field 7a between two equal circular plates which form an angle with each other is very non-homogeneous. The upper curve of Fig. 7a shows the sharply increased intensity at the point *A* where both plates are nearest together and the drop of field strength on both sides of said point *A*. In order to observe the effect of the short wave field, seeds have been introduced along the line of symmetry. These seeds, therefore, are exposed to about 8 times higher field strength at the point *A* than at the point *B*.[10] The result of the treatment is shown in Fig. 7b. At the point of maximum field strength all seeds are killed. Whether an effect of stimulation also occurred cannot be concluded from this picture as no pure seed cultures were used.

Experiments of this kind open an interesting aspect of the question of influence of the time factor in treatments with short wave fields. The material presented up to date does not allow any conclusion to be drawn about the effect of time, neither for the stimulation, nor for the lethal effect. It seems, however, indicated that the assumption of a simple law of the form: Dose = Intensity × time, is not justified.

[8] K. Leistner and H. Schaefer, Klin. Wochenschr. **14**, 899 (1935).

[9] Such fields will be described in a later paper.

[10] On the assumption that the field is not disturbed by the introduction of the seeds. This assumption may be justified since the size of the seeds is negligible compared to the dimensions of the field.

Erratum: The Penetrometer Method for Determining the Flow Properties of High Viscosity Fluids

[J. App. Phys. **14**, 170 (1943)]

WESLEY W. PENDLETON,
Westinghouse Research Laboratories, East Pittsburgh, Pennsylvania

EQUATIONS (48) and (50), page 178, quoted from W. Lethersich, are dimensionally incorrect.

These equations and the subsequent analysis were used to show the insignificance of the elastic force as compared with the viscous force in the penetrating needle system. This erroneous comparison was a side issue and had no bearing on the validity of the penetrometer equations or the method. Although the result of this comparison of elastic and viscous forces seemed to check experimental observation, the analytical comparison itself is questionable.

Thermionic Emission from an Oxide-Coated Cathode

H. Y. Fan
Radio Research Laboratory, National Tsing Hua University, Kunming, China
(Received May 18, 1943)

The properties of thermionic emission from a cathode coated with barium oxide are studied. The cathode is indirectly heated and its temperature is measured by a thermocouple. It is found that the emitted electrons have a Maxwellian distribution corresponding closely to the temperature of the cathode. The emission is studied with accelerating voltages up to 1300 volts. The current rises more steeply than predicted by Schottky's theory but begins to bend at the upper end. The variation of the work function and the factor A with the state of the cathode is studied by glowing the cathode at different temperatures. It is found that both the work function and the factor A vary. No appreciable decay of emission with time is observed. The effect of drawing emission on the work function and the factors A is small.

THERMIONIC emission from oxide-coated cathodes has been studied extensively. Many results are, however, contradictory and the properties of such emitters are not yet thoroughly clarified. We present in this paper the results of experiments made on a cathode coated with barium oxide. Emissions in retarding and accelerating fields were studied and the variations of emission constants with the state of the cathode were investigated. The experiments were made at low temperatures, so that the state of the cathode was not affected by the measurement itself.

EXPERIMENTAL ARRANGEMENT

For measurements of emission in a low field it is necessary to eliminate the potential drop along the cathode. In the case of oxide-coated cathodes the indirectly heated type is best suited for this purpose. The cathode used consists of a nickel alloy tubing, 2 mm in diameter and 4 cm long, with a loop of tungsten wire, embedded in alumina, serving as the heater. The coating is barium oxide, applied in the form of barium carbonate with amyl acetate and a trace of collodion as binder. The collector is a nickel cylinder, 1.29 cm in diameter and 1 cm long, with a nickel guard ring at each end. The guard rings are of the same diameter and 1.5 cm long each. They serve to eliminate the end effect of the applied field and the effect of the non-uniformity of the cathode temperature at the two ends.

The cathode temperature is usually measured by one of three methods: (1) direct optical pyrometer measurement; (2) measurement of the heating power input; (3) measurement of the core resistance. The first method is not applicable at low temperatures. The second method involves determination of the total emissivity of the coating surface, which varies with temperature. Besides, in the case of indirectly heated cathodes it is difficult to determine accurately how much of the total heating power is dissipated through the central portion of the cathode where the temperature is different from the two ends. In using the third method there is also the difficulty of non-uniform temperature of the cathode. In the case of filaments potential leads could be used to measure the resistance of the central portion. When the cathode is in the form of a tubing as in our case, this method is not applicable. We measure the temperature of the cathode by means of a thermocouple. A tungsten wire is spot-welded to the inside of the cathode near the center. The wire is held under tension, so that it does not touch the cathode at other places except the welded spot. The temperature of the core is measured by the thermal e.m.f. of this joint. This method is not applicable to filaments because of the fact that the wire welded to a filament disturbs its temperature. The core of our cathode is tubing 2 mils in thickness and the tungsten wire used is 3 mils in diameter. It is thought that the cathode should be massive enough for the disturbing effect of the tungsten wire to be negligible. To check this assumption

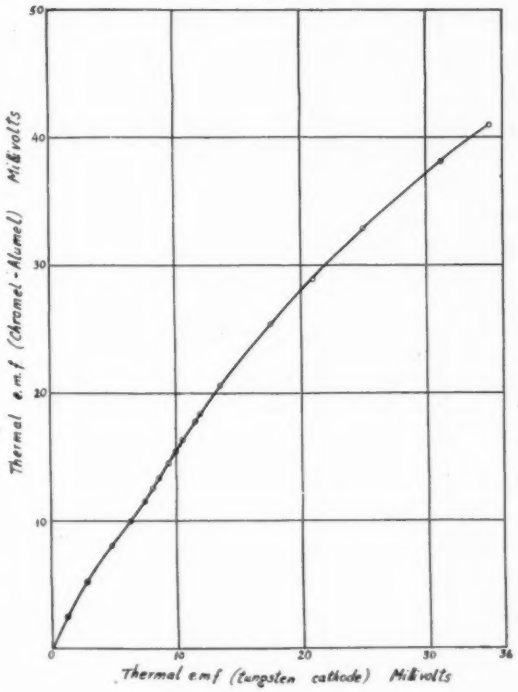

FIG. 1. Calibration of tungsten-cathode thermocouple.

a tube is made with two wires spot-welded to the cathode, one on the inside and one on the outside, at two different points on the same circumference. The outer wire should cool the welded joint whereas the inner wire, being nearer the heater, should heat the joint. For a wide range of the heater current the thermal e.m.f. of the two joints showed no difference. We feel, therefore, justified in using this method. The thermal e.m.f. of the tungsten-core couple is calibrated against a Chromel-Alumel thermocouple. For the calibration the two thermocouples are placed in an evacuated quartz tubing which is heated to different temperatures by an electric heater wound on the outside. To prevent any temperature difference the joints of the two thermocouples are spot-welded together and their thermal e.m.f.'s are taken simultaneously. Figure 1 shows the calibration curve. The thermocouple measures the temperature of the core. The temperature of the oxide surface should be lower. However, according to Moore and Allison[1] the temperature drop across the coating (thickness less than 100μ) cannot be more than a few degrees. Furthermore, in such a composite cathode the emission could not be a function of the oxide surface alone but should depend upon the temperature of the bulk of the oxide also. In view of these considerations we shall take the thermal e.m.f. as measuring the "cathode temperature."

The structure of the tube is shown in Fig. 2. To seal to the glass envelope the thermocouple wires have to be welded to lead-in wires. The joints between these wires are removed far from the rest of the tube to prevent them from heating up. Figure 2 shows also the electric circuit used for measurement. The emission current flows through a high resistance in the grid circuit of the FP54 tube. The potential drop across the resistance is balanced by the potentiometer P_1. There is, then, no potential difference between the collector and the guard rings during the measurement. The collector current is measured by the voltage supplied by the potentiometer P_1. The current is measured down to 10^{-12} ampere. The thermal e.m.f. indicating the cathode temperature can be measured with an accuracy of 0.02 mv, which corresponds to less than 1°C. The accuracy of the temperature measurements depends, however, upon the accuracy of the calibration of the Chromel-Alumel thermocouple, for which the table given by Hoskins Manufacturing Company in the *Handbook of Chemistry and Physics* is used. This table differs slightly from the table given in the *International Critical Tables*.

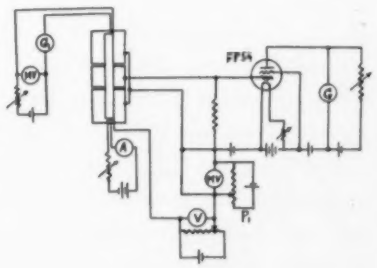

FIG. 2. Measurement circuit.

[1] G. E. Moore and H. W. Allison, J. App. Phys. 12, 431 (1941).

ELECTRON EMISSION IN A RETARDING FIELD

If the conduction electrons in the cathode have a Fermi-Dirac or Maxwellian distribution and if the surface potential barrier allows all electrons with velocities (normal to the surface) above a certain value to pass through and reflects all electrons with velocities less than this value, then the emitted electrons should have a Maxwellian energy distribution corresponding to the temperature of the cathode. Such results have been obtained for pure tungsten and platinum cathodes. For composite emitters, however, surface reflection may vary with the energy of the electrons in a more complicated manner. Indeed, Nottingham[2] has shown that electrons emitted from thoriated tungsten do not follow the Maxwellian distribution curve corresponding to the temperature of the cathodes and that at low retarding fields the emission current has a much smaller slope. Nottingham explains this as due to surface reflection of the type $R=e^{-Ex/e}$.

In the case of oxide-coated cathodes Koller[3] and Rothe[4] found that, although the energy distribution of the emitted electrons was Maxwellian, it corresponded to a temperature much higher than the observed cathode temperature. This, in fact, is similar to Nottingham's result for thoriated tungsten. On the other hand, Davisson[5] and Demski[6] found that the electron temperature calculated from the energy distribution curve agreed closely with the cathode temperature. The tube used by Rothe did not have suitable structure necessary for such measurement. The experiments of Davisson and Koller were not reported in detail. Demski measured the cathode temperature by an optical pyrometer and worked in the range 1110 to 1450°K. The electron temperature checked within a few percent with the temperature of the cathode, the difference becoming larger the higher the temperatures (13.3 percent at 1450°K). He explains this as due to variation of cathode activity with measurement. To avoid such trouble it is best to work at low temperatures. This is possible with our method of measuring cathode temperature.

Schottky[7] has shown that if the emitted electrons have Maxwellian energy distribution, then the relation between the current and the retarding potential is given by

$$i=i_0\frac{2}{(\pi)^{\frac{1}{2}}}\left\{\epsilon^{-eV/kT}\int_0^{(\rho eV/kT)^{\frac{1}{2}}}\epsilon^{-r^2eV/R^2kT}\times d\left[\left(\frac{eV}{kT}\right)^{\frac{1}{2}}\right]+\int_{(\rho eV/kT)^{\frac{1}{2}}}^{\infty}\epsilon^{-eV/kT}d\left[\left(\frac{eV}{kT}\right)^{\frac{1}{2}}\right]\right\}. \quad (1)$$

In our case $\rho^{\frac{1}{2}}=[R^2/(R^2-r^2)]^{\frac{1}{2}}=1.011$. Setting this factor equal to one, the second term on the left-hand side is the probability integral, the value of which can be taken from tables. If the ratio R/r is very large, the integral in the first term could be set equal to one. We have $R/r=6.43$; such a simplification would not be a good approximation. We calculate $\log i/i_0$ for different values of eV/kT, evaluating the integral by numerical integration. From such data theoretical curves for different values of T can be plotted. Figure 3 shows the experimental points and the corresponding theoretical curves for different temperatures of the cathode in the range 582 to 951°K. For curves 3, 4, 5, and 6, the saturation current was not measured. In fitting the experimental points to the theoretical curves we used the contact potential found from curves 1 and 2 to fix the relative horizontal positions, but the relative vertical positions were not fixed, the saturation currents not being known. The relative vertical positions of the experimental points and the theoretical curves shown for these curves are arbitrary. Each point was taken twice, on increasing and on decreasing voltage. In most cases the two readings differed so little from each other that, to avoid confusion, they are not shown separately.

We see from Fig. 3 that in cases 1 and 2 the experimental points fall very closely on the theoretical curves. In cases 3, 4, 5, and 6 we can at least say that the experimental points lie very nearly parallel to the theoretical curves. Actu-

[2] W. B. Nottingham, Phys. Rev. **49**, 78 (1936).
[3] R. Koller, Phys. Rev. **25**, 671 (1925).
[4] H. Rothe, Zeits. f. Physik **36**, 737 (1926).
[5] L. H. Germer, Phys. Rev. **25**, 795 (1925).
[6] A. Demski, Physik. Zeits. **30**, 291 (1929).
[7] W. Schottky, Ann. d. Physik **44**, 1011 (1914).

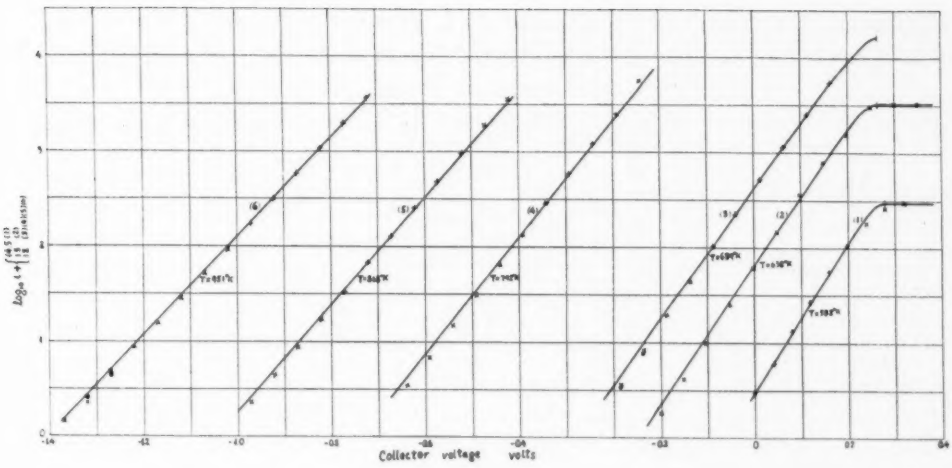

FIG. 3. Emission in retarding fields.

ally, in cases 2, 3, 4, and 5 the experimental points have a slightly steeper slope giving the energy distribution of the emitted electrons a temperature lower than that of the cathode. The difference between the two temperatures is, however, less than 5 percent in the worst case. We conclude that the emitted electrons have Maxwellian distribution corresponding to the cathode temperature within experimental error.

ELECTRON EMISSION IN AN ACCELERATING FIELD

Assuming mirror image force between the emitter and the electrons Schottky[8] derived the following relation between the emission current and the accelerating field E

$$i = i_0 \epsilon^{e^{\frac{1}{2}}E^{\frac{1}{2}}/kT}. \qquad (2)$$

The logarithm of i plotted against $\sqrt{E}$ should be a straight line with the slope $e^{\frac{1}{2}}/kT$. Experimentally this relation does not hold at low fields, since the emission current rises much faster with increasing field. The curve becomes a straight line with the predicted slope only at sufficiently high fields. For composite surfaces, such as thorium on tungsten, the departure from Schottky line depends upon the degree of activation, being larger for partially activated states. To explain such phenomena, the patch theory has been proposed. It takes into account the surface inhomogeneity of the emitter due to different emission properties of the various crystal facets in the case of clean metal cathodes, or due to different amounts of adsorbed active material at various parts of the surface in the case of composite cathodes. Becker[9] showed, by using a simplified model, that with the proper choice of the size of the areas of different activities and the degree of difference in activity a curve could be obtained to fit the experimental points. His calculations show that the smaller the size of the areas the higher must be the field for the current to approach the Schottky line and the larger the difference in work function between the various areas, the larger is the departure and the slower is the approach to the Schottky line. Electron-optical pictures[10] of emission from oxide-coated cathodes actually show strongly varying intensity. Thus one should expect departures from the Schottky line on the strength of the patch theory alone.

Figure 4 shows the experimental curves taken at various temperatures. There is some irregularity at small fields, the cause of which is not known. Above $E=150$ volt/cm the curves are straight within experimental error. The slopes are, however, over three times higher than the values predicted by Schottky's theory. The range of the accelerating voltage was then extended to

[8] W. Schottky, Physik. Zeits. **15**, 872 (1914).

[9] J. A. Becker, Rev. Mod. Phys. **7**, 95 (1935).

[10] Benjamin, Huck, and Jenkins, Proc. Phys. Soc. **50**, 345 (1938).

1300 volts. The results are shown in Fig. 5. The curves are straight up to $E=2500$ volt/cm, the

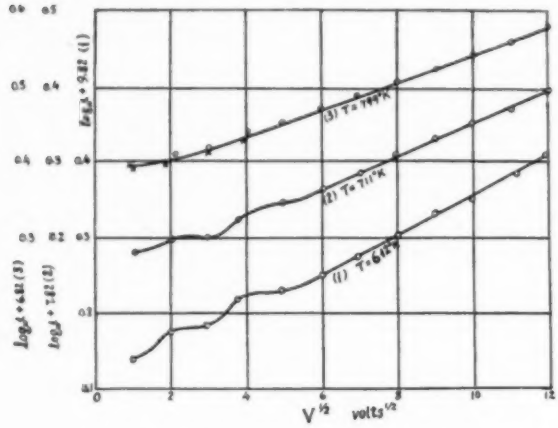

FIG. 4. Emission in accelerating fields.

slopes are given in Table I, together with the corresponding values according to Schottky's equation. The slopes of the experimental curves are much higher than predicted by Schottky's

TABLE I.

Temperature °K	Theoretical slope $\log_{10}$/volt$^{\frac{1}{2}}$	Experimental slope $\log_{10}$/volt$^{\frac{1}{2}}$	Ratio of the slopes
693	0.00635	0.0242	3.81
757	0.00581	0.0207	3.56
827	0.00536	0.0196	3.65

theory, but the ratios of two corresponding values are about the same for the three different temperatures. At the higher end of the voltage range the curves begin to bend with decreasing slope. Unfortunately, the insulation of the tube does not permit carrying the measurement to much higher voltages to see whether the curves will approach the Schottky line. In this connection, indirectly heated cathodes are not the most suitable type to use for investigation. On account of the large diameter of the cathode, very high voltages must be used to obtain large fields.

According to Benjamin, Huck, and Jenkins[10] the size of the areas with different activities corresponds to the size of carbonate particles from which the oxide coating is prepared. The particle size is usually of the order of 10^{-3} or 10^{-4} cm. It is interesting to note that this is the right order of magnitude required by Becker's patch theory.

VARIATION OF EMISSION CONSTANTS

The oxide coating of a thermionic cathode is an impurity semi-conductor with excess Ba, Sr, or Ca atoms as impurity supplying electrons to the conduction band. Fowler[11] has derived, on the basis of the theory of semi-conductors, the following equation for the emission current

$$i=De\frac{(8k^5\pi m)^{\frac{1}{2}}}{h^3}n^{\frac{1}{2}}T^{5/4}\epsilon^{\frac{1}{2}(\Delta E_1+\Delta E_2)-\Delta E_x/kT}$$

$$=DA'T^{5/4}\epsilon^{\frac{1}{2}(\Delta E_1+\Delta E_2)-\Delta E_x/kT}$$

$$=AT^{5/4}\epsilon^{\frac{1}{2}(\Delta E_1+\Delta E_2)-\Delta E_x/kT}, \quad (3)$$

where n is the concentration of impurity atoms in the oxide, ΔE_1 is the energy gap between the bottom of the conduction band and the top of the next lower band (2), ΔE_2 is the energy difference between the energy level of the impurity atoms and the top of band (2), ΔE_x is the energy difference between the top of band (2) and the energy of an electron at rest outside the oxide, and D is the transmission coefficient of the oxide surface. In contrast to the emission from clean metals, A' is not a universal constant but depends upon n. In fact, A for oxide-coated cathodes is very small compared with values for clean metals. This is not entirely due to D which may not be so greatly different from one. Thus

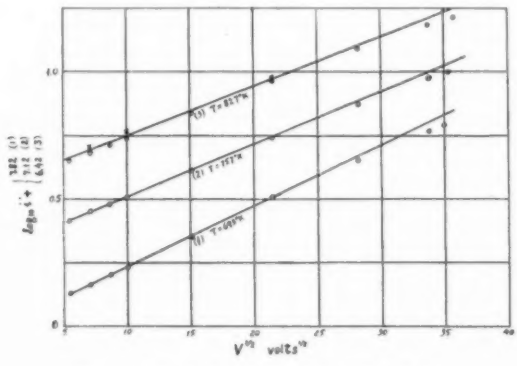

FIG. 5. Emission in accelerating fields.

[11] R. H. Fowler, *Statistical Mechanics* (Macmillan Company, New York, 1936), second edition, p. 401.

A should vary with the state of the oxide, both on account of its variation with n and on account of the variation of D with the surface condition.

The factor $\Delta E_x - \frac{1}{2}(\Delta E_1 + \Delta E_2)$ is equivalent to the work function. Of the three factors, ΔE_1 and ΔE_2 are approximately fixed for a given oxide, whereas ΔE_x may vary with the surface condition such as the amount of adsorption of barium or strontium and oxygen. Thus the work function should also vary with the state of activation. In this respect it is interesting to consider the point of view adopted by de Boer.[12] He considers the emission not as the passing of conduction electrons through the surface but as thermal ionization of the individual atoms adsorbed on the surface. According to this picture, the electrons inside the oxide pass from one barium atom to another, each time transforming these atoms into ions, until they reach the atoms adsorbed on the surface, where they are emitted by thermal ionization. So far as electron conduction inside the coating is concerned such a picture is merely an equivalent way of looking at the matter, but the factor A will depend not only upon the concentration of barium or strontium atoms inside the oxide due to its effect on electron conduction, but also upon the number of atoms adsorbed on the surface, being directly proportional to it. What is more important is that the work function is now the energy required for the thermal ionization of the adsorbed atoms. According to de Boer, when the adsorption is low (less than a full layer), the effect of the adsorbed atoms on the ionization energy of each other is negligible; consequently the work function of the oxide should be independent of the state of activation and should remain constant. It seems to us that even with this picture the work function should not remain constant, since the amount of adsorption certainly affects among other things, the difference between the energy levels inside and outside the oxide, on account of the double layer effect. The energy levels of the adsorbed atoms are more or less fixed with respect to those of the oxide. With variation of the amount of adsorption, the energy required to release an electron from an adsorbed atom and emit to the outside space should not remain unaffected. From the above considerations we expect that both A and the work function will vary with the state of activation of the oxide.

The experimental results conflict with each other. Some claim that the work function remains constant while A varies;[13] other results are just the opposite;[14] still others state that both A and the work function vary.[15] It seems, however, that most of these results are not reliable enough to be conclusive, because the temperature range used has been too short to give reliable Richardson plots or the temperature has been too high to prevent a change of the state of the oxide during measurement.

To determine the emission constants one has to measure the zero field emission. On account of the space charge there is no sharp breaking point where the curve goes through zero field. We find, however, that in the region of low accelerating voltage the current rises very slowly. The fact that our cathode has a large diameter and that the field increases rather slowly with the voltage is helpful in this respect. Negligible error is made if we take the current at 0.1 or 0.2 volt on the accelerating side, instead of at zero field. This is evident from Fig. 6, curve (a). We have observed a peculiar phenomenon: Sometimes the curve $\log i$ *versus* V shows a hump near zero field. The hump appears every time after glowing the cathode at a sufficiently high

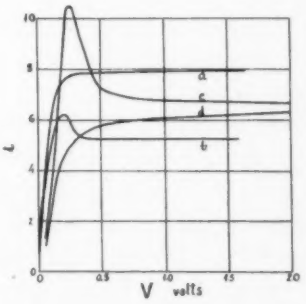

FIG. 6. Effect of potential difference between collector and guard rings.

[12] J. H. de Boer, *Electron Emission and Adsorption Phenomena* (Macmillan Company, New York, 1935).

[13] W. Espe, Wiss. Ver. Siemens-Konz. **5**, No. 3, 29, 46 (1927). H. Kniepkamp and C. Nebel, Wiss. Ver. Siemens-Konz, **11**, 75 (1932).

[14] W. Heinze and S. Wagener, Zeits. f. Physik **110**, 164 (1938).

[15] F. Detels, Zeits. f. Hochfrequenz. **30**, 10, 52 (1927); W. S. Huxford, Phys. Rev. **38**, 379 (1931).

temperature and disappears after a large current is drawn at sufficiently high temperature. We conclude that the hump is due to a contact potential difference between the collector and the guard rings. Although these are made of the same material, because of the difference in temperature between the central portion and the two ends of the cathode the rate of evaporation of barium and oxygen and their deposition on the collector and the guard rings is different, causing a potential difference. Curves (c) and (d), taken at the same time, are for the guard rings 0.1 volt positive with respect to the collector, in the case of curve (d), and 0.1 volt negative in the case of curve (c), and bear evidence to this explanation. Curve (c) has just the same shape as curve (b). The fact that only curves with a hump like curve (c), but none with poor saturation like curve (d), were observed, indicates that the collector is sometimes positive, but never negative, with respect to the guard rings. The magnitude of the hump of curve (c) far exceeds the worst case observed. Fortunately, with an accelerating voltage of over one volt, the two curves (c) and (d) approach the same value, which differs but little from the zero field current. It should be mentioned that the measurement of emission in retarding and accelerating fields was made with the tube in the condition showing no hump.

The contact potential between the collector and the cathode, as determined from the bending position of the log i *versus* V curve, varied from 0.1 to 0.7 volt. Had the surface condition of the collector remained unchanged, this variation of the contact potential difference should correspond to the change in the work function of the cathode. But the latter, as obtained from the Richardson plot, showed no correlation with the shift of the bending position of the log i *versus* V curve. Furthermore, since the collector is made of nickel, its work function should be around 5 ev, at the same time the work function of the cathode varied from 1.5 to 1.8 ev. The contact potential difference should thus be several volts. The fact that it was less than one volt, and varied with no apparent correlation with the work function of the cathode, shows that the surface condition of the collector was not that of clean nickel and that it varied with the treatment of the tube. Since barium as well as oxygen may be evolved from the cathode and deposited on the collector, such phenomena are not surprising. We found that, in general, after glowing the cathode at high temperature the bend in the curve log i *versus* V shifted to higher accelerating voltage, whereas drawing large emission had the opposite effect. For the determination of emission constants, low cathode temperatures were used, $480° < T < 720°$K, so that no change of contact potential difference took place during each set of measurement.

Figure 7 shows a set of log i *versus* V curves

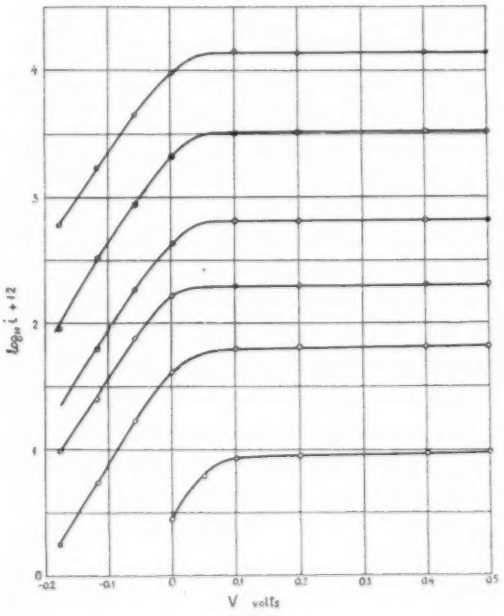

FIG. 7. Emission at different temperature.

and Fig. 8 shows the Richardson plots for various states of activation. Since the current i is not sensitive to the power of T in Eq. (3), we used T^2 instead of $T^{5/4}$ to reduce Eq. (3) to the form of Richardson equation for comparison with the data of others. Figure 8 shows that the points fall very closely on straight lines. The current measurement is accurate to within 2 or 3 percent. Any small deviation of the points must be due to inaccuracy in temperature measurement. The largest deviation of a point from the straight line corresponds to about 5°C. The experimental

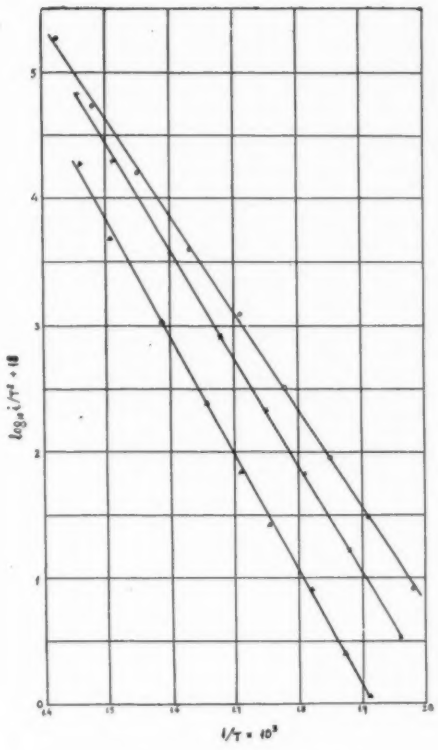

FIG. 8. Richardson plot.

points in the Richardson plots cover a range of more than 4 for $\log_{10} i$. The upper limit is imposed by the precaution against a change of the state of the cathode due to high temperature and large emission, whereas the lower limit is set by the tube leakage. Table II gives the emission constants determined after various treatments of the tube. The numbers of the Richardson plots in Fig. 8 correspond to the numbers in this table. An examination of the table shows that high temperature flashing increases both the work function and A, which come back to lower values after glowing the cathode at a lower temperature. Our cathode, being indirectly heated, has a large heat capacity, which makes its temperature variation slow. After flashing it may reactivate to some extent as the temperature drops slowly, so that we could not vary its state of activation over a wider range. The lowest value observed for the work function is about 1.5 ev. After flashing the cathode at high temperatures several times successively we could no longer bring the work function to this value: It was then about 1.6 volt. This is probably due to poising by oxygen liberated at high temperatures. Figure 9 shows the relation between the work function and $\log A$. Poor scattering of the points may be due to the inaccurate determination of the latter.

TABLE II.

No.	Cathode glowing Temperature °K	Duration min.	Work function ev	$\log_{10} A$
1	1390	7	1.691	−0.21
2	1350	4	1.571	−0.25
3	1200	30	1.520	−1.02
4	1270	10	1.571	−0.43
5	1320	7	1.689	−0.15
6	1300	10	1.590	−0.56
7	1100	30	1.521	−0.97
8	1320	4	1.641	−0.14
9	1320	7	1.696	−0.33
10	1120	60	1.551	−0.65
11	1200	30	1.560	−0.45
12	1150	45	1.503	−1.06
13	1390	7	1.830	+0.34
14	1140	30	1.605	−0.79

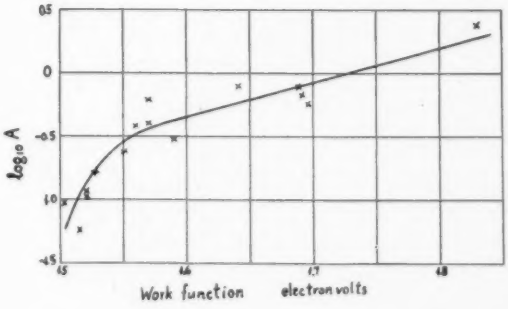

FIG. 9. Relation between work function and $\log A$.

EFFECT OF DRAWING EMISSION

It has been reported in several papers that when emission is drawn from an oxide-coated cathode the emission current decays with time, approaching a final value considerably smaller than the initial current, sometimes less by a factor of ten or more. In the range $650°K < T < 1000°K$, the greater part of the decay takes place in the first few minutes, and the lower the temperature the slower the approach to the

final value. All these measurements were made on cathodes coated with a mixture of barium and strontium oxides.[16]

In our case the measurements made for the Richardson plots were carried up to 700°K and in the measurements with accelerating fields the temperatures used were as high as 850°K. The emission current was steady and showed no sign of decay. To make sure of this fact four curves were taken at 790°K, 880°K, 950°K, and 990°K, with a constant voltage of 22.5 volts. The cathode was first glowed at the test temperature for some time. Then the collector voltage was applied by closing a switch and the emission current was taken at different time intervals. The curves are shown in Fig. 10. Curve 4 shows no change of

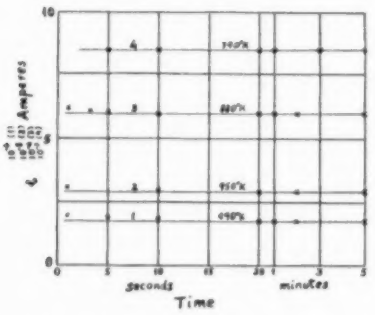

FIG. 10. Variation of emission with time.

emission with time, whereas curves 1, 2, and 3 show a slight drop within the first few seconds. However, in these cases the cathode temperature also dropped slightly as the voltage was applied. This was indicated by a deflection of galvanometer G_1 shown in Fig. 2. The galvanometer reading came back to the balanced position again when the collector voltage was removed. The slight drop in emission was thus apparently associated with the drop in cathode temperature due to emission.

The emission current has also the effect of heating the cathode by going through the oxide. Figure 11 shows the cathode temperature and

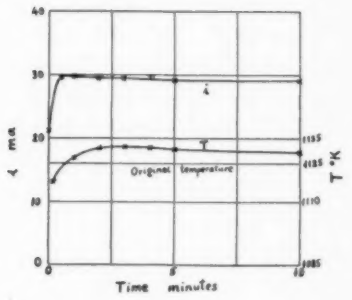

FIG. 11. Variation of emission and cathode temperature with time.

the emission current at 1125°K with an applied voltage $V=110$ volts. Upon applying the collector voltage the cathode temperature fell below the original value, then rose above it. Apparently the cooling was due to emission and the heating was due to conduction of the emission current through the oxide. The variation in emission was evidently to a great extent due to the variation of the cathode temperature.

It seems that, at temperatures and emission densities corresponding to the curves in Fig. 10, the emission of current has very little effect on the state of the oxide. In cases such as shown in Fig. 11 it is difficult to tell, due to the disturbing effect of the large variation of cathode temperature. Table III gives the emission constants

TABLE III.

No.	Cathode temperature °K	Tube treatment Emission drawing Voltage volt	Current ma	Duration min.	Work function ev	$\log_{10} A$
1	1065			120	1.592	−0.73
2	1065	20	2.5	120	1.592	−0.73
3	1120			120	1.648	−0.42
4	1120	60	13	90	1.620	−0.57
5	1120	110	30	45	1.608	−0.60
7	1065			180	1.598	−0.84
8	1065	110	8	60	1.590	−1.06

determined after various treatments of the tube. When emission was drawn the collector voltage was removed after the heating current, otherwise the effect of drawing emission might be reduced due to the slow cooling of the cathode. It is seen that the effect of drawing emission is small, both log A and the work function are slightly reduced.

[16] J. A. Becker, Phys. Rev. **34**, 1323 (1929); J. A. Becker and R. W. Sears, Phys. Rev. **38**, 2193 (1931); H. Kniepkamp and C. Nebel, reference 13; J. P. Blewett, Phys. Rev. **55**, 713 (1939).